

**DETERMINING CROP RESIDUE TYPE AND CLASS
USING SATELLITE ACQUIRED DATA**

A Thesis

Submitted to the Faculty

of

Purdue University

by

Xin Zhuang

**In Partial Fulfillment of the
Requirements for the Degree
of**

Master of Science in Engineering

December 1990

(NASA-CR-15**8961**) DETERMINING CROP RESIDUE
TYPE AND CLASS USING SATELLITE ACQUIRED DATA
M.S. Thesis Progress Report, Jun. 1990
(Purdue Univ.) 144 p CSCL 08A

N71-18460

Unclas
G3/43 0352284

PURDUE UNIVERSITY
GRADUATE SCHOOL
Thesis Acceptance

This is to certify that the thesis prepared

By Xin Zhuang

Entitled

Determining Crop Residue Type and Class
Using Satellite Acquired Data

Complies with University regulations and meets the standards of the Graduate School for
originality and quality

For the degree of Master of Science in Engineering

Signed by the final examining committee:

Donald Eng, chair
Don D. Jones
Edwin J. Moore
Philip H. Swain
Mason F. Baumgardner

Approved by:

R. J. Higgins Department Head 3 Dec 90 Date

This thesis is
 is not to be regarded as confidential

Donald Eng
Major Professor

Where there's a will there's a way.

— anonymous

This thesis is dedicated to my wife Jing Gu,
my parents Song Zhuang and Qi-fang Wei, and
my grandmother Cong-lan Li.

ACKNOWLEDGEMENTS

I would like to express my sincere thanks and great appreciation to all the individuals and organizations who made this study possible:

Dr. Bernard Engel, major professor, for his guidance and insight as a scientist committed to improving our biosphere.

Dr. Marion Baumgardner, Dr. Edwin Monke, Dr. Philip Swain, and Dr. Don Jones, for their guidance, assistance, and time throughout this research project and for serving on my advisory committee.

Jack Hart, for his collection of ground truth data for the study area and his kind cooperation in this research project.

Dr. David Landgrebe, for his permission to use the Image Processing Laboratory in the Department of Electrical Engineering, Purdue University, West Lafayette, IN.

Larry Biehl, for his infinite patience in assisting with the improvements of the MacLARSYS system and with computer problems.

Dr. Norberto Fernandez and Dr. Fabian Lozano, for their assistance in checking ground truth data and providing satellite image data and GIS data.

The National Aeronautics and Space Administration and the Laboratory for Applications of Remote Sensing at Purdue University, for providing the funding for this project. Special thanks to Dr. Chris Johannsen, and to Glenda Bauer and Beverly Sloniger for keeping everything organized.

Jon Benediktsson and Ranjan Muttiah, for their kindness and assistance.

This research was supported by NASA Research Grants NAGW-1472.

TABLE OF CONTENTS

	Page
1. INTRODUCTION	1
1.1 Objectives	4
1.2 Organization	4
2. LITERATURE REVIEW	6
2.1 Remote Sensing	6
2.1.1 Image Transformation	6
Spectral Ratioing	6
Principal Components	7
2.1.2 Image Classification	7
Supervised Classification	8
Unsupervised Classification	9
Hybrid Classification	10
2.1.3 Remote Sensing Applications in Agriculture	11
Crop Inventory	11
Soils	12
2.2 Neural Networks	14
2.2.1 Neural Network Terminology	15
What is a Neural Network?	15
The Brain and Neural Networks	16
Neural Network Operation	18
2.2.2 Historical Perspective	19
2.2.3 Back-propagation	19
2.2.4 Neuro-classification	21
2.3 Estimation of Crop Residues	22
2.3.1 Traditional Methods for Estimating Crop Residues	22
Meterstick Method	23
Line-Transect Method	23
Photographic Method	24
Scanning Microdensitometric Method	25
Empirical Method	25
2.3.2 Estimation of Crop Residues Using Remotely Sensed Data	27
3. MATERIALS AND METHODS	28
3.1 Site Description	28
3.2 Data Sources	29
3.3 Ground Truth Data	29

	Page
3.4 Neural Network Classifier	35
3.4.1 Neuro-classifier Algorithm: Back-propagation	35
3.4.2 Neural Networks for Classification	38
3.4.3 Neural Network Configurations	40
3.4.4 NASA NETS 2.0	41
3.5 Method for Estimating Residue Percentage	42
3.5.1 Preprocessing of Data	42
Information Class Creation	43
Principal Components	46
Spectral Ratioing	46
3.5.2 Classification Using Traditional Methods	47
3.5.3 Classification Using Neural Networks	47
3.5.4 Classification with the Aid of a GIS Layer	48
4. RESULTS AND DISCUSSION	50
4.1 Spectral Behavior of Crop Residues	50
4.1.1 Discrimination of Crop Residue Cover in March, 1987	50
4.1.2 Discrimination of Crop Residue Cover in April, 1988	53
4.2 Evaluation of Classification for the Original Data	54
4.2.1 Performance for March Data	55
4.2.2 Performance for April, 1988 Data	62
4.3 Evaluation of Classification for the Transformed Data	63
4.3.1 Performance for PC March, 1987 Data	63
4.3.2 Performance for PC April, 1988 Data	66
4.3.3 Performance for SR March, 1987 Data	70
4.4 Evaluation of GIS-Aided Classification	73
4.5 Comparison of the Classifiers for Different Data Sets	78
4.5.1 Comparison of ML Classifiers	79
4.5.2 Comparison of NN Classifiers	81
4.5.3 Comparison of the Best ML and NN	84
4.6 Evaluation of Neural Network Training	87
4. RESULTS AND DISCUSSION	50
4.1 Spectral Behavior of Crop Residues	50
4.1.1 Discrimination of Crop Residue Cover in March, 1987	50
4.1.2 Discrimination of Crop Residue Cover in April, 1988	53
4.2 Evaluation of Classification for the Original Data	54
4.2.1 Performance for March Data	55
4.2.2 Performance for April, 1988 Data	62
4.3 Evaluation of Classification for the Transformed Data	63
4.3.1 Performance for PC March, 1987 Data	63
4.3.2 Performance for PC April, 1988 Data	66
4.3.3 Performance for SR March, 1987 Data	70
4.4 Evaluation of GIS-Aided Classification	73
4.5 Comparison of the Classifiers for Different Data Sets	78

	Page
4.5.1 Comparison of ML Classifiers	79
4.5.2 Comparison of NN Classifiers	81
4.5.3 Comparison of the Best ML and NN	84
4.6 Evaluation of Neural Network Training	87
5. SUMMARY AND CONCLUSIONS	91
6. RECOMMENDATIONS FOR FURTHER RESEARCH	95
BIBLIOGRAPHY	97
APPENDICES	
Appendix A. Ground Truth Data Survey Form	101
Appendix B. Flown Aerial Photographs	117
Section 3:	117
Section 4:	118
Section 9:	120
Section 10:	121
Appendix C. NETS Interface Routine Code	122

LIST OF TABLES

Table	Page
1. Characteristics of surface samples of five mineral soils.	13
2. Neuron and processing element components.	18
3. Influence of various field operations on surface residue remaining.	26
4. Crop yields including residue cover after harvesting for Miami County, Indiana.	30
5. Residue cover percentage from ground truth data in section 9, 1986.	33
6. Residue cover percentage from ground truth data in section 9, 1987.	34
7. Representations for the neural network classifiers.	41
8. The characteristics of Landsat TM data.	43
9. Confusion matrix for the March, 1987 testing data classified using L1.	58
10. Confusion matrix for the March, 1987 testing data classified using ML.	58
11. Confusion matrix for the March, 1987 testing data classified using NN.	59
12. Confusion matrix for the April, 1988 testing data classified using L1.	59
13. Confusion matrix for the April, 1988 testing data classified using ML.	60
14. Confusion matrix for the April, 1988 testing data classified using NN.	60
15. Confusion matrix for the PC March, 1987 testing data classified using L1.	65
16. Confusion matrix for the PC March, 1987 testing data classified using ML.	65
17. Confusion matrix for the PC March, 1987 testing data classified using NN.	66
18. Confusion matrix for the PC April, 1988 testing data classified using L1.	67
19. Confusion matrix for the PC April, 1988 testing data classified using ML.	68

Table	Page
20. Confusion matrix for the PC April, 1988 testing data classified using NN.	68
21. Confusion matrix for the SR March, 1987 testing data classified using L1.	70
22. Confusion matrix for the SR March, 1987 testing data classified using ML.	71
23. Confusion matrix for the SR March, 1987 testing data classified using NN.	71
24. Confusion matrix for the March Plus testing data classified using L1.	74
25. Confusion matrix for the March Plus testing data classified using NN.	75
26. Confusion matrix for the April Plus testing data classified using L1.	76
27. Confusion matrix for the April Plus testing data classified using NN.	77
28. Training behavior for the neural classifiers.	89
9. Confusion matrix for the March, 1987 testing data classified using L1.	58
10. Confusion matrix for the March, 1987 testing data classified using ML.	58
11. Confusion matrix for the March, 1987 testing data classified using NN.	59
12. Confusion matrix for the April, 1988 testing data classified using L1.	59
13. Confusion matrix for the April, 1988 testing data classified using ML.	60
14. Confusion matrix for the April, 1988 testing data classified using NN.	60
15. Confusion matrix for the PC March, 1987 testing data classified using L1.	65
16. Confusion matrix for the PC March, 1987 testing data classified using ML.	65
17. Confusion matrix for the PC March, 1987 testing data classified using NN.	66
18. Confusion matrix for the PC April, 1988 testing data classified using L1.	67
19. Confusion matrix for the PC April, 1988 testing data classified using ML.	68
20. Confusion matrix for the PC April, 1988 testing data classified using NN.	68
21. Confusion matrix for the SR March, 1987 testing data classified using L1.	70

Table	Page
22. Confusion matrix for the SR March, 1987 testing data classified using ML.	71
23. Confusion matrix for the SR March, 1987 testing data classified using NN.	71
24. Confusion matrix for the March Plus testing data classified using L1.	74
25. Confusion matrix for the March Plus testing data classified using NN.	75
26. Confusion matrix for the April Plus testing data classified using L1.	76
27. Confusion matrix for the April Plus testing data classified using NN.	77
28. Training behavior for the neural classifiers.	89

Appendix
Table

1. Ground truth survey form A, 1986.	101
2. Ground truth survey form A, 1987.	102
3. Ground truth survey form A, 1988.	103
4. Ground truth survey form B.	104
5. Ground truth survey form C, 1986.	105
6. Ground truth survey form C, 1987.	106
7. Ground truth survey form C, 1988.	107
8. Ground truth survey form D, 1986.	108
9. Ground truth survey form D, 1987.	109
10. Ground truth survey form D, 1988.	110
11. Ground truth survey form E, 1986.	111
12. Ground truth survey form E, 1987.	112
13. Ground truth survey form E, 1988.	113
14. Ground truth survey form F, 1986.	114
15. Ground truth survey form F, 1987.	115
16. Ground truth survey form F, 1988.	116

LIST OF FIGURES

Figure	Page
1. Minimum distance to means classification strategy.	10
2. Equiprobability contours defined by a maximum likelihood classifier.	10
3. Representative reflectance spectra of surface samples of five mineral soils (Table 1).	14
4. Structure of a neuron.	17
5. Structure of a processing element.	17
6. Activation flows forward while errors flow back through the network.	20
7. Overview (inset) and close-up of the line-transect method.	24
8. Ownership boundaries for sections 3, 4, 9 and 10.	29
9. A sample of survey data form.	31
10. Network structure of a three-layer back-propagation system.	36
11. Matrix-mapping structure of the three-layer back-propagation system.	37
12. Three-layer back-propagation neural network.	39
13. Creation of the information classes for 1987.	44
14. Creation of the information classes for 1988.	45
15. Creation of Landsat TM Plus data.	48
16. Reflectance curves for the training data of March 23, 1987.	51
17. Reflectance curves for the training data of April 26, 1988.	52
18. Training performance for the March, 1987 data.	56
19. Testing performance for the March, 1987 data.	56
20. Training performance for the April, 1988 data.	61
21. Testing performance for the April, 1988 data.	61
22. Training performance for the PC March, 1987 data.	64
23. Testing performance for the PC March, 1987 data.	64

Figure	Page
24. Training performance for the PC April, 1988 data.	69
25. Testing performance for the PC April, 1988 data.	69
26. Training performance for the SR March, 1987 data.	72
27. Testing performance for the SR March, 1987 data.	72
28. Training performance for the March Plus data.	75
29. Testing performance for the March Plus data.	76
30. Training performance for the April Plus data.	77
31. Testing performance for the April Plus data.	78
32. Testing performance for of all MLs for the March, 1987 data.	80
33. Testing performance for of all MLs for the April, 1988 data.	80
34. Testing performance for of all NNs for the March, 1987 data.	82
35. Testing performance for of all NNs for the April, 1988 data.	82
36. The best classifiers for March, 1987 data.	83
37. The best classifiers for April, 1988 data.	83
38. Classification results for the Landsat TM data of March, 1987.	85
39. Classification results for the Landsat TM data of April, 1988.	86
40. Max errors for all neural trainings.	88
41. RMS errors for all neural trainings.	89
16. Reflectance curves for the training data of March 23, 1987.	51
17. Reflectance curves for the training data of April 26, 1988.	52
18. Training performance for the March, 1987 data.	56
19. Testing performance for the March, 1987 data.	56
20. Training performance for the April, 1988 data.	61
21. Testing performance for the April, 1988 data.	61
22. Training performance for the PC March, 1987 data.	64
23. Testing performance for the PC March, 1987 data.	64
24. Training performance for the PC April, 1988 data.	69
25. Testing performance for the PC April, 1988 data.	69
26. Training performance for the SR March, 1987 data.	72

Figure	Page
27. Testing performance for the SR March, 1987 data.	72
28. Training performance for the March Plus data.	75
29. Testing performance for the March Plus data.	76
30. Training performance for the April Plus data.	77
31. Testing performance for the April Plus data.	78
32. Testing performance for of all MLs for the March, 1987 data.	80
33. Testing performance for of all MLs for the April, 1988 data.	80
34. Testing performance for of all NNs for the March, 1987 data.	82
35. Testing performance for of all NNs for the April, 1988 data.	82
36. The best classifiers for March, 1987 data.	83
37. The best classifiers for April, 1988 data.	83
38. Classification results for the Landsat TM data of March, 1987.	85
39. Classification results for the Landsat TM data of April, 1988.	86
40. Max errors for all neural trainings.	88
41. RMS errors for all neural trainings.	89
Appendix	
Figure	
1. Photocopy A of flown aerial photograph for section 3, 1987.	118
2. Photocopy A of flown aerial photograph for section 4, 1987.	118
3. Photocopy B of flown aerial photograph for section 4, 1987.	119
4. Photocopy A of flown aerial photograph for section 9, 1987.	120
5. Photocopy A of flown aerial photograph for section 10, 1987.	121

ABSTRACT

Zhuang, Xin. M.S.E., Purdue University, December 1990. Determining Crop Residue Type and Class Using Satellite Acquired Data. Major Professor: Bernard A. Engel.

Landsat TM data for March 23, 1987 and April 26, 1988 with accompanying ground truth data for the study area in Miami County, IN were used in this study to determine crop residue type and class. Principal components and spectral ratioing transformations were applied to the Landsat TM data. One GIS layer of land ownership was added to each original image as the eighth band of data in an attempt to improve classification. Maximum Likelihood, Minimum Distance, and neural networks, which are an emerging artificial intelligence technique, were used to classify the original, transformed and GIS-enhanced remotely sensed data. Crop residues could be separated from one another and from bare soil and other biomass. Two types of crop residues and four classes were identified from each Landsat TM image. The Maximum Likelihood classifier performed the best classification for each original image without need of any transformation. The neural network classifier was able to improve the classification by incorporating a GIS-layer of land ownership as an eighth band of data. The Maximum Likelihood classifier was unable to consider this eighth band of data and thus its results could not be improved by its consideration.

1. INTRODUCTION

Crop residues are the portions of a crop that are left in the field after harvest. They are a tremendous natural resource — not a waste as some have termed them. They add organic matter content to soils and this adds plant nutrients; improves soil structure; influences soil water, air, and temperature relations; helps control runoff and erosion; and makes tillage easier. Crop residues can also improve water quality. Therefore, the management of crop residues has a large impact on the quantity and quality of soil and water resources.

Soil erosion is a problem in the United States. Water erosion is more serious than wind erosion in Indiana and most of the Midwest. Recent U.S. Department of Agriculture surveys (Mannering, 1990) of average erosion rates on Indiana cropland estimate 7½ tons per acre per year on gentle slopes (2-6%), 11 tons annually on moderate slopes (6-12%), and 29 tons on steep slopes (12-18%). This indicates that on sloping croplands the rates of soil loss are exceeding the annual rate of soil formation, which is considered to be about five tons per acre or less. Erosion rates greater than five tons per acre will eventually reduce soil productivity.

Studies relating cropland agriculture to water quality show that 4-5 billion tons of sediment are being deposited in this nation's streams each year, with over half coming from cropland (Mannering, 1990). It gets there largely as a result of runoff associated with rainstorms. Moreover, sediment often carries chemicals, such as phosphorus, that cause contamination of water.

Conservation tillage is the best nation-wide solution to maintaining soil productivity and improving water quality. A conservation tillage system is a tillage system which reduces runoff and soil loss either by: 1) leaving appreciable crop residues on the soil surface; 2) leaving the surface rough and cloddy or ridged; or 3) a combination of the two.

Surface residue is effective because it protects the soil from detachment; it minimizes surface crusting, thus increasing infiltration rates; and it slows runoff velocities, thus reducing its ability to transport sediment.

Research on residue effectiveness in reducing soil erosion (Wischmeier, 1978) showed that if 50% of the surface is covered, soil loss will be reduced to 32% of that with no mulch present. A surface cover of 80% will reduce soil loss to 13% of that with no mulch, and 100% cover will practically eliminate soil loss. At low mulch application rates, a well-anchored mulch covering 20% of the soil surface will reduce soil loss to 60% of that with no mulch.

Modeling soil erosion is useful for understanding its control. Several soil erosion models require residue cover data. They include the Universal Soil Loss Equation (USLE) (Wischmeier and Smith, 1978), the Areal Nonpoint Source Watershed Environmental Response Simulation (ANSWERS) (Beasley *et al.*, 1980), the Water Erosion Prediction Project (WEPP) (Foster and Lane, 1987), and the Chemical, Runoff and Erosion Agricultural Management System (CREAMS) (Knisel, 1980).

The estimation of cropland residue cover is vital for conservation tillage programs. Five methods of estimating crop residues have been commonly used. They are the meterstick method (Hartwig, 1978), the line-transect method, the photographic method, the scanning microdensitometry method (Lowery *et al.*, 1984), and the empirical method (Hill *et al.*, 1989). Each of them has limitations to a range of cover and topographic conditions.

Remotely sensed data, such as satellite images have been used in the applications of crop inventory and land use and have potential for determining crop residue type and amount. One satellite image covers a much larger area than the conventional methods mentioned previously. For example, a Landsat TM scene covers $185 \times 185 \text{ km}^2$. Given the ground truth corresponding to a portion of a satellite scene, the scene can be classified to estimate crop residue cover. Based on research in the area of remote sensing, the hybrid classification of satellite images, i.e. the combination of supervised classifications and unsupervised classifications, nearly always presents the best result for the applications of crop inventory and land use.

Research in the discipline of artificial intelligence has shown that neural networks, one branch of artificial intelligence, are the latest alternative for classification of multispectral remotely sensed data. A neural network (NN) is a computing system with a number of simple, highly interconnected processing elements which process information in parallel by their dynamic state response to external inputs. The classification of a satellite image using a neural network with back-propagation, which is a widely-used learning rule for neural networks, is called *neuro-classification* in this research.

Although neuro-classification follows procedures similar to conventional (statistical) classifications such as Maximum Likelihood and L1 Minimum Distance, it has major advantages over them in terms of statistical assumptions. In addition, it can theoretically integrate non-remotely sensed data into the process to improve classification accuracy. However, neuro-classification did not perform better than conventional classifications on a very high dimensional (more than 20 channels) image (Benediktsson *et al.*, 1990b).

1.1 Objectives

The primary objective of this research is to develop methods for determining crop residue type and class using satellite data.

Specific objectives required to achieve the primary objective are:

1. to determine crop residue type and class (amount) using conventional classification methods.
2. to explore improvements to classification methodology using neural networks.
3. to make a comparison of the classification results from objectives 1 and 2.

1.2 Organization

This thesis documents the methodology of estimating crop residue cover using remotely sensed data and several remote sensing techniques.

The next chapter, LITERATURE REVIEW, reviews the related background literature. The first portion of this chapter includes several remote sensing techniques and applications in agriculture. The second portion of this chapter is a review of neural networks which are an emerging artificial intelligence technique, including the concept, a most commonly-used learning algorithm, *back-propagation*, and the application in image classification. The third portion of this chapter examines five conventional techniques for measuring crop residues. These methods are the meterstick method, the line-transect method, the photographic method, the scanning microdensitometry method and the empirical method.

Chapter 3 is **MATERIALS AND METHODS**. It describes the data resources, ground truth data processing, neural network classifiers and the remote sensing methods for estimating crop residue cover developed in this study.

The next chapter, **RESULTS AND DISCUSSION**, presents and discusses the results obtained from all methods used in this study. Comparisons for the different methods are made based on the results. Consequently, the best methods are recommended.

Chapter 5 presents a **SUMMARY AND CONCLUSIONS** from this study. The final chapter, **RECOMMENDATIONS FOR FURTHER RESEARCH**, provides suggestions for further study.

2. LITERATURE REVIEW

This chapter will review: applications of remote sensing related to agriculture; neural networks with a learning rule suitable for image processing; and methods of estimating crop residues.

2.1 Remote Sensing

The review of image transformations, three conventional types of classification of remotely sensed data, and the applications of remote sensing in agriculture follows.

2.1.1 Image Transformation

Image transformations can either enhance multispectral image data or improve image classification. This review focuses on the two most-commonly used transformations, *spectral ratioing* and *principal components*.

Spectral Ratioing

An image generated from spectral ratioing is the enhancement resulting from the division of digital number values in one spectral band by the corresponding values in another band. It is often useful for discriminating subtle spectral variations in a scene because of the following two

reasons (Mather, 1987): a) certain aspects of the shape of spectral reflectance curves of different Earth-surface cover types can be brought out by ratioing; and b) undesirable effects on the recorded radiances such as the effect of variable illumination resulting from variations in topography can be reduced.

Principal Components

The principal components transformation is used to transform image data to uncorrelated data in a new coordinate system and to reduce the dimension of multispectral information. That is, the principal components transformation is one of the techniques designed to compress the multispectral information into a smaller number of bands. As a preprocessing procedure prior to image classification, this transformation generally increases the computational efficiency of the classification process because of the uncorrelated transformed data and the ability of analysis based on a smaller number of bands. All of the information represented are usually dominated by the first few *components* in the new coordinate system and this subset of wavelength bands may then be used for viewing and for classification. However, the importance of the lower-order principal components was pointed out by P.M. Mather (1987). The principal components transformation does not enhance separability since it is a linear transformation that rotates and translates the original coordinate system.

2.1.2 Image Classification

The purpose of computer classification of remotely sensed data is to categorize all pixels based on their numerical properties into physical classes. One way to categorize conventional types of classification is as follows:

- a. supervised,
- b. unsupervised, and
- c. hybrid, i.e. the combination of supervised and unsupervised.

Supervised Classification

In supervised classification, every pixel is categorized into one of the training classes which are determined from ground reference data. Training fields are chosen interactively by the analyst.

L1 Minimum Distance is one of the supervised classifiers that identifies an unknown pixel by computing the absolute distance between the value of the unknown pixel and each of the information class means. The information category means are calculated before classification. An example of this classifier is illustrated in Figure 1. The unknown pixels have been plotted at points 1 and 2. The distance between unknown pixel 1 and each class mean value is shown by dashed lines in Figure 1. After computing the distances, the unknown pixel (Pixel 1) is assigned to the "closest" class, in this case "corn."

L1 Minimum Distance is mathematically simple and computationally efficient, but it has certain limitations. Most importantly, it is insensitive to different degrees of variance and correlation in the spectral response data (Lillesand and Kiefer, 1987). In Figure 1, unknown pixel 2 would be assigned by this classifier to the category "sand," in spite of the fact that the greater variability in category "urban" suggests that "urban" would be a more appropriate class assignment. Because of such problems, this classifier is not widely used in applications where spectral classes are close to one another in the measurement space and have high variances.

Maximum Likelihood is the most widely used supervised classifier for remote sensing

image data. It quantitatively evaluates both the variance and covariance, as well as the mean, of the class spectral response patterns when classifying an unknown pixel. Under the assumption of normality, the distribution of a class response pattern can be completely described by the mean vector and the covariance matrix. Given these parameters, we may compute the statistical probability of a given pixel value being a member of a particular land-cover class.

Compared to L1 Minimum Distance, Maximum Likelihood almost always presents an acceptable result, if the distribution of data is Gaussian, though it is mathematically and computationally complicated. Figure 2 illustrates a Maximum Likelihood classifier applied to the same data set as shown in Figure 1. In this case, the classification of unknown pixel 1 was in agreement with that in Figure 1, but unknown pixel 2 was correctly identified as "urban" by the Maximum Likelihood classifier.

L1 Minimum Distance and Maximum Likelihood are often used because they are easily implemented on a computer. As described above, L1 Minimum Distance considers only the first order statistic, *mean*; while Maximum Likelihood includes both the first order and second order statistics, *mean* and *covariance*. Therefore, the latter one is better in classification than the former one if the decision boundaries are not easy to separate the classes in the measurement space.

Unsupervised Classification

In unsupervised classification, all pixels in an image are first aggregated into the natural spectral groupings or clusters presented in the scene based on the given criteria. There is no training data as the basis for classification. Then, these clusters are identified and labeled by comparing to ground reference data.

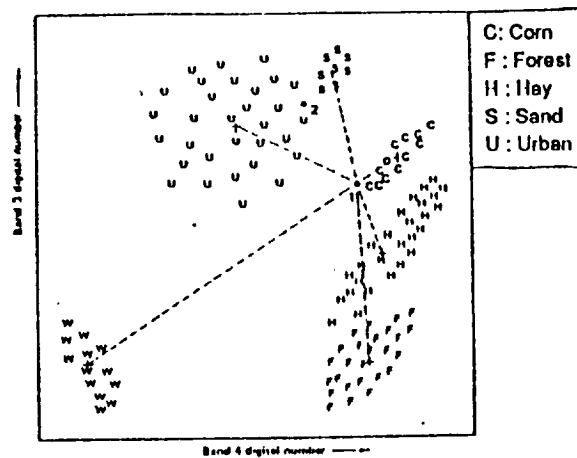


Figure 1. Minimum distance to means classification strategy.
(Source: Lillesand and Kiefer, 1987)

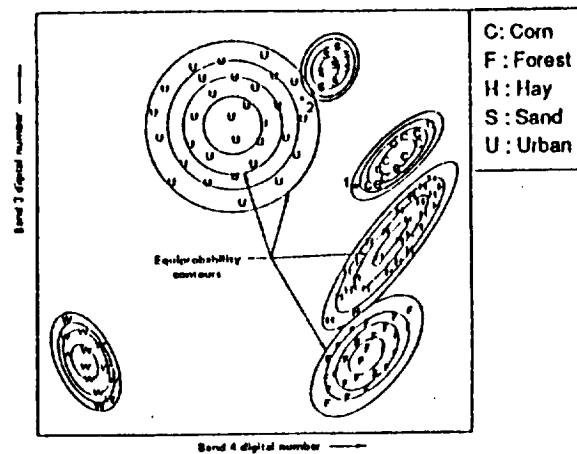


Figure 2. Equiprobability contours defined by a maximum likelihood classifier.
(Source: Lillesand and Kiefer, 1987)

Hybrid Classification

Usually, ground reference data are available for only a portion of the area of an image. It is difficult to select training samples for some areas such as rivers and streams. Therefore, the

types of classification described above have to be used together. In classification, training samples are first chosen for the fields for which ground reference data has been collected. Then clustering is performed for those areas without ground truth data or for which adequate pixels cannot be selected. The clustering groups are labeled and added into the training samples as a whole afterwards. Finally, the image is classified based on the entire training set using the supervised approach. The entire process is called *hybrid classification*. Hybrid classification almost always gives a higher result accuracy than either supervised or unsupervised classification alone.

2.1.3 Remote Sensing Applications in Agriculture

The development of remote sensing started more than twenty years ago. Certainly, there are more than the two applications in agriculture which will be described below. However, what is presented here focuses on applications in crop inventory and soils.

Crop Inventory

Crop inventory has long been recognized as an important application of remote sensing. With the rapidly increasing world demand for food, the value of accurate and timely crop production information is substantial. The wide-area, sequential coverage from Landsat combined with the capabilities of computer processing offers a new opportunity to improve the accuracy, precision and timeliness of crop production estimates.

Quantitative evaluations of computer processed Landsat data show that major crop species can be accurately identified. Comparisons of area estimates from Landsat classifications and conventional surveys agree well, and the Landsat estimates have a very small sampling

error compared with estimates from ground surveys (Colwell, 1983). Current investigations are verifying the applicability of computer-aided analysis of Landsat data for identifying crops and making area estimates over a wide range of environments with differing soils, weather and cultural practices.

In other studies the use of remotely sensed data for determining crop condition and predicting yield is being investigated. The extent and severity of stresses, such as disease and drought, have been determined from remotely sensed data. At this time, remotely sensed data are being used for the prediction of crop yields.

Soils

Soil investigations, soil survey, and soil mapping are three types of applications using remotely sensed data. They include three kinds of studies: the effects of soil properties on reflectance, the influence of soil surface conditions on reflectance, and the use of imagery in soil mapping (Wu, 1988).

The research on the characteristic variations in soil reflectance (Baumgardner and Stoner, 1982) showed five distinct soil spectral reflectance curves (see Table 1 and Figure 3), considering curve shape, the presence or absence of absorption bands, and the predominance of soil organic matter, iron oxide composition and soil moisture. The results are important for the study of spectral reflectance of low residue cover since reflectance is influenced by soil beneath.

Remotely sensed data also were used to monitor conservation tillage practices with an acceptable classification accuracy (DeGloria, 1986) and to estimate the crop rotation (C) values for the USLE (Stephen, 1985). The estimation of crop residues using remotely sensed data will be described in more detail following the next section.

Table 1. Characteristics of surface samples of five mineral soil.

	Reflectance curve form				
	organic dominated (a)	minimally altered (b)	iron affected (c)	organic affected (d)	iron dominated (e)
Soil series	Drummer	Jal	Talbot	Onaway	(not given)
Horizon sampled	Ap	All	Ap	Ap	Allp
Soil subgroup	Typic Haplaquoll	Typic Calciorthid	Typic Hapludalf	Alfic Haplorthod	Typic Haplorthox
Sample location	Champaign Co. IL, USA	Lea Co. NM, USA	Kutherford Co. TN, USA	Delta Co. MI, USA	Londrina, Paraná, Brazil
Climatic zone	humid mesic	semiarid thermic	humid thermic	humid frigid	humid hyperthermic
Parent material	loess over glacial drift	fine textured alluvium or lacustrine	clayey limestone residuum	glacial drift	basalt
Drainage class	poorly drained	well drained	well drained	well drained	excessively drained
Textural class	silty clay loam	loamy fine sand	silty clay loam	fine sandy loam	clay
Moist soil	10YR 2/1	10YR 5/3	7.5YR 4/6	7.5YR 3/2	2.5YR 3/6
Munsell colour	black	brown	strong brown	dark brown	dark red
Contents of:					
Organic matter	5.61%	0.59%	1.84%	3.3%	2.28%
Iron oxide	0.76%	0.03%	3.68%	0.81%	25.6%
Moisture at .1 bar tension	41.1 %	17.0 %	28.2 %	27.3 %	33.1 %

(Source: Baumgardner and Stoner, 1982)

ORIGINAL PAGE IS
OF POOR QUALITY

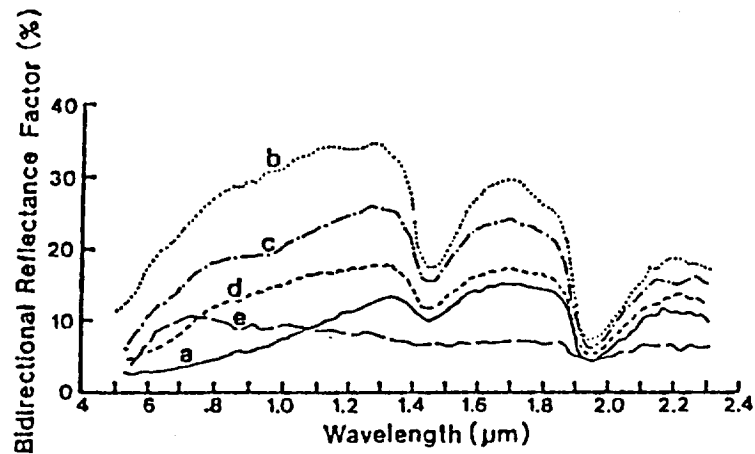


Figure 3. Representative reflectance spectra of surface samples of five mineral soils (Table 1):

- a. organic-dominated (high organic content, moderately fine texture)
- b. minimally altered (low organic, medium iron content)
- c. iron-affected (low organic, medium iron content)
- d. organic-affected (high organic content, moderately coarse texture)
- e. iron-dominated (high iron content, fine texture)

(Source: Baumgardner and Stoner, 1982)

2.2 Neural Networks

Development of neural networks in engineering in recent years has been rapid and surprising, although neural networks have been studied biologically for a couple of decades. Applications of neural networks include pattern recognition, knowledge data bases for stochastic information, optimization computation, robot control and decision making. Neural networks

have been proposed for tasks ranging from battlefield management to minding the baby (Wasserman, 1989). Potential applications are those where intelligent functions are performed effortlessly and conventional computation has proven cumbersome or inadequate.

The following section introduces the concepts of neural networks, back-propagation (which is a widely-used neural network learning algorithm) and classification of remotely sensed data using neural networks.

2.2.1 Neural Network Terminology

Neural networks are brain-like computers. Like all computers, they have hardware and software. What is presented in the following section focuses on their software.

The human brain is the oldest, the most complex, powerful and mystified computer known to man. The brain's powerful thinking, remembering, and problem-solving capabilities have inspired several generations of scientists to attempt computer modeling of its operation. Some scientists have sought a computer model to mimic the functionality of the brain in a very simplified manner, i.e. the study of neural networks.

What is a Neural Network?

A neural network is a computing system that is made up of numerous simple, highly interconnected processing elements which process information in parallel by their dynamic state response to external inputs. This means that the neural network does not execute a series of instructions; it responds, in parallel, to the inputs presented to it. The results are stored in both distributed and associative memory, namely called neural computing memory, after it has reached some equilibrium condition. Neural networks don't "execute programs" as much as

they "behave", given a specific input. Instead, they "react," "self-organize," "learn," and "forget" (Caudill, 1988).

Neural networks can mimic the human brain functionally in that there are different weights for connections which are similar to those on human synapses (Zhuang and Engel, 1990a). This is a key point for neural network applications in many areas.

Neural networks do not work well at precise, numerical computation such as calculating the payroll (Wasserman, 1989). On the other hand, this form of computation is not a natural application for people either. A neural network is an excellent partner to more traditional systems, such as expert systems or simulation. Combined systems will coexist with neural networks performing the tasks for which they are best suited.

The Brain and Neural Networks

The structure of neural networks in contrast with the nervous system will be described. The neuron is the fundamental cellular unit of the nervous system and in particular of the brain. In a neural network, the corresponding unit is a processing element (PE). Figures 4 and 5 illustrate the structures of a neuron and a PE, respectively. The basic components of a neuron and a PE are listed in Table 2.

The human brain consists of tens of billions of densely interconnected neurons. However, a neural network usually is made up of several thousand PEs at most, considering the capability and speed of a computer. They join in a manner similar to that shown in Figure 5. Elements are then organized into a sequence of layers which can be described by matrices with full or random connections between successive layers.

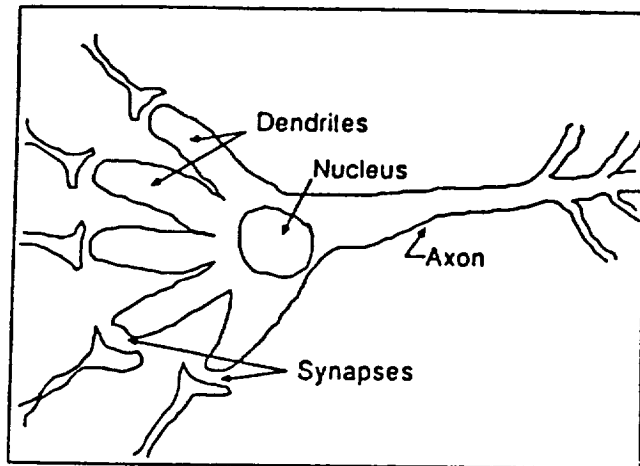


Figure 4. Structure of a neuron.
(Source: NeuralWare, 1989)

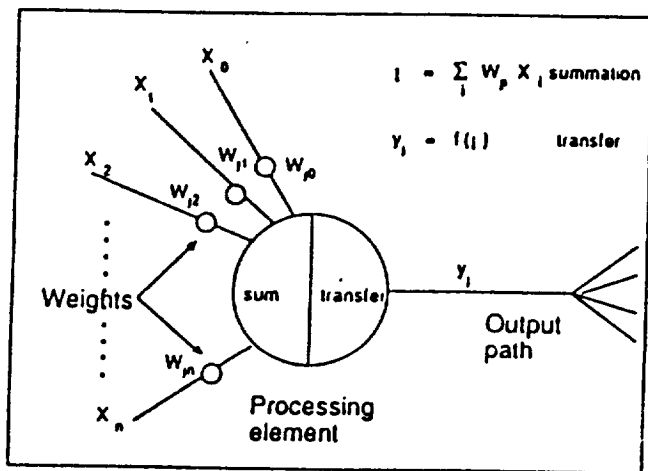


Figure 5. Structure of a processing element.
(Source: NeuralWare, 1989)

Table 2. Neuron and processing element components.

Component Name	Function
Nucleus Sum & Transfer Function	Receives & combines signals from its dendrites. Combines input values and thresholds them.
Dendrite Input Path	Channel from other neurons. Channel from other PEs.
Axon Output path	Passes output signals to other neurons. Passes output signals to other PEs.
Synaptic strength Weight	Amount of signal transferred across synapse* A major parameter of connection

* Synapse : a junction from a neuron to the dendrites of another one.

Neural Network Operation

There are two main phrases in the operation of a neural network — learning and recall (NeuralWare, 1989). *Learning* is the process of self-adjusting the connection weights in response to stimuli presented at the input layer and optionally at the output layer. If a desired output to a given input is shown, the learning is supervised learning; if a desired output is not shown, the learning is unsupervised learning. There is still a third kind of learning falling between supervised and unsupervised learning called reinforcement learning where an external teacher indicates whether the response to an input is good or bad. *Recall* refers to how the network globally processes a stimulus presented at its input layer and creates a response at the output layer.

2.2.2 Historical Perspective

The work of scientists and biologists in the past thirty years has shaped the development of neural networks. The first project in neural computing, *Perceptron* (NeuralWare, 1989), was initiated in 1957 by Frank Rosenblatt at Cornell Aeronautical Lab. Two years later, Bernard Widrow, at Stanford University, contributed a great deal in neural computing with his *adaptive linear element* called *Adaline* (Widrow and Hoff, 1960). James A. Anderson continued his work developing the *linear associator* (NeuralWare, 1989). Can neural networks self-organize? The answer is provided by the *Kohonen model*, proposed by Teuvo Kohonen of the Helsinki Technology University in Finland. *Self-organization* (Kohonen, 1984) means to learn without being given the correct answer for a set of inputs. The neurode wins through competitive learning. This kind of philosophy is called "winner takes all". One of the most complex neural networks ever invented was developed by Stephen Grossberg and Gail Carpenter of the Center for Adaptive Systems at Boston University which is based on *adaptive resonance theory (ART)* (Caudill, 1988). ART networks and algorithms maintain the plasticity required to learn a new pattern, while preventing the modification of patterns that have been learned previously (Wasserman, 1989).

2.2.3 Back-propagation

The most popular, successful and widely used learning algorithm today is back-propagation. To solve a problem with a back-propagation network, you show it training inputs with the desired outputs, namely called I/O pairs, over and over, while the network learns by adjusting its weights on connections. Once it arrives at the desired error, it will have found a set

of weights that produce the correct output for every input, and remembers these weights which will be used to solve the problem.

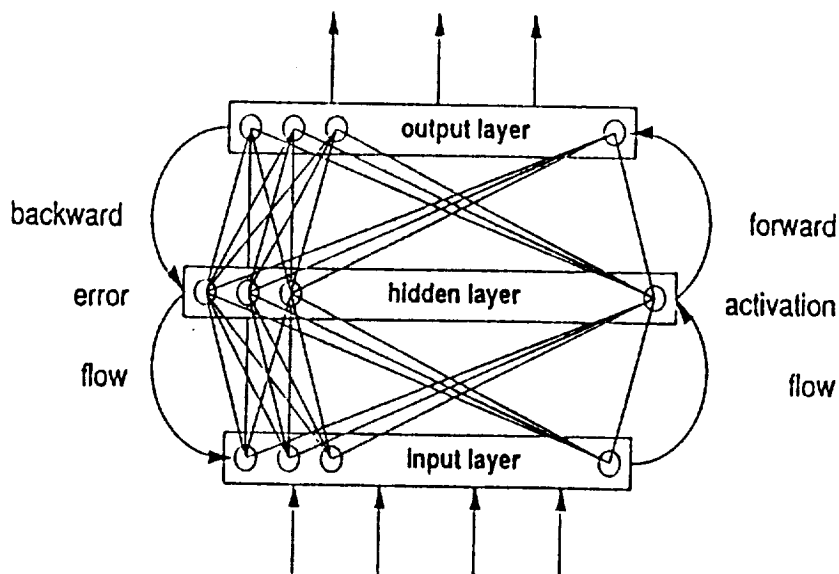


Figure 6. Activation flows forward while errors flow back through the network.

Back-propagation consists of two passes, as shown in Figure 6, which are the forward pass and backward pass. In the forward pass, inputs proceed through the network and generate an output. Then, in the backward pass, the difference between the actual and desired outputs generates an error signal that is propagated back through the network to teach it to come closer to producing the desired output.

The first generation of the back-propagation algorithm was the *Delta rule* or *Least Mean Squared (LMS) rule* (Widrow and Hoff, 1960). The best known network using the Delta rule is called ADALINE which uses the Delta rule to adjust the weights on its input connections to learn to sort input patterns into categories. Another generation of the Delta rule is called the *generalized delta rule* which adjusts the weights on internal units based on the error at the out-

put. It is currently used by most back-propagation neural networks.

2.2.4 Neuro-classification

Although improvements in remote sensing techniques have been made continuously, few of them have had the impact on quality and quantity of classification as has classification using neural networks. Neuro-classification of Landsat data has created a new horizon for remote sensing.

The advantage of neuro-classification over conventional approaches lies in that we do not need to make a distribution assumption about the image data, and can easily combine other than remotely sensed data that may improve the classification accuracy. Neuro-classification is non-parametric. The key point of successful neuro-classification is the representativeness of its training data.

Neural networks have been applied to several types of classification of multispectral remotely sensed data. Neuro-classification, when applied to Landsat MSS data merged with geographic data including elevation, slope, and aspect, was better than conventional classifications (Benediktsson *et al.*, 1990a), and was worse than them when it was employed to very high dimensional data (more than 20 channels) (Benediktsson *et al.*, 1990b). A four-band (bands 1, 2, 3 and 4) Landsat TM image (459 x 368 pixels) with four land-cover classes (water, urban, forest and grass) was classified by Hepner *et al.* (1990). It was concluded that the neural classifier, which used a minimal training set compared with the Maximum Likelihood classifier, performed well for all areas including those for which the conventional approach did not. Decatur's (1989) conclusion concerning his classification of the SAR data (896 x 1024 pixels)

with three classes (urban, park and ocean) was that the neuro-classifier presented better results than the Bayesian classifier when accurate assumptions about probability density functions could not be made and a *priori* probability could not be given. A merged image of AVHRR and SMMR data for an Arctic area was classified by Key *et al.* (1989) using traditional and neural classifiers. They showed that the neural classifier had greater flexibility than the Maximum Likelihood classifier for classifying indistinct classes, for example, classes containing pixels with spectral values that differ significantly from those in the training areas, while ignoring assumptions of statistical normality.

2.3 Estimation of Crop Residues

Crop residue cover estimation is not only useful in planning field operations to maintain erosion control and water quality but is sometimes needed to determine if a particular field qualifies for certain federal, state, or local conservation programs (Hill *et al.*, 1990). It is also useful for determining pesticide and fertilizer application rates.

2.3.1 Traditional Methods for Estimating Crop Residues

Following are five methods for estimating the percentage of crop residue cover in an area. They are the meterstick method, the line-transect method, the photographic method, the scanning microdensitometric method, and the empirical method. The first four are accomplished with field observations; the last requires generalizations and calculations and is used primarily for conservation planning purposes.

Meterstick Method

The meterstick method (Hartwig *et al.*, 1978) involves placing a meterstick on the soil surface perpendicular to the plant row. Beginning at one row and ending at an adjacent row, the total length of residue under the meterstick, along one edge of the meterstick, is measured. The percentage of the total row width covered by residue is the residue cover value. The meterstick method is seldom used now because of the effort required to collect the data.

Line-Transect Method

For the line-transect method (Hill *et al.*, 1989), a commercially available tape or rope, 50 feet long, is stretched diagonally across the crop rows (see Figure 7). The percentage of residue is then determined by counting the number of foot marks that intersect or lie directly over a piece of residue and multiplying by two. At least five measurements at sites typical of the entire field, except in turn-way areas, are taken and averaged to obtain the residue estimate.

The line-transect method is actually a sampling procedure used to estimate the percentage of the length of a line over residue. If used properly, without operator bias, it is an accurate method. However, significant effort is required to collect the residue data.

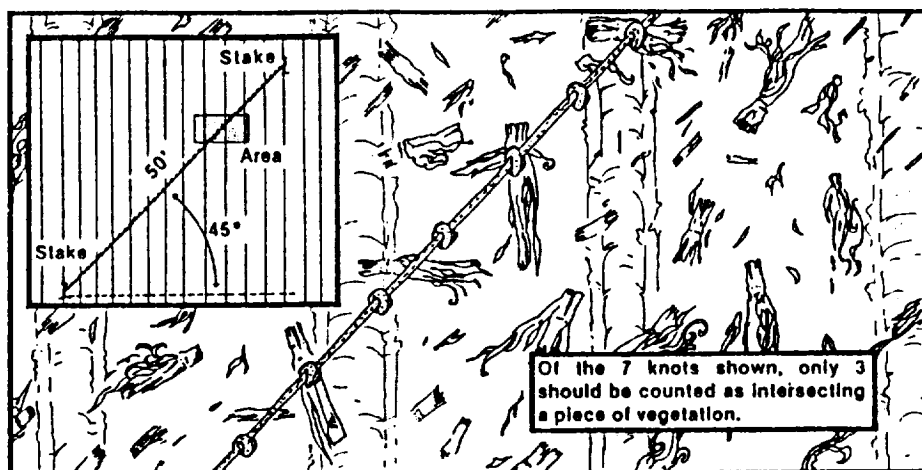


Figure 7. Overview (inset) and close-up of the line-transect method.
(Source: Hill *et al.*, 1989.)

Photographic Method

The photographic method consists of photographing the area between adjacent crop rows from a nearly vertical angle. The slide is then projected on a gridded screen. Residue cover is the percentage of the intersections of the grid over residue. An alternative procedure is to photograph a grid on the ground surface and to determine from the projected slides the percentage of intersections over residue.

The photographic method is also a sampling procedure used to estimate the percentage of an area covered with residue. However, it has a lower accuracy than the line-transect method (Lafren *et al.*, 1981). This method also requires a significant amount of time to collect residue data for large areas.

ORIGINAL PAGE IS
OF POOR QUALITY

Scanning Microdensitometric Method

The scanning microdensitometer assigns digital values to light intensities on a photograph. The device measures density by shining light through film transparencies. The amount of light passing through a transparency depends on the opacity of the image. The darker the image, the less light passes through and the higher the density. The percentage of residue cover is determined by the density (Lowery *et al.*, 1984). The densitometric method produces results with similar accuracies to the three methods discussed above but requires less time and labor.

Empirical Method

This method is different from those described above in that the empirical method calculates the likely percentage of residue cover after weathering and individual tillage operations, rather than requiring field observation (Hill *et al.*, 1989). This method is adequate for long-range conservation planning and for predicting tillage effects on residue cover, although it is less accurate on a year-to-year basis due to variation in weathering and tillage equipment use.

Table 3 shows the ranges in percent of residue remaining after various tillage or planting operations. For a given implement, actual percentage remaining is a result of several factors, including operating speed, operating depth, and soil and residue condition. In the table, the lower end of the percentage ranges should be used for fragile residues like soybeans, while the upper range corresponds to corn residue.

Table 3. Influence of various field operations on surface residue remaining.

Tillage and planting implements	Residue remaining after each operation*
Moldboard plow	3 to 5%
Chisel plow	
Straight points	50 to 80%
Twisted points	30 to 60%
Knife-type fertilizer applicator	50 to 80%
Disk (tandem or offset)	
3" deep	40 to 80%
6" deep	30 to 60%
Field cultivator	50 to 80%
Planter	
Smooth or no coulters	90 to 95%
Narrow ripple coulters (less than 1.5" flutes)	85 to 90%
Wide fluted coulters (greater than 1.5" flutes)	80 to 85%
Sweeps or double disk furrowers (till-plant)	60 to 80%
Drills	
Disk openers	90 to 95%
Hoe openers	50 to 80%
Winter weathering	75 to 85%

* Use higher values for corn residue and lower values for fragile residue, such as from soybeans.

(Source: Hill *et al.*, 1989.)

For an estimate of residue remaining after planting, a multiplication of initial crop cover (approximately 95% for 120-bu corn, 85% for 38-bu. soybeans), winter weathering loss, and the appropriate percentage for each operation that makes up a tillage-planting system is performed. The empirical method provides only rough estimates since the variables involved prevent accurate determination of residue cover. However, Table 3 can be helpful in comparing tillage systems because it empirically gives the residue data remaining after specific tillage and planting operations.

2.3.2 Estimation of Crop Residues Using Remotely Sensed Data

Remotely sensed data, which refers to aerial photographs and satellite images, have advantages in the range of cover and topographic conditions for which it is applicable compared to the conventional methods for determining residue cover. This method could also substantially reduce the field time needed to ensure compliance of agricultural conservation practices in the U.S. Department of Agriculture cost-sharing programs (Whiting *et al.*, 1987).

Compared to an aerial photograph, a satellite scene is less expensive on an area basis, less disturbed, and larger in the area of cover, and thus, the estimation of residue cover using satellite images is of interest for large areas and will be discussed further.

Using this method, the training and testing fields corresponding to sound ground truth within the area of coverage are first selected. The ground truth of residue cover on the area can be collected using one of the methods described in the previous sections or be calculated by the empirical method according to information on crop yields, weathering, tillage and planting. Then based on the satisfactory classification of these fields, the satellite image corresponding to the entire area of interest can be classified to determine crop residues for the entire area.

The project that estimated crop residues in Seneca County, Ohio using Landsat TM data showed that if sound ground truth could be obtained, determining crop residues using satellite data could be a fast and cost effective way of monitoring tillage (Olsen, 1986). However, improvements in the classification process and accuracy of results are needed.

3. MATERIALS AND METHODS

3.1 Site Description

A study area of approximately 2.56×10^3 acres was included in this research. It was composed of sections 3, 4, 9 and 10 located in T28N, R5E Richland township of Miami County, Indiana. The four sections' land uses included corn, soybeans, grasslands, forest, roads, an abandoned railroad, farmsteads and the Eel River. Portions of the area are owned by 58 farmers (see Figure 8). This area is representative of much of northern Indiana and other Midwestern U.S. states.

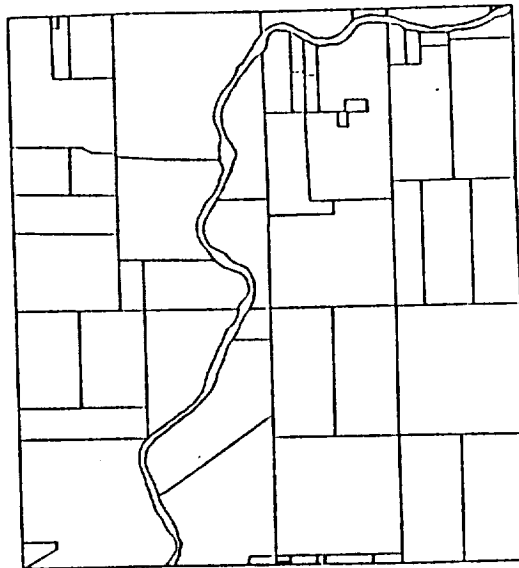


Figure 8. Ownership boundaries for sections 3, 4, 9 and 10.

3.2 Data Sources

The following were the data sources utilized in this study:

1. Ground cover survey data for section 9 for years 1986, 1987 and 1988.
2. Landsat thematic mapper data for March 23, 1987, and April 26, 1988.
3. Copies of airphoto mosaics for Miami County, T28N, R5E Richland township, sections 3, 4, 9 and 10, 1987, approximate scale: 1:24,000.
4. USGS (U.S. Geological Survey) topographic map (Roann, Indiana Quadrangle), 1:24,000.
5. Digitized ownership map, scale: 1:24,000.

Since the latest Landsat TM data were not provided by NASA for this study, the corresponding ground truth data had to be collected through a survey which will be described in the following section. Theoretically speaking, ground truth data should be collected at the same time as the satellite crosses the area of interest.

3.3 Ground Truth Data

Since the ground truth data could not be collected directly from the fields for the dates corresponding to the Landsat data (March 23, 1987 and April 26, 1988), estimates of crop residues were obtained through a survey. Ground truth data accompanying the corresponding

copies of the flown aerial photographs of the area were provided by Jack Hart of the Cooperative Extension Service office of Miami County, Indiana in the form shown in Figure 9. They contain the information about ownership, field number, acreage, crop type, tillage-planting systems used, date of Fall or Spring tillage, date of planting, date of harvest, and soil management. All survey data are listed in Appendix A. The copies of the flown aerial photographs are listed in Appendix B. Crop yields were obtained in the form of average values from the Extension office and are listed in Table 4.

Table 4. Crop yields including residue cover after harvesting for Miami County, Indiana.

Year	Corn (bu/%)	Soybeans (bu/%)	Wheat (bu)	Oats (bu)	Hay (tons)
1986	124 / 98%*	38 / 85%	44	79	3.1
1987	137 / 100%	44 / 98%	62	73	3.7
1988	80 / 63%	28 / 63%	48	44	1.7

CROPPING HISTORY FOR FARMS IN SECTIONS SELECTED
FOR NASA SATELLITE RESEARCH PROJECT
SOIL MANAGEMENT PHASE

Farmer's (or operator's) name: LESTER & DORIS RAY

Farm location: SECTION 9/28N/5E SOUTHEAST 1/4
Rd 800N WEST OF 600E

Cropping year (1986 - (1987) - 1988) Circle one
-- Fill out one sheet for each year --

Field Number:	1	2	3	4
No. of Acres:	44	22.2	12.5	8.2
Crop:	Soybeans	Soybeans	Soybeans	Soybeans
Primary Tillage System Used: (check)				
No-Till				
Ridge Till				
Chisel Straight or Twisted Pts:	✓	✓	✓	✓
MB Plow				
Disk 3 or 8 inches				
Planter has Smooth or no coulters:	✓	✓	✓	✓
Narrow Ripple Coulters (<1.5")				
Date of Fall or Spring tillage:	APR 87	MAY 87	APR 87	APR 87
Date of Planting:	MAY 20	MAY 20	MAY 20	MAY 20
Date of Harvest:	OCT	OCT	OCT	OCT
Soil Mgt. Practices: (Answer yes No)				
Terraces:	NO	NO	NO	NO
Contours:	NO	NO	NO	NO
Strip Crop:	NO	NO	NO	NO
Tile Drained:	NO	NO	NO	NO
Irrigation:	NO	NO	NO	NO
If Crop was CRP or Set-aside What was Seeded?				

Figure 9. A sample of survey data form.

ORIGINAL PAGE IS
OF POOR QUALITY

Residue cover percentage (*i.e.* ground truth data) was calculated by the following formula (Hill, 1989):

$$R = I \times W \times T \times P \quad [3.1]$$

where

R is the residue cover percentage,

I is initial crop residue cover related to yields (given in Table 4),

W is the winter weathering loss (if not Fall moldboard plowed): 85% for corn and 75% for soybeans.

T is the tillage operation(s) factor given in Table 3.

P is the planting operation factor given in Table 3.

The residue cover results are for the Spring after harvesting the crop. However, there were no satellite data in agreement with the exact time for which residue data were available, and the crops of corn, soybeans and wheat were planted at different times. Therefore, besides the residue cover after the spring planting, the residue cover percentage coinciding with each satellite crossing date was also computed and listed in Tables 5 and 6.

As shown in each table, all information related to field number, acreage, crop type, tillage-planting practices, harvesting time and crop yield were preprocessed and listed. The last two columns in the tables refer to residue percentages: the first one corresponding to residue cover after the next spring planting, and the second corresponding to residue cover on the satellite crossing date of that year (March 23, 1987 or April 26, 1988).

Sample #	Field #	Acres #	Crop/Yields	Weather	MB Plow/Date	Chisel/Date	Disk/Date	Planter/Plan/Date	Residue%	Mar 23, 1987/TM
A-01	1	21.5	Fallow							
B-01	1	60	Pasture							
C-01	7	57	100.00% Corn/124			Twisted/Oct22 60.00%				
D-01	7	13	98.00% Corn/124	85.00%	Yes/Apr.			Smooth//Apr25 95.00%	47.48%	50.00%
D-02	11	6.4	98.00% Soybeans/38	85.00%	3.00%			Smooth/Soybeans/May.	2.50%	83.00%
D-03	11A&11B	26	85.00% Soybeans/38	75.00%			37/Apr. 40.00%	Smooth/ACR/May 90.00%	22.95%	64.00%
D-04	12	27	85.00% Alfalfa	75.00%	Yes/May		37/Apr. 40.00%	Smooth/May20 90.00% /May	22.95%	64.00%
E-01	1A	10	100.00% ACR							
E-02	1B	131.8	100.00% Corn/124							
E-03	2A	6.9	98.00% Corn/124	85.00%		Twisted/Oct28 60.00%		Ripple//Apr25 90.00%	44.98%	50.00%
E-04	2B	26.6	98.00% ACR	85.00%		Twisted/Oct28 60.00%		Ripple//Apr25 90.00%	44.98%	50.00%
F-01	1	44	100.00% Soybeans/38							
F-02	2	22.2	85.00% Soybeans/38	75.00%		Twisted/Apr. 30.00%		Smooth/May20 90.00%	19.51%	64.00%
F-03	3	12.5	85.00% Soybeans/38	75.00%		Twisted/Apr. 30.00%		Smooth/May20 90.00%	19.51%	64.00%
F-04	4	8.2	85.00% Soybeans/38	75.00%		Twisted/Apr. 30.00%		Smooth/May20 90.00%	19.51%	64.00%

Table 5. Residue cover percentage from ground truth data in section 9, 1986.

Sample #	Field #	Acre #	Crop/Yields Fallow	Weather	MB Plow/Date	Chisel/Date	Disk/Date	Planter/Plant/Date	Residue %	Apr. 26, 1988/TM
A-01	1	21.5								
B-01	1	60	Pasture 100.00%							
C-01	7	57	Corn/137 100.00%	85.00%		Twisted/Nov04 60.00%				
D-01	7	13	Soybeans/44 98.00%	75.00%				Smooth//Apr30 95.00%	48.45%	51.00%
D-02	11	6.4	ACR					3*/May10 40.00%	26.46%	74.00%
D-03	11A&11B	26	Soybeans/44 100.00%					3*/May10 40.00%		
D-04	12	27	Hay/3.7 tons 100.00%	75.00%	Yes/May10 3.00%			Smooth//May10 90.00%	26.46%	74.00%
E-01	1A	10	ACR					/Alfalfa.Hay		
E-02	1B	131.8	100.00%							
E-03	2A	6.9	Corn/137 100.00%	85.00%		Twisted/Nov01-Apr15 60.00%				
E-04	2B	26.6	100.00%	85.00%		Twisted/Nov01 60.00%			51.00%	51.00%
F-01	1	44	100.00%							
F-02	2	22.2	Soybeans 98.00%	75.00%				3*/Apr. 40%	29.40%	74.00%
F-03	3	12.5	Soybeans 98.00%	75.00%				3*/Apr. 40.00%	29.40%	74.00%
F-04	4	8.2	Soybeans 98.00%	75.00%				3*/Apr. 40.00%	29.40%	74.00%

Table 6. Residue cover percentage from ground truth data in section 9, 1987.

3.4 Neural Network Classifier

The learning algorithm used for the neural network classifier, *back-propagation*; the neural network configurations used for classifications of original, transformed, and generated images; the neural network software package used in this study; and its interface routines will be discussed in detail in the following sections.

3.4.1 Neuro-classifier Algorithm: Back-propagation

The three-layer back-propagation system used by the classifiers previously shown in Figure 6 will be described. Its result can be extended to systems with more than three layers by induction. A t -D input vector v shown in Figure 10, for which every component denotes a unit (neurode or node) in the input layer, is first multiplied by the matrix N , which is a $s \times t$ matrix and illustrates the connection between the input layer and the hidden layer, to produce a s -D vector z for the set of hidden units:

$$z = Nv, \quad [3.2]$$

and then z is multiplied by M , which is a $r \times s$ matrix and illustrates the connection between the hidden layer and the output layer, to produce a r -D output vector u :

$$u = Mz. \quad [3.3]$$

in which its every component denotes a unit in the output layer. Substituting Nv for z yields the response for the composite system:

$$\mathbf{u} = \mathbf{M}(\mathbf{N}\mathbf{v}). \quad [3.4]$$

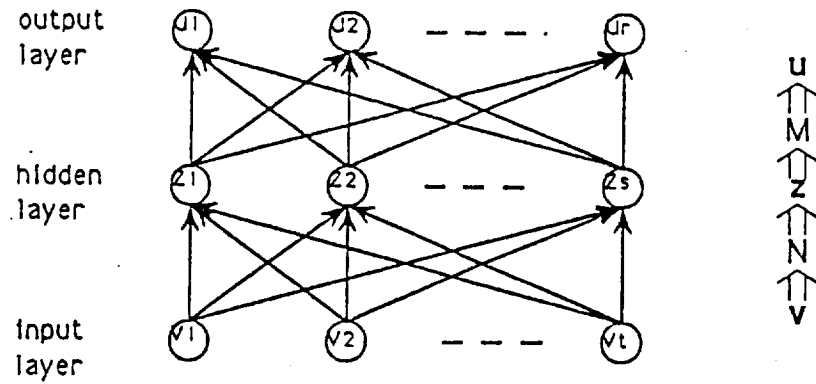


Figure 10. Network structure of a three-layer back-propagation system.

This equation relates the input vector \mathbf{v} to the output vector \mathbf{u} . Substituting \mathbf{W} for $(\mathbf{M}\mathbf{N})$, the equation becomes:

$$\mathbf{u} = \mathbf{M}(\mathbf{N}\mathbf{v}) = (\mathbf{M}\mathbf{N})\mathbf{v} = \mathbf{W}\mathbf{v}. \quad [3.5]$$

The i, j th element of \mathbf{W} is the inner product of the i th row of \mathbf{M} with the j th column of \mathbf{N} . Note that matrix multiplication is not commutative. Figure 11 shows a matrix-mapping structure of the three-layer back-propagation system. Therefore, there will be k transform matrices for a $k+1$ layered system; the number of transform matrices in a specific system equals the number of layers minus one, that is:

$$W = N_k \dots N_2 N_1. \quad [3.6]$$

Here, N_i refers to the connection between the i th layer and the $i+1$ th layer in one system. Note that the *order* of multiplication is important. The matrix denoting the connection with the successive layer must be premultiplied each time.

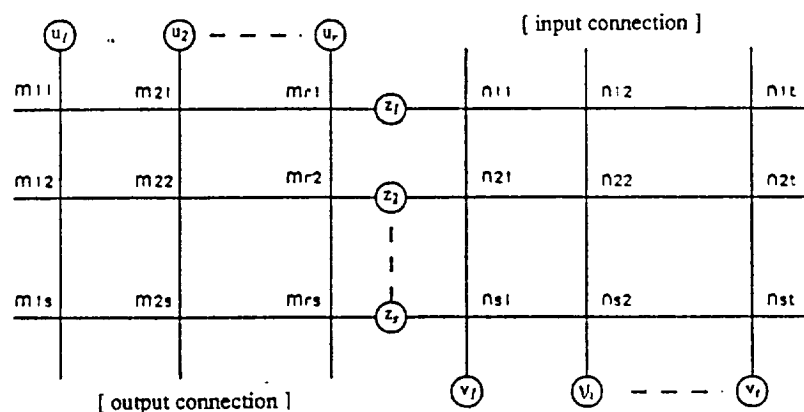


Figure 11. Matrix-mapping structure of the three-layer back-propagation system.
 $n_{i,j}$: an entry of matrix N
 $m_{i,j}$: an entry of matrix M

In matrix notation the back-propagation algorithm can be written as:

$$W(n+1) = W(n) + \eta \delta(n) v^T(n) + \alpha (W(n) - W(n-1)) \quad [3.7]$$

$$n = 1, 2, \dots$$

where $W(n)$ is the state of the connection matrix after n presentations, $v(n)$ is the input presented on the n th presentation, η is the learning constant which is a scalar constant referring to learning speed, α is the momentum constant which is a scalar and determines the effects of

past weights on the convergence in weight space, and $\delta(n)$ is the difference between the desired and actual output on trial n , such that

$$\delta(n) = t(n) - W(n-1)v(n) \quad [3.8]$$

where $t(n)$ is the desired output for presentation n and $W(n-1)v(n) = u(n)$ is the output actually produced on that presentation. $W(0)$ is assumed to be an identity matrix.

3.4.2 Neural Networks for Classification

Based on research previously done in neuro-classification of satellite image data, the three-layer back-propagation scheme was employed for the neural networks used in this study. The data preprocessing methods for neural networks including coding and connections are described in this section.

Decimal coding was tested for the input layer, but the neural training did not converge. This was most likely because the normalization of this coding diminished the feature of each input unit rather than increasing it. If the normalization was not performed, the unit value range was too great (256 levels) to learn for the neural network. Therefore, a two dimensional array of units with binary coding was used for the input layer. Because 8-bit Landsat TM data was used, each of the eight units of a column in the input layer referred to one bit and each of the units in a row represented one spectral channel. Therefore, the two dimensional array was seven units in row length by eight units in column length (i.e. 7×8 units) for Landsat TM data. Since each image had different spectral features, each neural network had its own representation for the hidden layer.

Thermometer coding was adopted for the output layer. Units in this layer were designed in one dimension, and the number of its units equals the number of spectral classes. For example, class 5 out of 10 possible categories would be represented as 1 in the first five nodes and 0 in the remaining five nodes (e.g. $5 = 1\ 1\ 1\ 1\ 1\ 0\ 0\ 0\ 0\ 0$).

The full connection was applied to the linkages of layers *input* to *hidden* and layers *hidden* to *output*. This indicates that each unit in a layer was connected with every unit in adjacent layers. There were no connections between nodes located in a common layer. Although this type of connection takes a lot of memory and computation, it makes the design of the network simple, the weight-adjustment easy, and the training able to be monitored and adjusted.

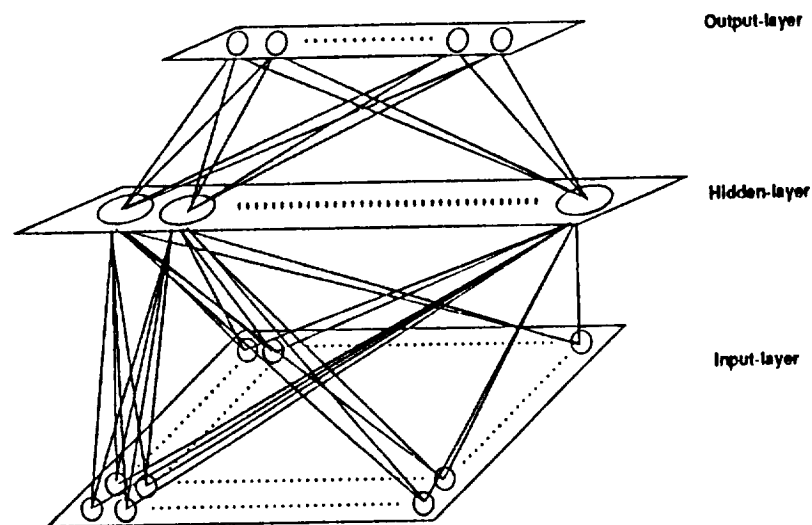


Figure 12. Three-layer back-propagation neural network.

3.4.3 Neural Network Configurations

The three-layer back-propagation configuration for the neural network classification was used, as shown in Figure 12. Representations for each input layer, hidden layer, and output layer for all neural networks used are listed in Table 7. As seen in Table 7, there are seven images listed. In addition to the two original Landsat TM images (March 23, 1987 and April 26, 1988), there were another five images which were transformed and generated from the original images. They will be defined in later sections. The determination of representations for each input layer was based on the definition in the last section. The representations for each hidden layer were initialized with thirty units. After initial training, they were changed to arrive at the values shown in Table 7. The rule for changing the initial number of units in a hidden layer was based on the two monitoring parameters set up in NASA NETS. They are the Max and RMS errors. A Max error was the maximum among the differences between each actual output and desired output on the output layer, whereas a RMS error referred to the root mean square of the differences. If Max and RMS errors decreased very slow or did not decrease, increasing the number of hidden layer units was required; if Max errors decreased during 25 or 30 cycles, and then went up again and stayed at a very high error value, decreasing the number of hidden layer units was required. The reason for assigning seven units for every output layer will be discussed in a later section as will information class creation.

Table 7. Representations for the neural network classifiers.

Image description	Input layer (units)	Hidden layer (units)	Output layer (units)
Landsat TM data March 23, 1987	7 × 8 array	35	7
PC ^a transformed data March 23, 1987	7 × 8 array	25	7
Landsat TM data April 26, 1988	7 × 8 array	35	7
PC ^a transformed data April 26, 1988	7 × 8 array	35	7
SR ^b transformed data March 23, 1987	7 × 8 array	21	7
Landsat TM Plus ^c data March 23, 1987	8 × 8 array	35	7
Landsat TM Plus ^c data April 26, 1988	8 × 8 array	35	7

^aPrincipal components.

^bSpectral ratioing.

^cGIS-enhanced Landsat TM data.

3.4.4 NASA NETS 2.0

The neural network simulator tool used was NASA NETS (Baffes, 1989). It can be run on a variety of machines including SUN workstations and PCs. The simulator's primary functions are twofold: 1) to provide a flexible system for manipulating a variety of neural network configurations using the *generalized delta back propagation* learning algorithm; and 2) to provide the general user community a means for learning about neural network technology without the need for specialized hardware (Baffes, 1989). The NETS software used for image classification was run on SUN SPARC workstations.

The interface routines, including those for converting an ERDAS BIL file (ERDAS, 1988) to an ASCII file, subsetting an image, encoding and decoding an image as required by

NETS, and computing classification accuracy, were written to make it possible for NETS to be used for image classification. NETS was incorporated with MacLARSYS* allowing it to be utilized more effectively because MacLARSYS provides a *LIST* function that can list training and testing data or a portion of or an entire image in ASCII format. The results of classification can be easily imported back into MacLARSYS for display. These routines for interfacing NETS with MacLARSYS are listed in Appendix C.

3.5 Method for Estimating Residue Percentage

3.5.1 Preprocessing of Data

Although both TM data sets were collected in early Spring (March 23, 1987 and April 26, 1988), there were differences among them. In March, the weather is still cool, tillage-planting practices have not yet started and there are no or few leaves growing on plants. In contrast, the weather has changed significantly in late April, some fields have been tilled and planted, and young leaves are growing on trees. The spectral response patterns were different in each of the seven Landsat TM wavelength bands for the images, but the tendency of reflectance changes followed a similar pattern. The spectral ranges for different wavelengths of all seven Landsat TM bands are listed in Table 8. The color composition of band 4 (near infrared) for red, band 3 (red) for green, and band 5 (middle infrared) for blue was adopted for the data sets to enhance

* MacLARSYS is an image processing software package running on the Macintosh computer and has been developing by the Laboratory for Application of Remote Sensing (LARS) at Purdue University, West Lafayette, Indiana.

the visualization of crop residue classes when the image was displayed.

Table 8. The characteristics of Landsat TM data.

Band	Wavelength (μm)	Nominal spectral location	Spatial resolution (m)
1	0.45 - 0.52	Blue	30
2	0.52 - 0.60	Green	30
3	0.63 - 0.69	Red	30
4	0.76 - 0.90	Near-infrared	30
5	1.55 - 1.75	Mid-infrared	30
6 ^a	2.08 - 2.35	Mid-infrared	30
7 ^a	10.4 - 12.5	Thermal infrared	120

^aBands 6 and 7 were switched when the original TM images were down-loaded from tape.

Information Class Creation

According to the ground truth data, there were water, trees, bare soil (fallow), crop residues, and five types of pasture/grass including red clover, alfalfa, oats, CRP¹ and ACR². Since the focus of this research was on crop residues, the decision-making tree analysis method of systems engineering was adopted to construct the decision-making tree of the information classes. In order to look at how many branches, nodes, and leaves existed for the tree, a top-down analysis was applied to the ground truth data. Two hierarchical decision trees of the information classes resulted as shown in Figures 13 and 14 corresponding to the two TM data sets. Then a bottom-up analysis was employed to produce the information classes from each tree. Consequently, two sets of training classes were generated with seven training classes each as listed in Figures 13 and 14. Therefore, there would be seven units in an output layer of each neural network used for classification.

1 Conservation Reserve Program which could refer to weeds or grasses.

2 Agriculture Crop Reserve which could refer to different types of grasses.

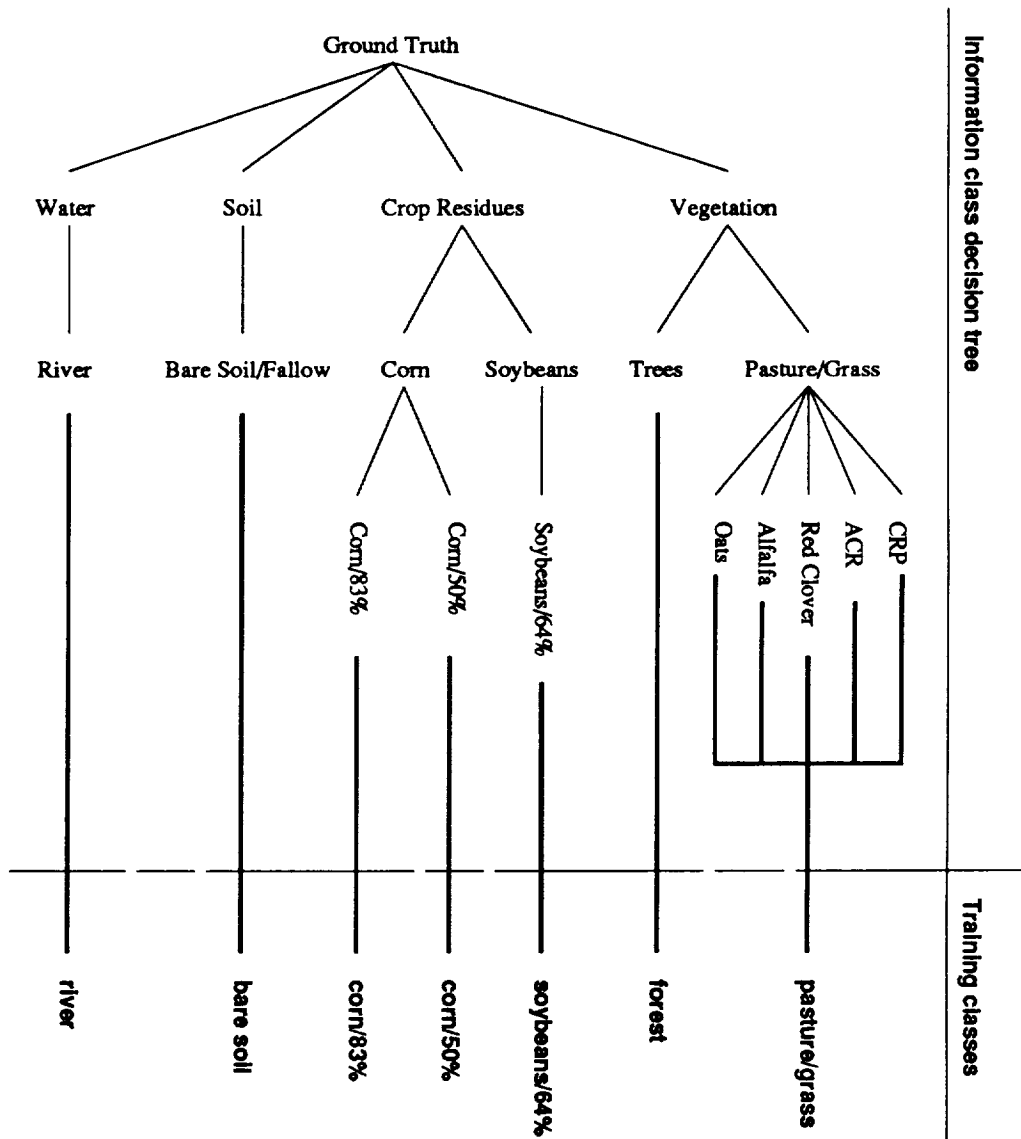


Figure 13. Creation of the information classes for 1987.

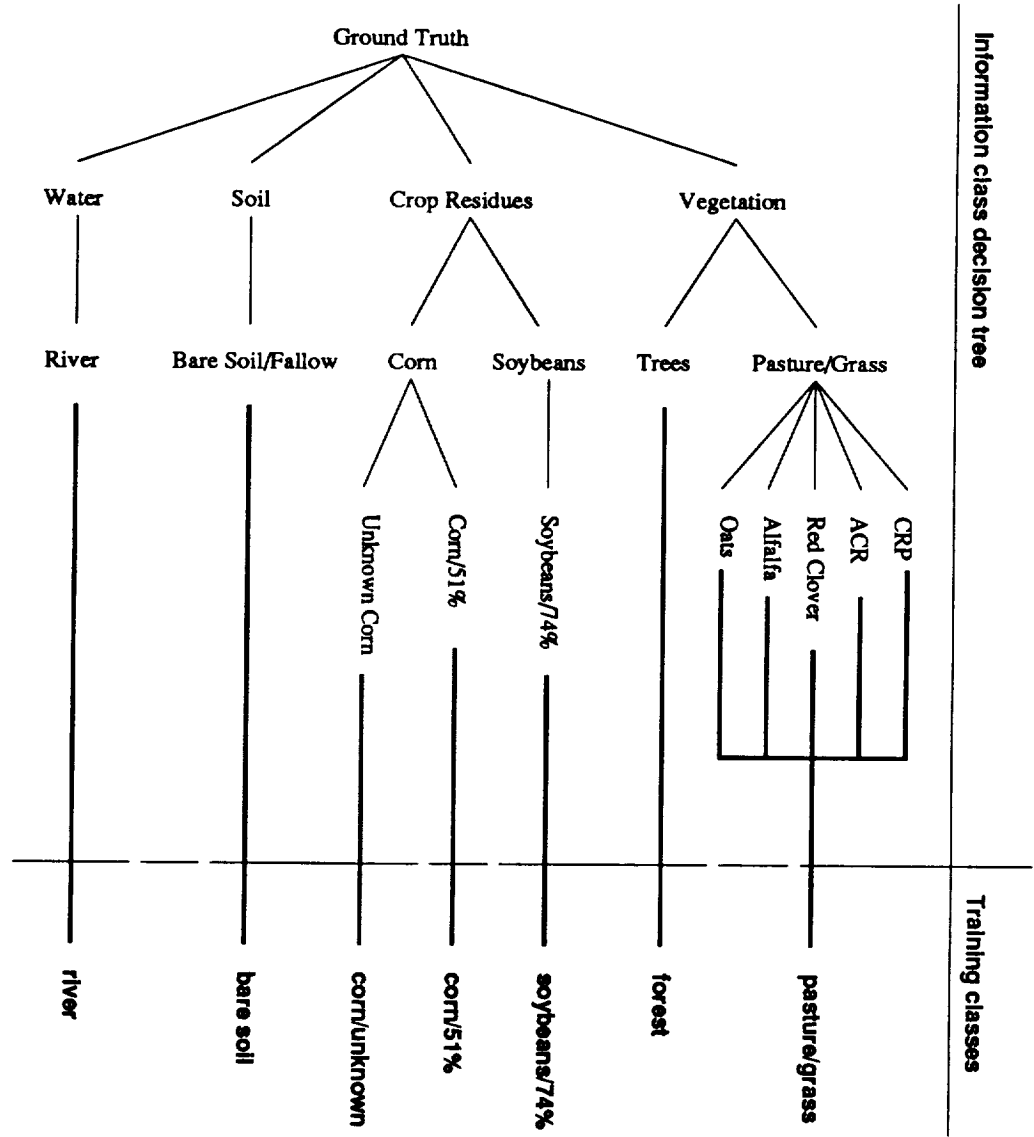


Figure 14. Creation of the information classes for 1988.

Principal Components

Principal components transformation was performed to enhance images with maximum contrast and to make images visually more interpretable. Although principal components transformation does not enhance separability for the traditional classification techniques as reviewed earlier, it was employed to investigate whether neural network classification techniques perform differently after such a transformation. A neural classifier treated the transformed data, which was uncorrelated after transformation in the multispectral vector space, as a new image and determined the features from the transformed training data.

Principal components transformation was applied to the two Landsat TM data sets. Considering the awareness of the lower-order principal components reviewed earlier and the configuration of the neural networks, all seven components were utilized in this study.

Spectral Ratioing

As reviewed in Chapter 2, an enhanced image can be generated from the division of digital values in one spectral band by the corresponding values in another band. These ratios clearly portray the variations in the slopes of the spectral reflectance curves between the two bands involved.

In this research, the difference between crop residues and bare soil was greater in band 5 than in band 6 for March data. Therefore, spectral ratioing was applied for crop residue discrimination. The function of this computing procedure was a modification of the *Normalized Difference Vegetation Index (NDVI)* (Mather, 1987). It can be called the *Normalized Difference Residue Index (NDRI)* and was defined as:

$$\text{NDRI} = \frac{X_5 - X_6}{X_5 + X_6} \times 255. \quad [3.9]$$

The symbols X_5 and X_6 refer to the values of Landsat TM bands 5 and 6, respectively. The transformed data were used to replace the thermal infrared band of data (band 7) for the March 23, 1987 scene.

3.5.2 Classification Using Traditional Methods

With the aid of displaying an image given the color composition defined previously, training fields were selected interactively for section 9. In addition to portions of known fields, extra training data were chosen from the other three sections (sections 3, 4 and 10) based on the spectral features of fields. The training data for class *river* were obtained by statistical clustering.

Two traditional methods, Maximum Likelihood and L1 Minimum Distance (reviewed in Chapter 2), were used to classify images. The same procedure was applied to all image data.

3.5.3 Classification Using Neural Networks

Neural network training was different from the training approach for traditional classification. However, the training data sets were the same in both cases to allow comparisons of classification results. The training data sets used for traditional methods were first exported from MacLARSYS. Then the digital values corresponding to each training field were binary-coded, the class numbers matching each training field were thermometer-coded, and they were

coupled as input-output pairs to be used as inputs for the training of the neural network classifier.

3.5.4 Classification with the Aid of a GIS Layer

Motivated by the successful classification of Landsat MSS data merged with geographic data (Benediktsson *et al.*, 1990a) and the performance of neural networks integrated with GIS (Arnold *et al.*, 1990), a GIS layer was incorporated into the neuro-classification technique. The GIS layer was the ownership map associated with the four sections studied. It was digitized using ERDAS and then added as an eighth band to the original Landsat TM image data, as illustrated in Figure 15. The eight-band merged data were called *Landsat TM Plus*.

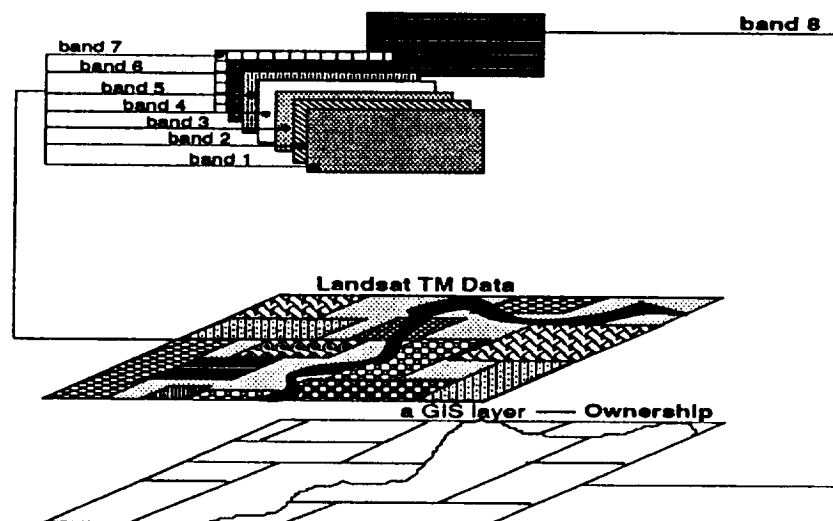


Figure 15. Creation of Landsat TM Plus data.

The reasons of choosing the ownership layer were that a) the boundaries representing different owners matched training field boundaries, b) an enclosed region stood for one owner, c) one area was coded with a digital number (i.e. there existed the same reflectance inside one area), and d) the classification results may be improved because of the unique digital number inside a polygon.

For these types of data, Maximum Likelihood sometimes does not work because one spectral class may only exist inside one region. This means that the class exhibits the same digital value in the eighth band and thereby there is no variance in the band. Consequently, elements related to this band in the corresponding covariance matrix are zero and the determinant for the covariance matrix is zero. Therefore, the covariance matrix cannot be inverted and thereby Maximum Likelihood classification cannot be performed in this case. However, this is not a problem for a neural classifier because it does not address the second order statistic, *variance*. Minimum Distance can also be applied to the classification of these types of data because it considers only the first order statistic, *mean*.

Neural networks and L1 Minimum Distance were used for the classifications of this merged eight-band data. All procedures involved were similar to those adopted in the classifications of seven-band data.

4. RESULTS AND DISCUSSION

4.1 Spectral Behavior of Crop Residues

Crop residue cover changes as a result of the season's changing from Winter to Spring, *i.e.*, the temperature goes up and earth becomes defrosted in that time period. In Indiana, planting usually starts in April. Reflectance differences between crop residues and other biomass and a river were included in this study. Spectral variations caused by the changing season are discussed in the following sections.

4.1.1 Discrimination of Crop Residue Cover in March, 1987

Figure 16 shows the spectral curves for the selected six-band Landsat TM data* of March 23, 1987, which were plotted based on the training class means in each of the six wavelength bands. Each of them corresponds to one category in the study sections. There are three curves indicating crop residues which are classes *corn/50%*, *corn/83%* and *soybeans/64%*. These crop residue classes were previously generated from the corresponding ground truth data.

* Band 7, thermal infrared band, is not included in Figure 16 because of its 120m resolution.

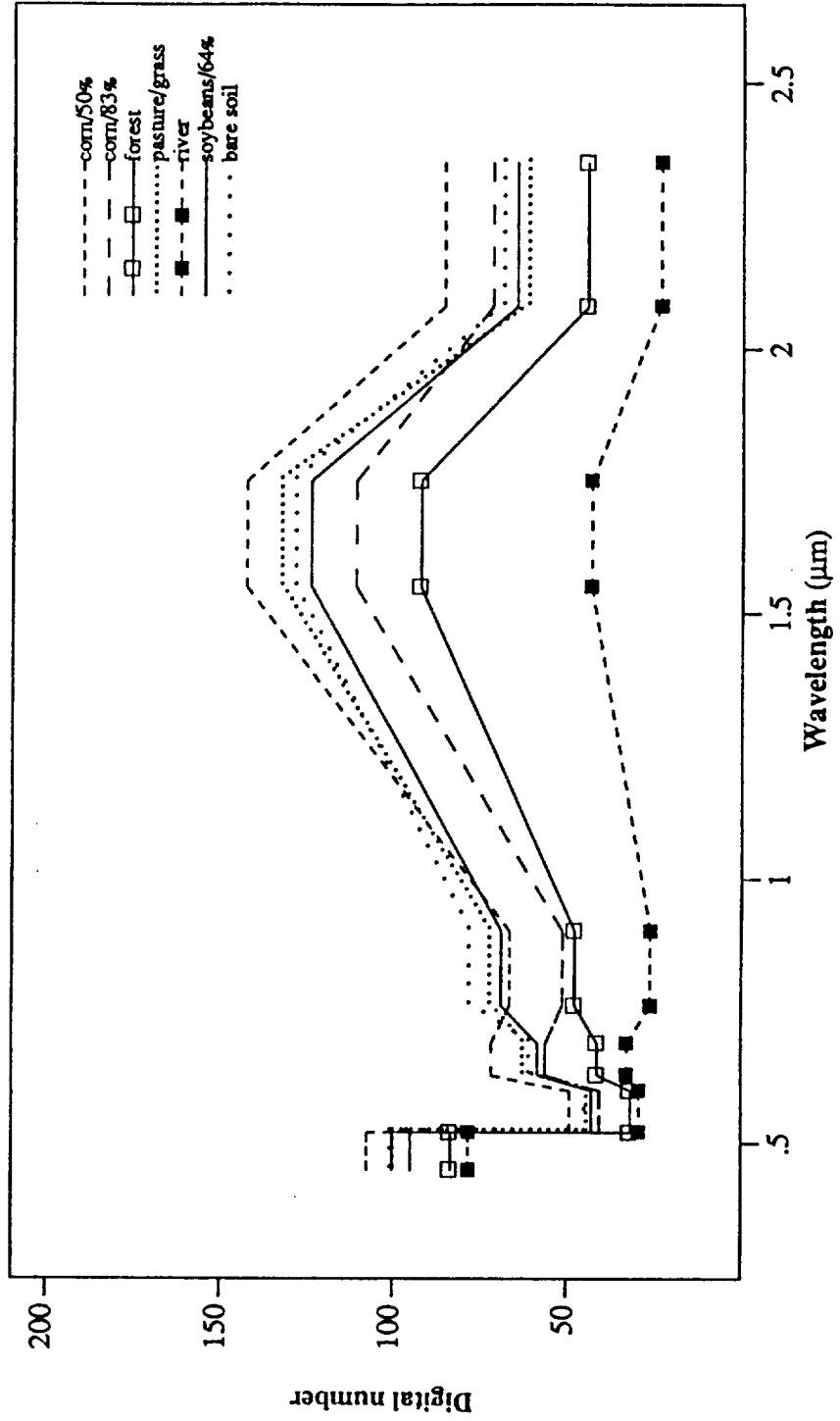


Figure 16. Reflectance curves for the training data of March 23, 1987.

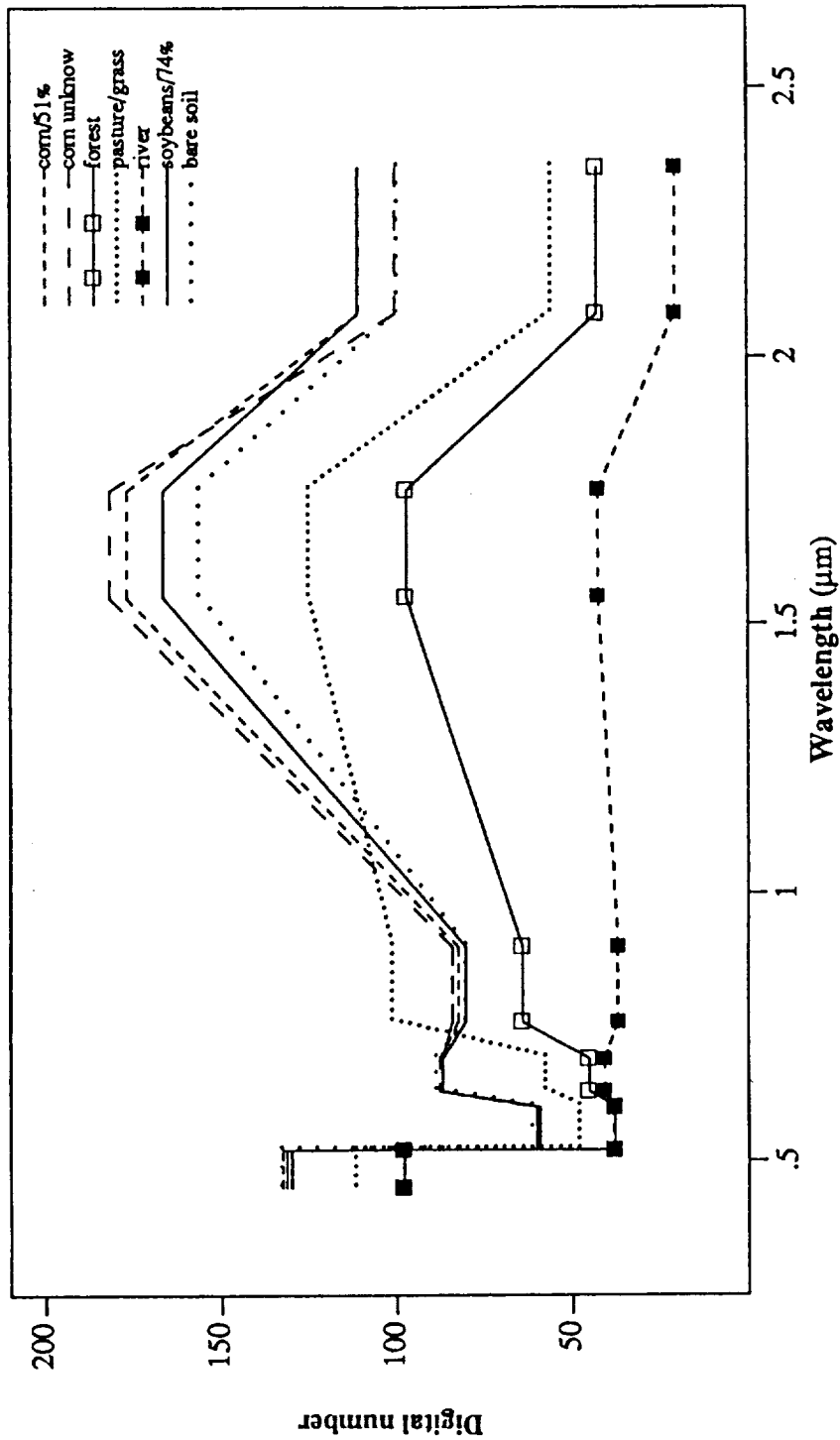


Figure 17. Reflectance curves for the training data of April 26, 1988.

It can be seen in Figure 16 that both intra-discrimination of crop residues, including inside one category like *corn*, and inter-discrimination of biomass categories were distinguishable, especially in the first middle infrared wavelength, 1.55 to 1.75 μm . Class *corn/50%* had the highest reflectance in this wavelength because it held less moisture than any other class. Class *river* had the lowest reflectance in every band as water should exhibit. Classes *corn/83%* and *soybeans/64%* ranked in the middle but the former had a smaller digital number than the latter in the middle infrared wavelength. Class *forest* showed the second lowest reflectance in every band because leaves were not on trees at that time. Classes *pasture/grass* and *bare soil* had lower reflectance values than class *corn/50%* and higher reflectance than any other class, probably because they were moderately dry.

Moreover, class *corn/50%* had higher reflectance in every wavelength band than class *corn/83%*. The reason is that class *corn/50%* has a lower density than class *corn/83%*, and thus, it has less moisture content and absorbs less electromagnetic energy. In other words, class *corn/50%* radiates more energy than class *corn/83%*. Therefore, it can be concluded that the lower the residue percentage, the higher the reflectance and the greater the digital number. This is similar to soil spectral characteristics changing along with moisture content as reviewed previously.

4.1.2 Discrimination of Crop Residue Cover in April, 1988

The spectral characteristics of the crop residues and bare soil had changed markedly in April as seen in Figure 17. All crop residue classes could be separated from class *bare soil* only in the first middle infrared wavelength. Class *corn/51%* had higher reflectance than the compar-

able class, *corn/50%* in March, 1987. Similarly, class *bare soil* had higher reflectance values in April, 1988 than in March, 1987. The reasons are that the moisture content for March, 1987 data was higher than that of April, 1988 and crop residues have lower density than bare soil. However, the decrease of soil moisture content is usually slower than that of crop residues since crop residues reside above the land surface and their moisture contents are more directly influenced by weather. The difference between the two corn residue classes is very small, most likely because the residue percentage of class *corn/unknown* was close to that of class *corn/51%*. Class *soybeans/74%* had a smaller digital number than the corn residue classes because it had a higher density of residue coverage. Moreover, each crop residue class and the bare soil class had apparent increases of their individual digital numbers in every spectral wavelength band because of dryer conditions and higher solar angle in April, especially their digital values in the first middle infrared wavelength that were greater than 150 as compared to less than this value in March as shown in Figure 16. Class *pasture/grass* had a similar trend in the near infrared wavelength due to chlorophyll in young grass leave cells. However, classes *river* and *forest* had the first and second lowest reflectance in every wavelength band even though most trees had buds or young leaves in April.

4.2 Evaluation of Classification for the Original Data

The classification results for both training and testing data for March 23, 1987 and April, 1988 are shown in Figures 18 through 21. These training and testing data were selected from the two original images without any transformation. The discussion of the classification performances for the March and April data follows.

4.2.1 Performance for March Data

As seen in Figure 18, the neural classifier (NN) obtained the highest accuracy, whereas L1 Minimum Distance (L1) had the lowest accuracy among the three classifiers compared for the training data set. Although Maximum Likelihood (ML) did not have as high an accuracy as NN, it gave more than 95% accuracy for both individual classes and the entire training data set. The reason for the 100% accuracy of the training data set for NN is that NN was able to completely learn the training data set. Comparable performances were obtained for each of the other training data sets which will be discussed in latter sections

The classifiers performed differently for the testing data as shown in Figure 19. The relative performances for NN and ML are switched with each other. ML achieved 90% or better accuracy for each class and 96% accuracy for the entire testing data set, whereas the NN's lowest accuracy was 81% for the soybean residue class and 92% accuracy for the entire testing data set. L1 obtained 70% accuracy for both the soybean residue class and the entire testing data set which was not as good as ML and NN classifiers. Because the class *pasture/grass* was a mixture of several types of pasture and grass, it had variable spectral features and L1 had a 67% classification error (accuracy: 33%) for this class due to its consideration of first order statistics alone.

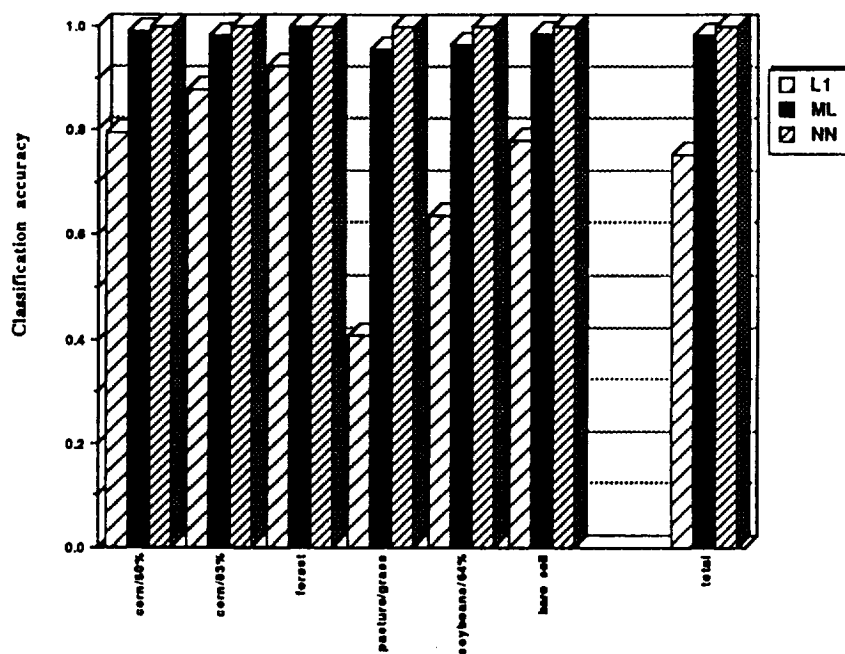


Figure 18. Training Performance for the March, 1987 data.

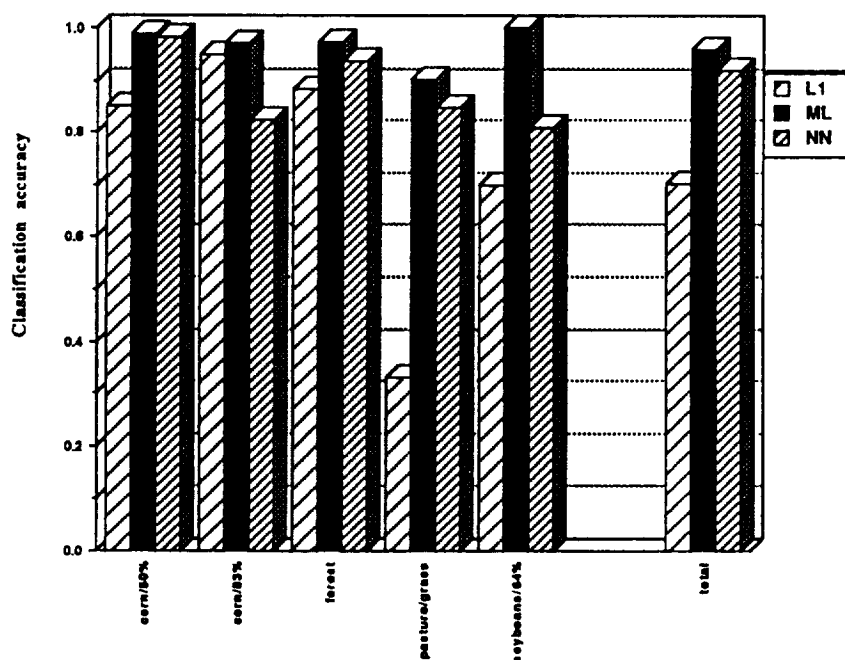


Figure 19. Testing performance for the March, 1987 data.

One confusion matrix for each classifier was produced from the classification of the testing data, and they are listed in Tables 9, 10 and 11. The percentages listed in the tables represent the proportion of ground truth pixels, in each case, correctly and incorrectly labeled by the classifier. The numbers without percentages beside them indicate that their corresponding percentages were less than 0.5%. In each table, columns refer to errors of omission corresponding to those pixels belonging to the class of interest that the classifier has failed to recognize; rows refer to errors of commission corresponding to pixels from other classes that the classifier has labeled as belonging to the class of interest (Richards, 1989). For example, the value located in column 5 and row 1 in Table 9 indicates that 6 pixels belonging to class *soybeans/64%* have failed to be recognized by L1. In other words, 10% of the class *soybeans/64%* has been mislabeled by L1 to *corn/50%*. For the confusion tables (including those shown in later sections), ground truth classes *river* and *bare soil* are not included because adequate numbers of pixels could not be selected for training, and the name of the class *pasture/grass* was shortened to *pasture*.

As seen in Tables 9, 10 and 11, the classification confusion between the crop residue classes and the bare soil class is 5% for class *soybeans/64%* for L1, 1% for class *corn/50%* for ML and 3% for *soybeans/64%* for NN. In addition, confusion exists among crop residue classes. The maximum confusion is 10% (class *soybeans/64%*) for L1, 3% (class *corn/83%*) for ML and 18% (class *corn/83%*) for NN.

Table 9. Confusion matrix for the March, 1987 testing data classified using L1.

		Ground truth classes					Total
		corn/50%	corn/83%	forest	pasture	soybeans/64%	
TM classes	corn/50%	721(85%)	0	0	87(14%)	6(10%)	814
	corn/83%	47(6%)	183(95%)	12(4%)	9(1%)	2(3%)	253
	forest	0	2(1%)	244(88%)	9(1%)	0	255
	pasture	32(4%)	0	0	199(33%)	8(13%)	239
	river	0	0	19(7%)	0	0	19
	soybeans/64%	45(5%)	8(4%)	1	215(36%)	44(70%)	313
	bare soil	3	0	0	85(14%)	3(5%)	91
Number of ground truth pixels		848	193	276	604	63	1984

Table 10. Confusion matrix for the March, 1987 testing data classified using ML.

		Ground truth classes					Total
		corn/50%	corn/83%	forest	pasture	soybeans/64%	
TM classes	corn/50%	838(99%)	6(3%)	0	1	0	845
	corn/83%	4	187(97%)	0	0	0	191
	forest	0	0	269(97%)	3(1%)	0	272
	pasture	0	0	7(3%)	554(90%)	0	551
	river	0	0	0	0	0	0
	soybeans/64%	0	0	0	21(3%)	63(100%)	84
	bare soil	6(1%)	0	0	35(6%)	0	41
Number of ground truth pixels		848	193	276	604	63	1984

Table 11. Confusion matrix for the March, 1987 testing data classified using NN.

		Ground truth classes					Total
		corn/50%	corn/83%	forest	pasture	soybeans/64%	
TM classes	corn/50%	833(98%)	34(18%)	4(1%)	23(4%)	1(2%)	895
	corn/83%	8(1%)	159(82%)	5(2%)	13(2%)	3(5%)	188
	forest	1	0	259(94%)	13(2%)	0	273
	pasture	4	0	7(3%)	513(85%)	5(8%)	529
	river	0	0	1	11(2%)	1(2%)	13
	soybeans/64%	2	0	0	26(4%)	51(81%)	79
	bare soil	0	0	0	5(1%)	2(3%)	7
Number of ground truth pixels		848	193	276	604	63	1984

Table 12. Confusion matrix for the April, 1988 testing data classified using L1.

		Ground truth classes					Total
		corn/51%	corn/unknown	forest	pasture	soybeans/74%	
TM classes	corn/51%	489(57%)	0	0	0	23(23%)	512
	corn/unknown	65(8%)	183(77%)	0	0	0	211
	forest	0	0	259(92%)	187(37%)	0	446
	pasture	5(1%)	0	0	311(62%)	2(2%)	318
	river	0	0	24(8%)	3(1%)	0	27
	soybeans/74%	236(27%)	2(1%)	0	0	39(40%)	277
	bare soil	69(8%)	42(22%)	0	3(1%)	34(35%)	148
Number of ground truth pixels		864	190	283	504	98	1939

Table 13. Confusion matrix for the April, 1988 testing data classified using ML.

		Ground truth classes					Total
		corn/51%	corn/unknown	forest	pasture	soybeans/74%	
TM classes	corn/51%	637(74%)	10(5%)	0	0	20(20%)	667
	corn/unknown	0	177(93%)	0	0	0	177
	forest	0	0	278(98%)	1	0	279
	pasture	5(1%)	3(2%)	4(1%)	503(100%)	0	520
	river	0	0	1	0	0	1
	soybeans/74%	220(25%)	0	0	0	73(74%)	293
	bare soil	2	0	0	0	0	2
Number of ground truth pixels		864	190	283	504	98	1939

Table 14. Confusion matrix for the April, 1988 testing data classified using NN.

		Ground truth classes					Total
		corn/51%	corn/unknown	forest	pasture	soybeans/74%	
TM classes	corn/51%	704(81%)	34(18%)	7(2%)	1	45(46%)	792
	corn/unknown	23(3%)	146(77%)	16(6%)	12(2%)	4(4%)	201
	forest	7(1%)	0	226(80%)	91(18%)	1(1%)	325
	pasture	12(1%)	7(4%)	22(8%)	382(76%)	11(11%)	434
	river	1	0	12(4%)	10(2%)	0	23
	soybeans/74%	113(13%)	2(1%)	0	6(1%)	37(38%)	158
	bare soil	4	0	0	2	0	6
Number of ground truth pixels		864	190	283	504	98	1939

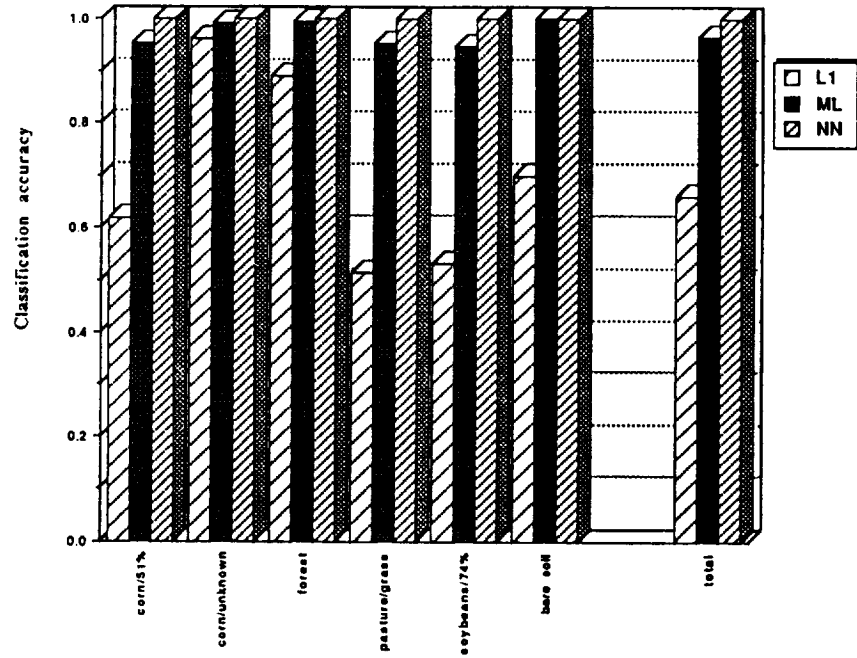


Figure 20. Training performance for the April, 1988 data.

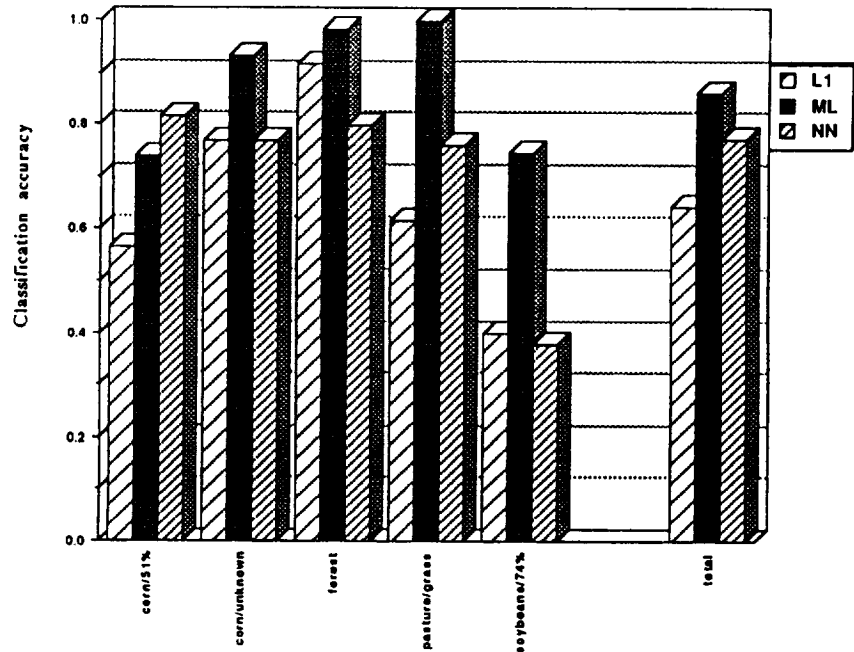


Figure 21. Testing performance for the April, 1988 data.

4.2.2 Performance for April, 1988 Data

Figures 20 and 21 illustrate classification results obtained by using L1, ML, and NN for the training and testing data. As shown in Figure 20, these three classifiers showed a similar tendency to that of the March, 1987 training data, *i.e.* NN obtained perfect accuracy, ML 96% accuracy and L1 66% accuracy. L1 dropped seven percent compared to 73% for the March, 1987 training data. This is because the differences of reflectance among the crop residue classes and between the crop residue classes and the bare soil class for the April, 1988 data were less than those for the March, 1987 data, as described earlier.

Although these three classifiers had the same tendency of performance for the testing data as they did for the March, 1987 testing data, NN and L1 obtained less than 50 percent accuracy for the soybean residue class and the overall testing accuracy for all three classifiers as a whole decreased 10 percent on average compared to that for the March testing data. ML, as it did for the March data, performed with the highest accuracy. Confusion matrices were also generated for the April, 1988 testing data, and are listed in Tables 12, 13 and 14 corresponding to classifiers L1, ML, and NN. From these tables, the maximum confusion among crop residue classes is 27% (class *corn/51%*) for L1, 25% (class *corn/51%*) for ML and 46% (class *soybeans/74%*) for NN, and the confusion between crop residues and bare soil is 8% from class *corn/51%*, 22% from class *corn/unknown* and 35% from class *soybeans/74%* for L1. This type of confusion was less than 0.5% for ML and NN. Therefore, the confusions among the crop residue classes and between the crop residue classes and the bare soil class are much greater than those for the March, 1987 testing data. The reason is the same as that for the April, 1988 training data mentioned above.

4.3 Evaluation of Classification for the Transformed Data

Two types of transformations, principal components and spectral ratioing, were performed to enhance the images. Principal components transformation was applied to both March 1987 and April, 1988 data whereas spectral ratioing transformation only to March, 1987 data. For the following descriptions, the three images were called *PC March* and *PC April* corresponding to the original March and April data transformed by principal components and *SR March* corresponding to the original March data transformed by spectral ratioing. The classification results for training and testing data from these transformed images are discussed in the following sections.

4.3.1 Performance for PC March, 1987 Data

As seen in Figure 22, the three classifiers had classification results similar to those for the untransformed March data, *i.e.*, the order of performance from best to worst was NN, ML and L1 for the training data set. For the testing data, the order of performance changed as shown in Figure 23. This also happened for the March testing data. ML presented 96% or better accuracy for the crop residue classes and 97% accuracy for the entire testing data set. L1 had an 82% accuracy for the entire testing data set. NN performed at 81% accuracy for the soybean residue class, 91% or better for the corn residue classes, and 91% for the entire training data set. The confusion matrices for the testing data are listed in Tables 15, 16 and 17. There was no confusion between crop residues and bare soil for any of the classifiers. The maximum confusion among crop residue classes is 12% (from corn/50%) for L1, 2% (from corn/50%) for ML and 9% (from class corn/83%) for NN. Therefore, the testing classification result for the class

corn/83% was improved by applying NN to the PC March, 1987 data. This indicates that NN treated the PC transformed data as a new data set.

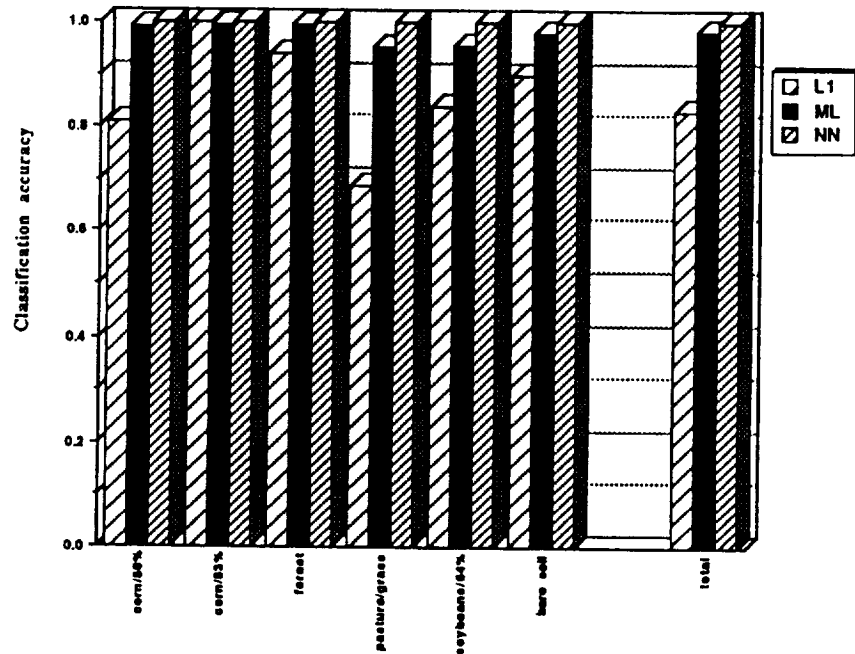


Figure 22. Training performance for the PC March, 1987 data.

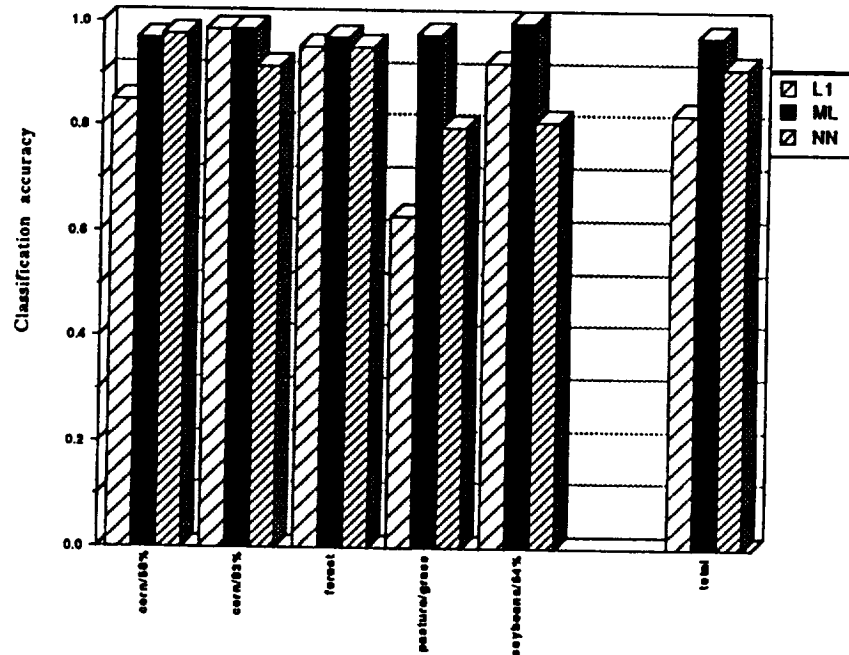


Figure 23. Testing performance for the PC March, 1987 data.

Table 15. Confusion matrix for the PC March, 1987 testing data classified using L1.

		Ground truth classes					Total
		corn/50%	corn/83%	forest	pasture	soybeans/64%	
TM classes	corn/50%	782(85%)	1(1%)	0	10(2%)	5(6%)	798
	corn/83%	111(12%)	139(99%)	1	4(1%)	2(2%)	257
	forest	0	0	300(95%)	3(1%)	0	303
	pasture	11(1%)	0	3(1%)	301(63%)	0	315
	river	0	0	9(3%)	0	0	9
	soybeans/64%	18(2%)	1(1%)	2(1%)	52(11%)	83(92%)	156
	bare soil	0	0	0	109(23%)	0	109
Number of ground truth pixels		922	141	315	479	90	1947

Table 16. Confusion matrix for the PC March, 1987 testing data classified using ML.

		Ground truth classes					Total
		corn/50%	corn/83%	forest	pasture	soybeans/64%	
TM classes	corn/50%	892(97%)	2(1%)	0	0	0	894
	corn/83%	21(2%)	139(96%)	0	0	0	160
	forest	0	0	306(97%)	1	0	307
	pasture	1	0	9(3%)	467(97%)	0	477
	river	0	0	0	0	0	0
	soybeans/64%	8(1%)	0	0	5(1%)	90(100%)	103
	bare soil	0	0	0	6(1%)	0	6
Number of ground truth pixels		922	141	315	479	90	1947

Table 17. Confusion matrix for the PC March, 1987 testing data classified using NN.

		Ground truth classes					Total
		corn/50%	corn/83%	forest	pasture	soybeans/64%	
TM classes	corn/50%	900(98%)	12(9%)	4(1%)	13(3%)	2(2%)	931
	corn/83%	19(2%)	129(91%)	3(1%)	0	2(2%)	153
	forest	1	0	300(95%)	16(3%)	5(6%)	322
	pasture	1	0	6(2%)	383(80%)	8(9%)	389
	river	1	0	2(1%)	5(1%)	0	8
	soybeans/64%	0	0	0	12(10%)	73(81%)	123
	bare soil	0	0	0	12(3%)	0	12
Number of ground truth pixels		922	141	315	479	90	1947

4.3.2 Performance for PC April, 1988 Data

Figures 24 and 25 show the classification results obtained by using L1, ML and NN for the training and test data. As seen in Figure 24, both ML and NN were more than 90 percent accurate for each training class, whereas L1 was 73% accurate for the entire training data set (66% for class *corn* 51%, 99% for class *corn/unknown* and 86% for class *soybeans* 74%). The testing accuracies for L1, ML and NN were 78%, 88% and 83%, respectively. However, L1 and NN only obtained about 51% accuracy for class *soybeans* 74%. The confusion matrices are listed in Tables 18, 19 and 20. From these tables, the confusion between crop residues and bare soil is 5% for class *corn*/51%, 7% for class *corn/unknown* and 11% for class *soybeans*/74% for L1 classification. There is little confusion for ML and NN classifiers. However, confusion among crop residue classes still exists. The maximum confusion percentages for L1, ML and NN are 35% for class *soybeans*/74%, 15% for class *corn*/51% and 36% for class *soybeans*/74%.

respectively. Again, the maximum confusion percentage was decreased 10% by applying NN to the PC transformed data set. The confusions among the crop residue classes for the April, 1988 PC data were greater than those for the March, 1987 PC data. This indicates that the April, 1988 PC data was more difficult to classify than the March, 1987 PC data.

Table 18. Confusion matrix for the PC April, 1988 testing data classified using L1.

		Ground truth classes					Total
		corn/51%	corn/unknown	forest	pasture	soybeans/74%	
TM classes	corn/51%	589(71%)	0	0	0	47(35%)	636
	corn/unknown	71(9%)	115(93%)	0	0	0	186
	forest	0	0	125(84%)	73(12%)	1(1%)	199
	pasture	0	0	1(1%)	546(88%)	2(1%)	549
	river	0	0	20(14%)	0	0	20
	soybeans/74%	120(15%)	0	0	0	70(52%)	190
	bare soil	44(5%)	9(7%)	2(1%)	1	15(11%)	71
Number of ground truth pixels		824	124	148	620	135	1851

Table 19. Confusion matrix for the PC April, 1988 testing data classified using ML.

		Ground truth classes					Total
		corn/51%	corn/unknown	forest	pasture	soybeans/74%	
TM classes	corn/51%	692(84%)	7(6%)	0	0	16(12%)	715
	corn/unknown	2	106(85%)	0	0	0	108
	forest	0	0	117(79%)	6(1%)	0	123
	pasture	4	11(9%)	12(8%)	614(99%)	13(10%)	654
	river	0	0	3(2%)	0	0	3
	soybeans/74%	123(15%)	0	0	0	105(78%)	228
	bare soil	3	0	16(11%)	0	1(1%)	20
Number of ground truth pixels		824	124	148	620	135	1851

Table 20. Confusion matrix for the PC April, 1988 testing data classified using NN.

		Ground truth classes					Total
		corn/51%	corn/unknown	forest	pasture	soybeans/74%	
TM classes	corn/51%	692(84%)	19(15%)	0	4(1%)	48(36%)	763
	corn/unknown	38(5%)	103(83%)	2(1%)	3	2(1%)	148
	forest	3	2(2%)	138(93%)	72(12%)	4(3%)	219
	pasture	9(1%)	0	7(5%)	536(86%)	12(9%)	564
	river	0	1(1%)	2	0	0	3
	soybeans/74%	78(9%)	0	0	3	69(51%)	150
	bare soil	4	0	0	0	0	4
Number of ground truth pixels		824	124	148	620	135	1851

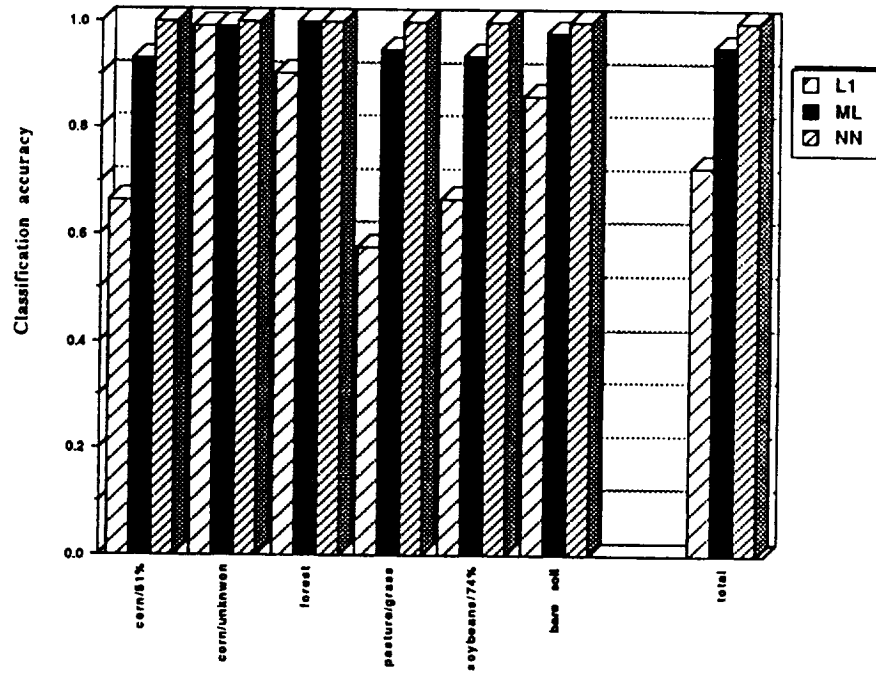


Figure 24. Training performance for the PC April, 1988 data.

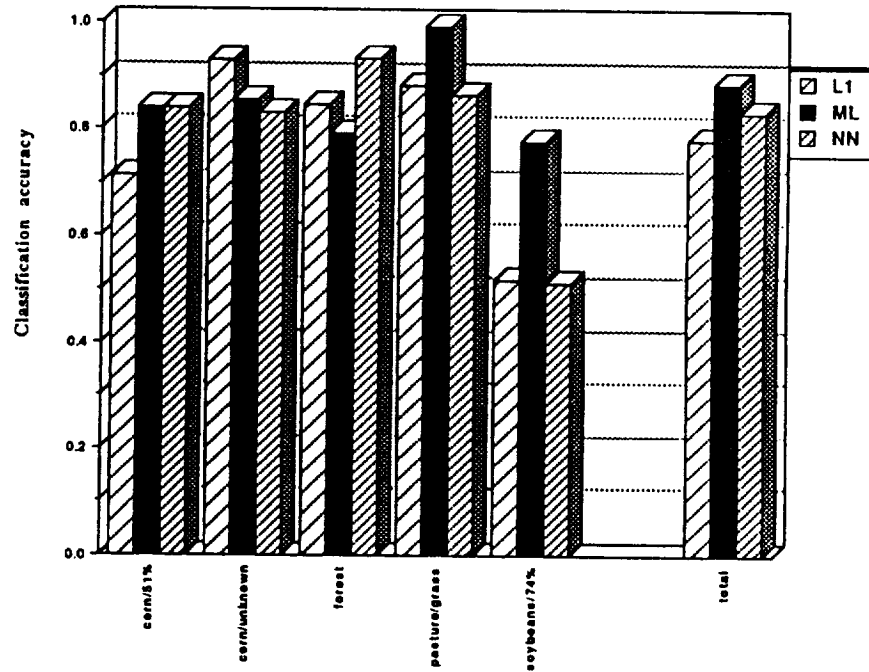


Figure 25. Testing performance for the PC April, 1988 data.

4.3.3 Performance for SR March, 1987 Data

As seen in Figure 26, L1, ML and NN obtained 82%, 98% and 100% accuracies for the training data, respectively. This coincided with the performances of these classifiers for the March and PC March training data. However, the testing accuracies of the SR March data, as shown in Figure 27, were less than those of the March and PC March data for ML and NN whereas the testing accuracy for the SR March data (87%) was higher than the March and PC March data for L1 classification. The confusion matrices corresponding to the three classifiers are listed in Tables 21, 22 and 23. There is almost no confusion between crop residues and bare soil as shown in these tables. The confusion among the crop residue classes has maximums of 11% (class *corn/50%*) for L1, 4% (class *corn/83%*) for ML and 29% (class *corn/83%*) for NN.

Table 21. Confusion matrix for the SR March, 1987 testing data classified using L1.

		Ground truth classes					Total
		corn/50%	corn/83%	forest	pasture	soybeans/64%	
TM classes	corn/50%	839(86%)	1(1%)	0	3(1%)	3(3%)	846
	corn/83%	108(11%)	112(99%)	0	0	1(1%)	221
	forest	0	0	188(87%)	7(1%)	1(1%)	196
	pasture	4	0	8(4%)	516(86%)	6(6%)	534
	river	0	0	9(3%)	0	0	25
	soybeans/64%	20(2%)	0	0	22(1%)	81(87%)	123
	bare soil	0	0	0	50(8%)	1(1%)	51
Number of ground truth pixels		971	113	217	602	93	1996

Table 22. Confusion matrix for the SR March, 1987 testing data classified using ML.

		Ground truth classes					Total
		corn/50%	corn/83%	forest	pasture	soybeans/64%	
TM classes	corn/50%	874(90%)	4(4%)	0	1	0	879
	corn/83%	7(1%)	109(96%)	0	0	0	116
	forest	0	0	193(89%)	2	0	195
	pasture	61(6%)	0	11(5%)	506(84%)	2(2%)	580
	river	0	0	13(6%)	5(1%)	0	18
	soybeans/64%	28(3%)	0	0	6(1%)	91(98%)	125
	bare soil	1	0	0	82(14%)	0	83
Number of ground truth pixels		971	113	217	602	93	1996

Table 23. Confusion matrix for the SR March, 1987 testing data classified using NN.

		Ground truth classes					Total
		corn/50%	corn/83%	forest	pasture	soybeans/64%	
TM classes	corn/50%	880(91%)	33(29%)	2(1%)	4(1%)	3(3%)	922
	corn/83%	27(3%)	80(71%)	1	1	2(2%)	111
	forest	4	0	137(63%)	9(1%)	0	150
	pasture	44(5%)	0	56(63%)	558(93%)	30(32%)	688
	river	3	0	21(10%)	13(2%)	0	37
	soybeans/64%	13(1%)	0	0	11(2%)	57(61%)	81
	bare soil	0	0	0	6(1%)	1	7
Number of ground truth pixels		971	113	217	602	93	1996

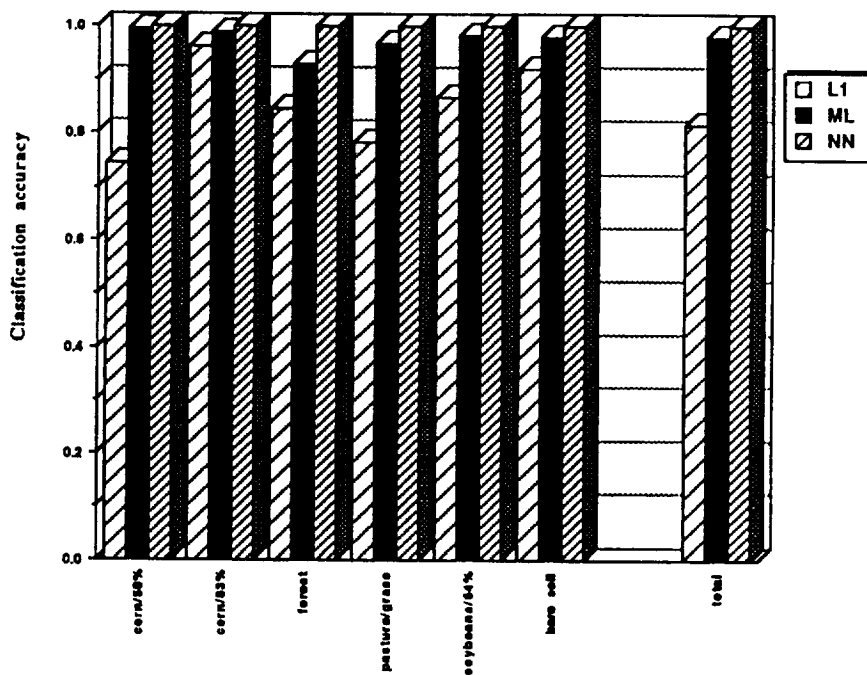


Figure 26. Training performance for the SR March, 1987 data.

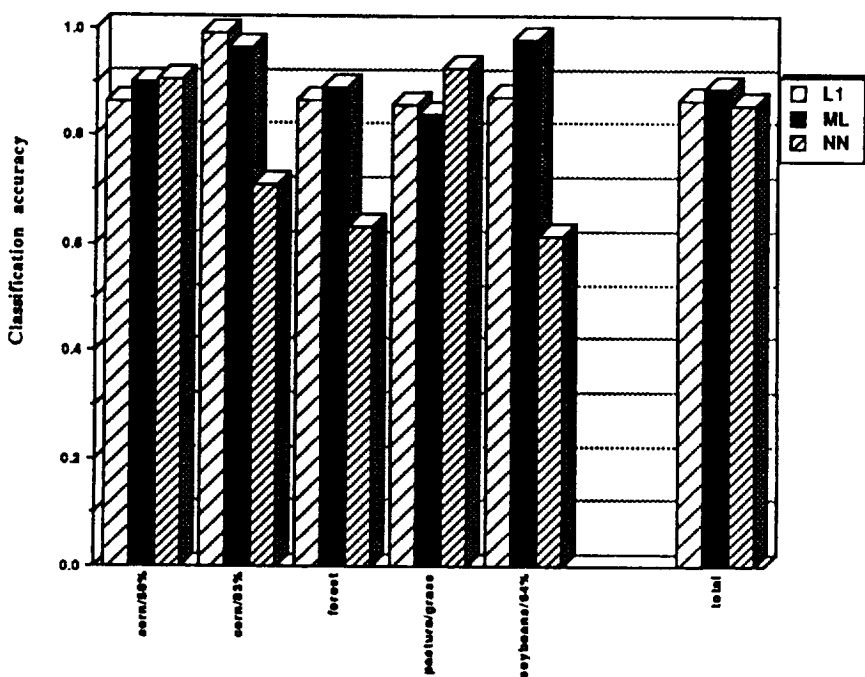


Figure 27. Testing performance for the SR March, 1987 data.

4.4 Evaluation of GIS-Aided Classification

A GIS layer, *ownership*, was added to each of the original data as an eighth band of data and called *March Plus* and *April Plus* data as described previously. The classification results for both image dates are shown in Figures 28 through 31. The training and testing data were selected from the two eight-band Landsat TM Plus images. The discussion related to the April Plus data follows the explanation of the March Plus data.

As seen in Figure 28 and 29, ML is not included due to the inability to invert the covariance matrix because of the *river* class. L1 obtained only 27% and 39% accuracies for the March Plus training and testing data for class *pasture/grass* because of its consideration of only the first order statistic as discussed earlier. However, NN still obtained a perfect classification as before for the training data, and about 90% accuracy for individual classes of the testing data and 95% for the entire testing data set. Confusion matrices corresponding to L1 and NN are listed in Tables 24 and 25. It can be seen that L1 mis-classified 13% of class *corn 50%* into class *soybeans 64%*, 5% of class *corn 83%* into class *soybeans 64%*, and 5% of class *soybeans 64%* into class *corn 50%*. Confusion between the crop residue classes still existed for L1. The confusion between crop residues and bare soil was 3% for L1. However, there is none of this type of confusion for the NN classification. The confusion among crop residue classes for NN is 12% for class *corn/50%* and 1% for class *soybeans/64%*. Therefore, the overall testing classification accuracy was better by applying NN to the March Plus data set than to the March, 1987 data set, the PC March, 1987 data set and the SR March, 1987 data set, and the NN's classification accuracy for the entire March Plus testing data was similar to ML's classification accuracy for the March, 1987 testing data set.

Figures 30 and 31 show the classification performance for the training and testing of April Plus data. Again, ML could not be used for the same reason as for the March Plus data set. L1 obtained 62% and 54% accuracies, while NN obtained 100% and 87% accuracies for the training and testing data set, respectively. As seen in Tables 26 and 27, there is a certain amount of confusion between the crop residue classes and bare soil for L1 but no confusion for NN. Again, the overall testing classification accuracy was much better by applying NN to the April Plus data set than to the April, 1988 data set and the PC April, 1988 data set, and the NN's classification accuracy for the entire April Plus testing data set was higher than ML's classification accuracy for the April, 1988 testing data set. Therefore, the classification for the April, 1988 data set was improved by applying NN to the GIS-enhanced April data set.

Table 24. Confusion matrix for the March Plus testing data classified using L1.

		Ground truth classes					Total
		corn/50%	corn/83%	forest	pasture	soybeans/64%	
TM classes	corn/50%	589(81%)	2(3%)	0	2	4(5%)	597
	corn/83%	14(2%)	66(88%)	2(1%)	7(2%)	1(1%)	90
	forest	0	2(3%)	133(92%)	2	0	137
	pasture	4(1%)	1(1%)	0	176(39%)	0	181
	river	0	0	10(7%)	0	0	10
	soybeans/64%	96(13%)	4(5%)	0	167(37%)	78(94%)	345
	bare soil	22(3%)	0	0	95(21%)	0	117
Number of ground truth pixels		725	75	145	449	83	1477

Table 25. Confusion matrix for the March Plus testing data classified using NN.

		Ground truth classes					Total
		com/50%	com/83%	forest	pasture	soybeans/64%	
TM classes	com/50%	723(100%)	9(12%)	1(1%)	17(4%)	1(1%)	751
	com/83%	1	66(88%)	0	6(1%)	0	73
	forest	1	0	144(99%)	5(1%)	1(1%)	151
	pasture	0	0	0	401(89%)	5(6%)	406
	river	0	0	0	1	1(1%)	2
	soybeans/64%	0	0	0	12(3%)	75(90%)	87
	bare soil	0	0	0	7(2%)	0	7
Number of ground truth pixels		725	75	145	449	83	1477

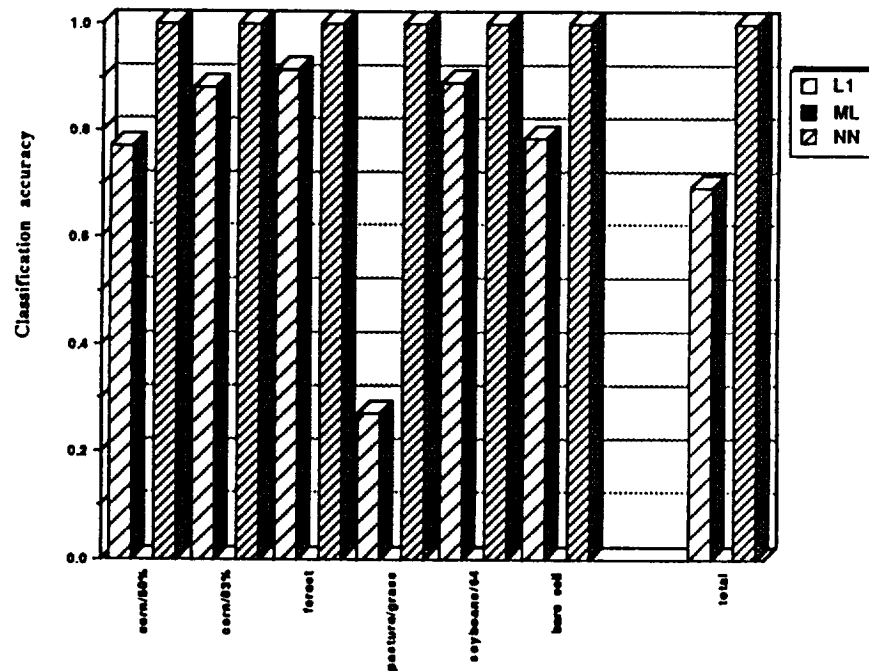


Figure 28. Training performance for the March Plus, 1987 data.

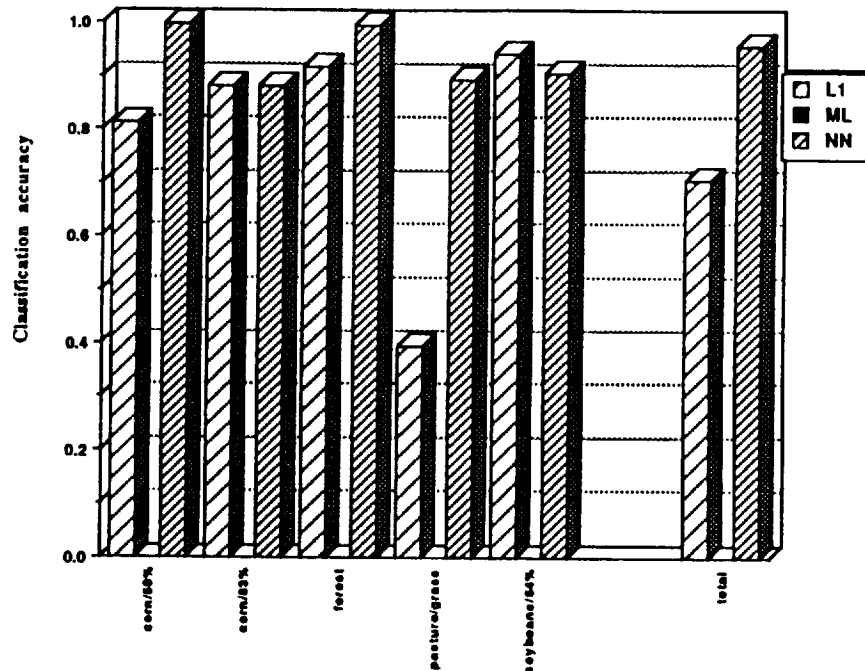


Figure 29. Testing performance for the March Plus, 1987 data.

Table 26. Confusion matrix for the April Plus testing data classified using L1.

		Ground truth classes					Total
		com/51%	com/unknown	forest	pasture	soybeans/74%	
TM classes	com/51%	383(62%)	0	0	4(1%)	68(53%)	455
	com/unknown	92(15%)	70(66%)	0	85(20%)	3(2%)	250
	forest	0	0	123(77%)	133(31%)	0	256
	pasture	0	3(3%)	0	156(36%)	2(2%)	161
	river	0	0	37(23%)	0	0	37
	soybeans/74%	142(23%)	0	0	10(2%)	53(42%)	205
	bare soil	3	33(31%)	0	43(10%)	1(1%)	80
Number of ground truth pixels		620	106	160	431	127	1444

Table 27. Confusion matrix for the April Plus testing data classified using NN.

		Ground truth classes					Total
		com/51%	com/unknown	forest	pasture	soybeans/74%	
TM classes	com/51%	582(94%)	12(11%)	0	34(8%)	4(3%)	632
	com/unknown	24(4%)	83(78%)	0	34(8%)	3(3%)	144
	forest	10(2%)	1(1%)	153(96%)	35(8%)	2(2%)	201
	pasture	3	10(9%)	7(4%)	328(76%)	2(2%)	350
	river	0	0	0	0	1(1%)	1
	soybeans/74%	1	0	0	0	115(91%)	116
	bare soil	0	0	0	0	0	0
Number of ground truth pixels		620	106	160	431	127	1444

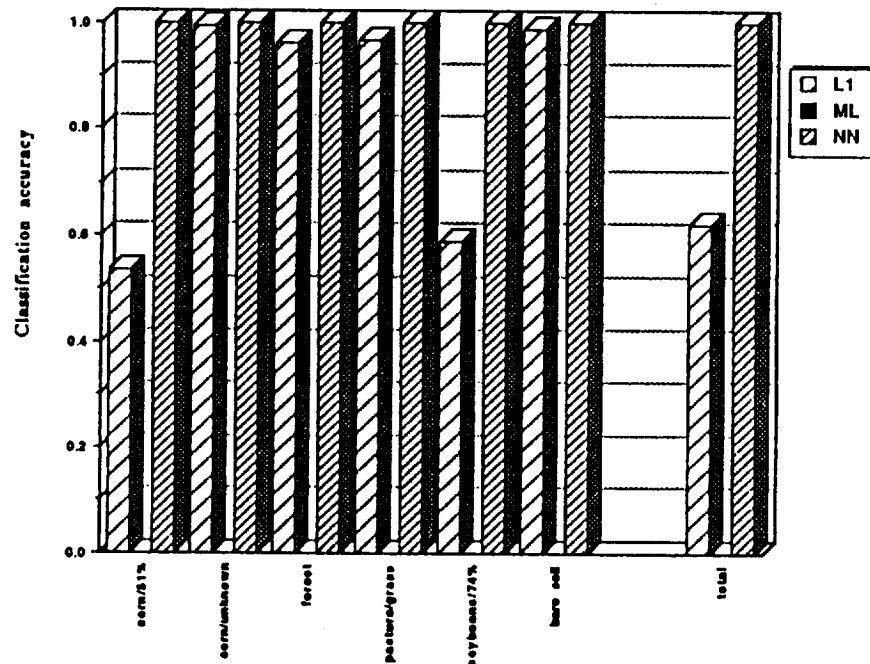


Figure 30. Training performance for the April Plus data.

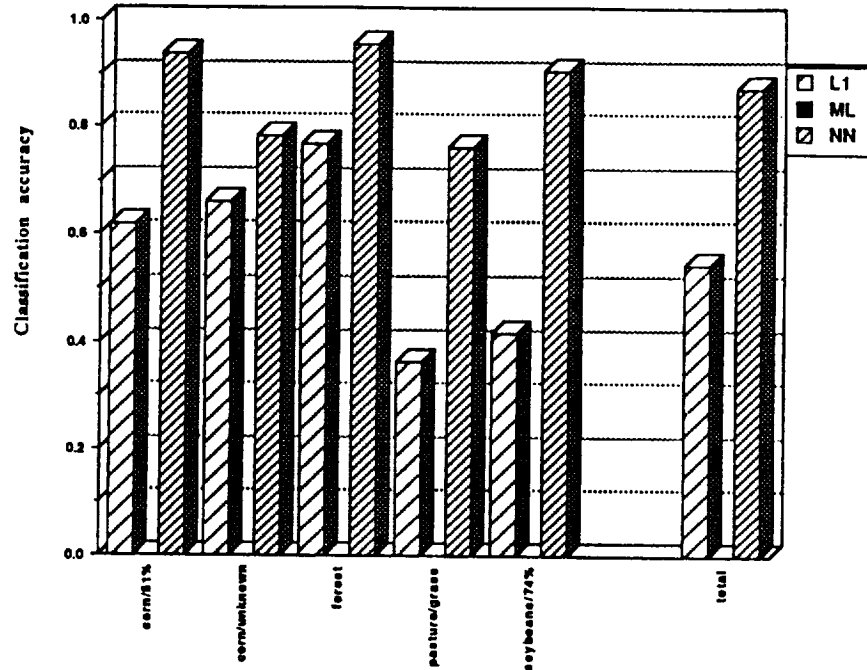


Figure 31. Testing performance for the April Plus data.

4.5 Comparison of the Classifiers for Different Data Sets

The three classifiers, L1, ML and NN, used for each type of data (the original data, the principal components transformed data, the spectral ratioing transformed data and the original data incorporating a GIS layer) obtained different classification results. Before the comparisons are to be made, it is necessary to point out that L1 is not going to be included because of the unsatisfactory results obtained with it as discussed in the previous sections. Therefore, the classifiers to be compared are ML and NN. The comparison between ML and NN will be made after comparisons of each classifier applied for all types of data are made.

4.5.1 Comparison of ML Classifiers

Figure 32 illustrates the testing performance of the ML classifier for the three types of March, 1987 data while Figure 33 shows the testing performance of the ML classifier for the two types of April, 1988 data. In each legend of the figures, *ML-1*, *ML-2* and *ML-3* refer to the ML used for the Landsat TM data, the PC transformed data and the SR transformed data, respectively. ML is not shown in both Figure 32 and Figure 33 for the Landsat TM Plus data because ML could not classify them, and *ML-3* is not shown in Figure 33 because there was no SR April, 1988 data.

As seen in Figures 32 and 33, the differences between the comparable classification accuracies which were obtained by applying ML to the original and PC data for the March and April images, are 1% and 2% respectively. The differences are because of the slightly different training data. Therefore, using the original data would cost less because it does not required a transformation, although principal components transformed images were visually more interpretable than the original ones when displayed on a screen. However, the testing accuracies for the April data decreased about ten percent each compared to 96% and 97% accuracy for the March, 1987 data and the PC March, 1987 data. This indicates that the March images were easier to classify than the April images whether principal components transformation was applied or not. In addition, the accuracies for both individual classes and the entire testing data set for the SR March, 1987 data are less than those for the other two types of data as shown in Figure 32.

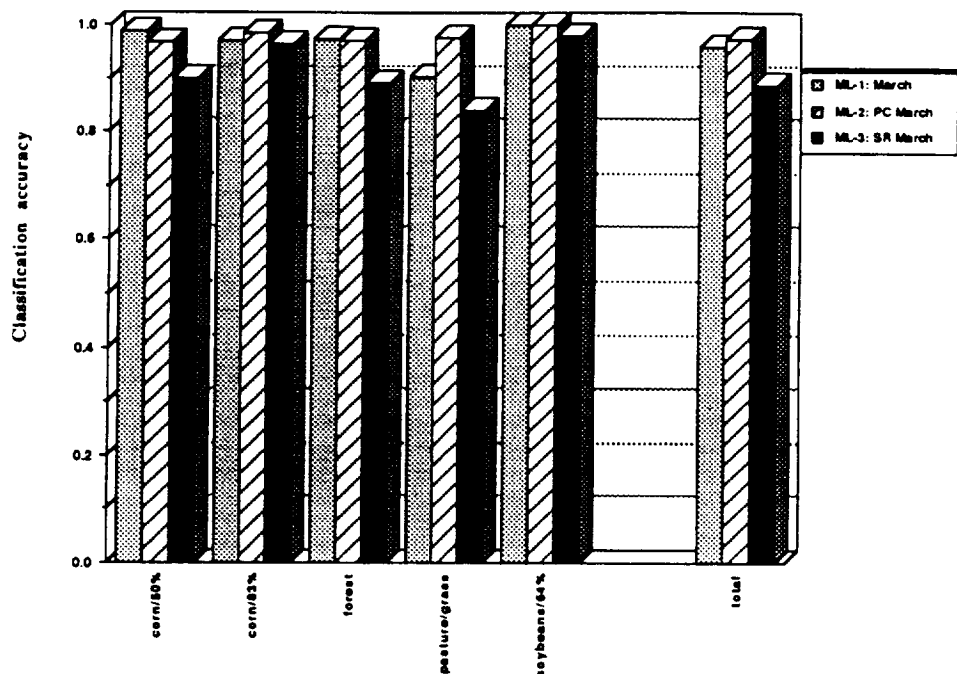


Figure 32. Testing performance of all MLs for March, 1987 data.

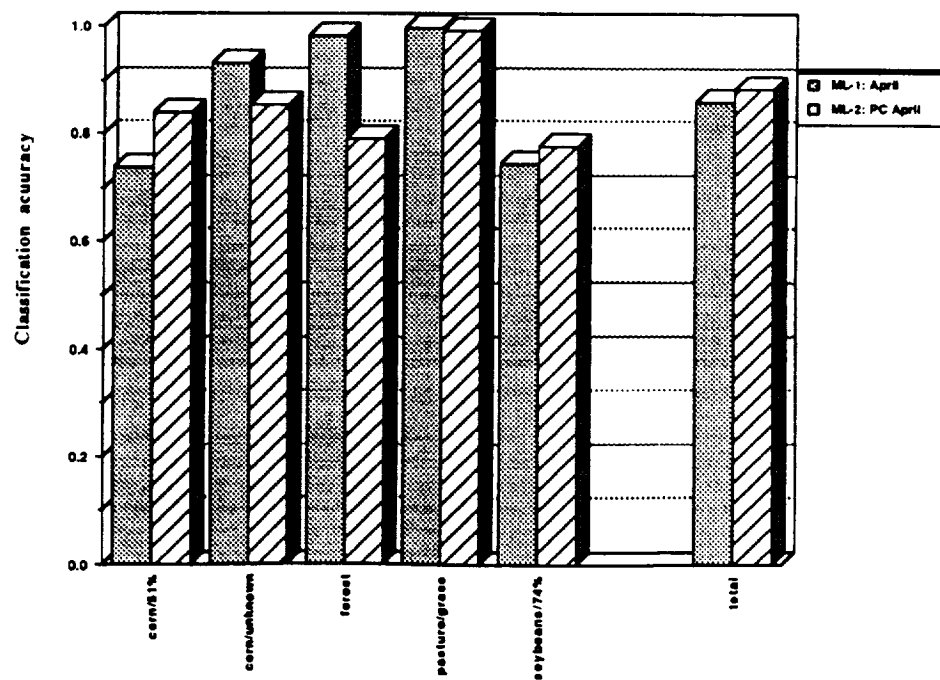


Figure 33. Testing performance of all MLs for April, 1988 data.

4.5.2 Comparison of NN Classifiers

The testing NN classification results for all types of March and April data are depicted in Figures 34 and 35. In each legend of the figures, *NN-1*, *NN-2*, *NN-3* and *NN-4* refer to the NN used for the Landsat TM data, the PC transformed data, the SR transformed data and the Landsat TM Plus data, respectively. *NN-3* is not listed in Figure 35 because there was no SR April, 1988 data,

As shown in Figures 34 and 35, neuro-classification of Landsat TM Plus data (*NN-4*) gave the highest accuracies for both the March and April images and a marked accuracy increase for each crop residue class. Moreover, as reported earlier, there was no confusion between the crop residue classes and the bare soil class for both the March and April Plus data. This indicates that the separability for the crop residue classes and the bare soil class has been increased after incorporating the GIS-layer, *ownership*, as the eighth band of data for each original Landsat TM image, and thus classification results improved. Neuro-classification of PC transformed data (*NN-2*) almost always presented better accuracies for each individual crop residue class except for class *corn/50%* for March, 1987 data, and had a higher accuracy than that of the original April, 1988 data. Neuro-classifications had almost the same accuracies for the March, 1987 testing data set and the March Plus testing data set. Therefore, it can be concluded that NN performed equally well or better for the principal components transformed images. However, the testing accuracies related to the SR March, 1987 data are less than any other in Figure 34.

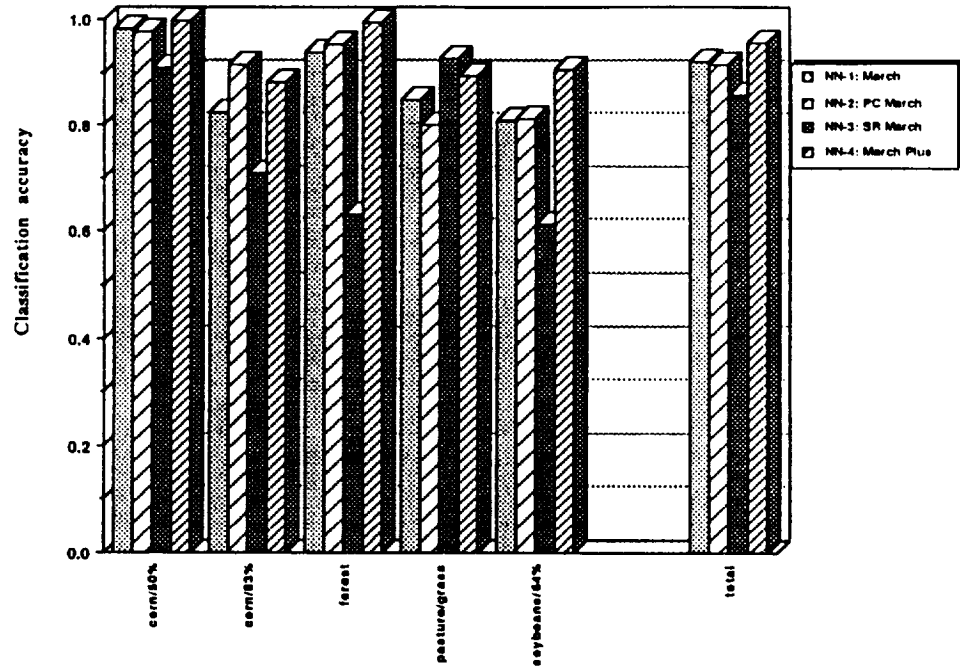


Figure 34. Testing performance of all NNs for March, 1987 data.

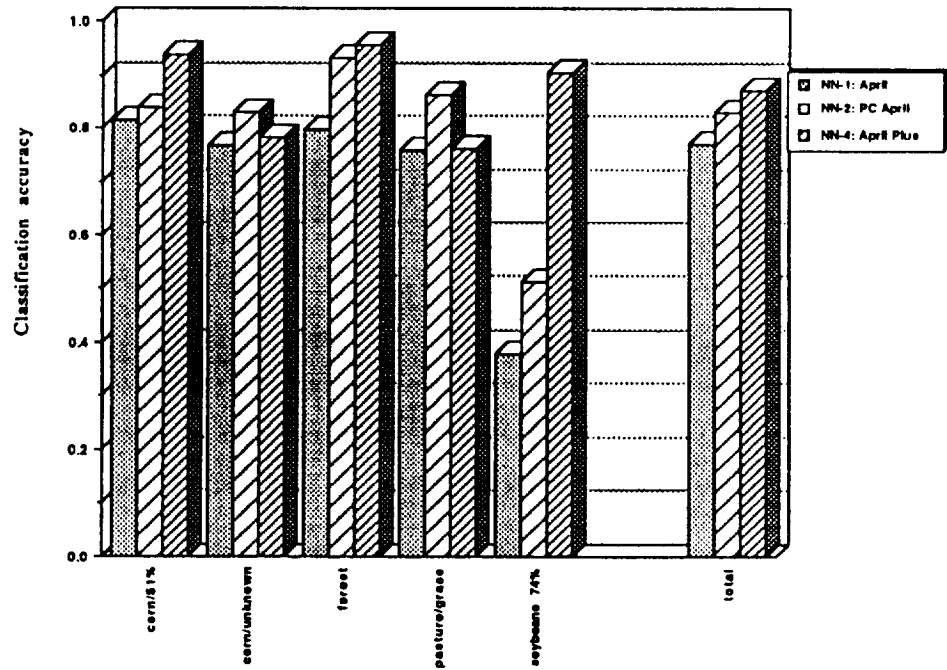


Figure 35. Testing performance of all NNs for April, 1988 data.

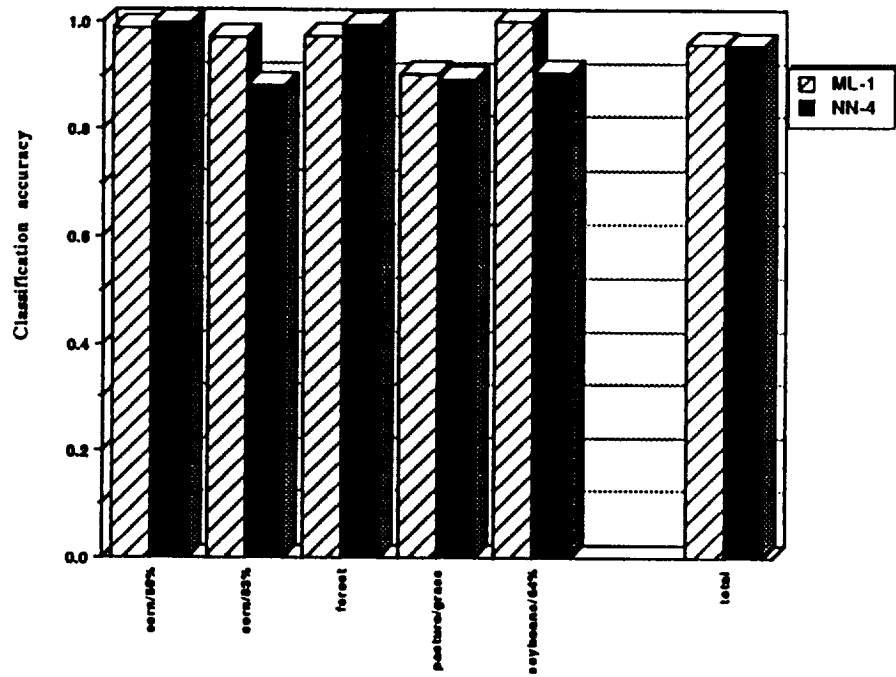


Figure 36. The best classifiers for March, 1987 data.

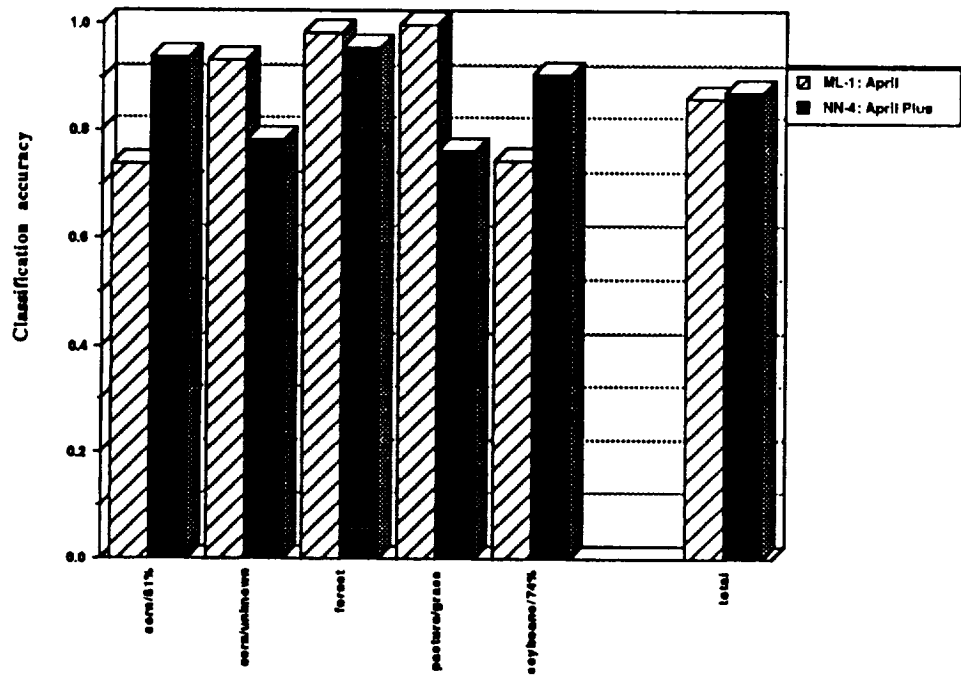


Figure 37. The best classifiers for April, 1988 data.

02

4.5.3 Comparison of the Best ML and NN

Based on the results shown in the sections above, the best classifiers in this study for each data set were selected and are illustrated in Figures 36 and 37. The best classifier for each original Landsat TM image was ML, whereas the best classifier for each Landsat TM Plus image generated by incorporating a GIS-layer was NN. As seen in Figures 36 and 37, NN presented equal or better accuracies than ML for the entire testing data sets of March and April. Therefore, if the image processing system was integrated with a GIS, it would be better to incorporate some GIS layer like *ownership* field boundaries, into an original image and then to classify it using a neural network classifier. In addition to the quantified performances, it can be seen in Figures 38 and 39 that the classification results of the study area for NN showed less or similar confusion among the crop residue classes, higher absolute classification accuracies for the crop residue classes and the bare soil class than those for ML, and very clear crop residue fields and their boundaries. In Figure 38, the NN's result shows some noise inside *soybean/74%* and *corn/83%* fields as indicated in their confusion matrices shown earlier, whereas the ML's result has many pixels mis-classified into class *bare soil* in addition to a field confusion with class *corn/83%* shown in the upper center portion of the figure. In Figure 39, the NN's result shows some confusion as indicated in the corresponding confusion matrices, whereas the ML's result has much more confusion among the crop residue classes, especially between class *corn/51%* and class *soybeans/74%*, which was also shown earlier in their confusion matrices. In both cases, the corresponding L1's results obtained by classifying the original images were also depicted to illustrate the large amount of mis-classification. For NN classification, if the image processing system is not integrated with a GIS, it would require a certain amount of work merging a GIS layer into the original satellite image before image classification.

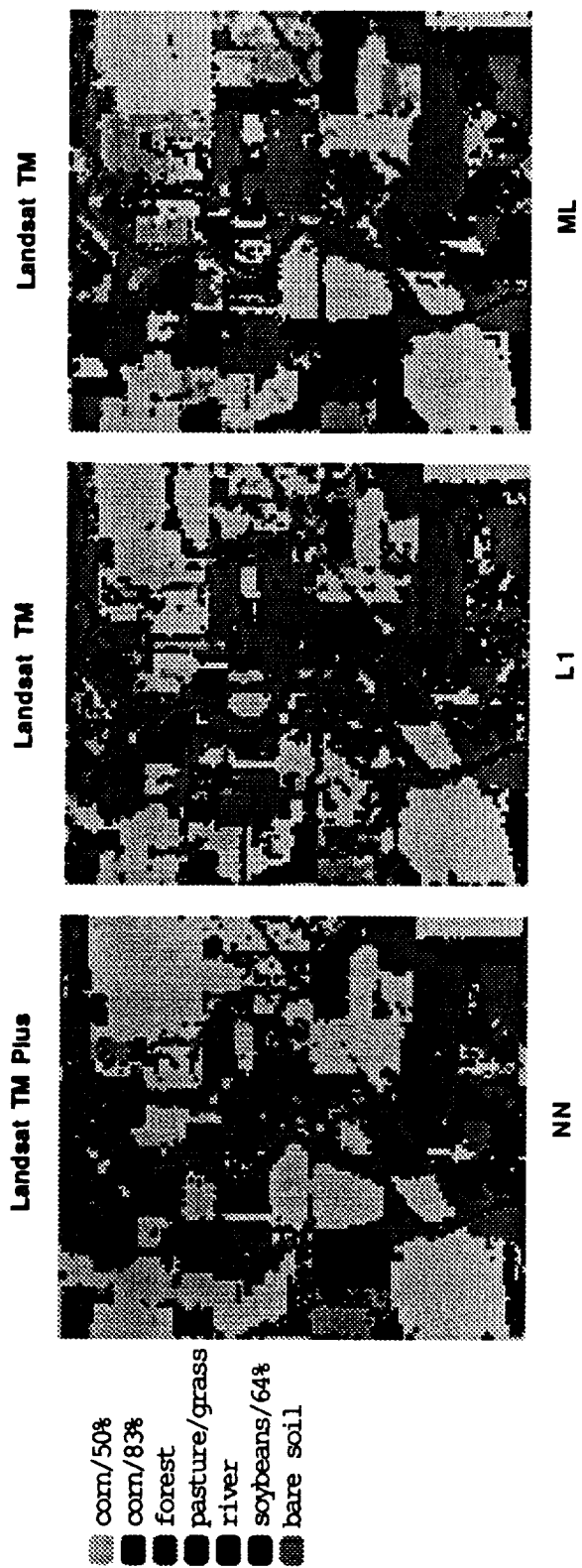


Figure 38. Classification results for the Landsat TM data of March 23, 1987.

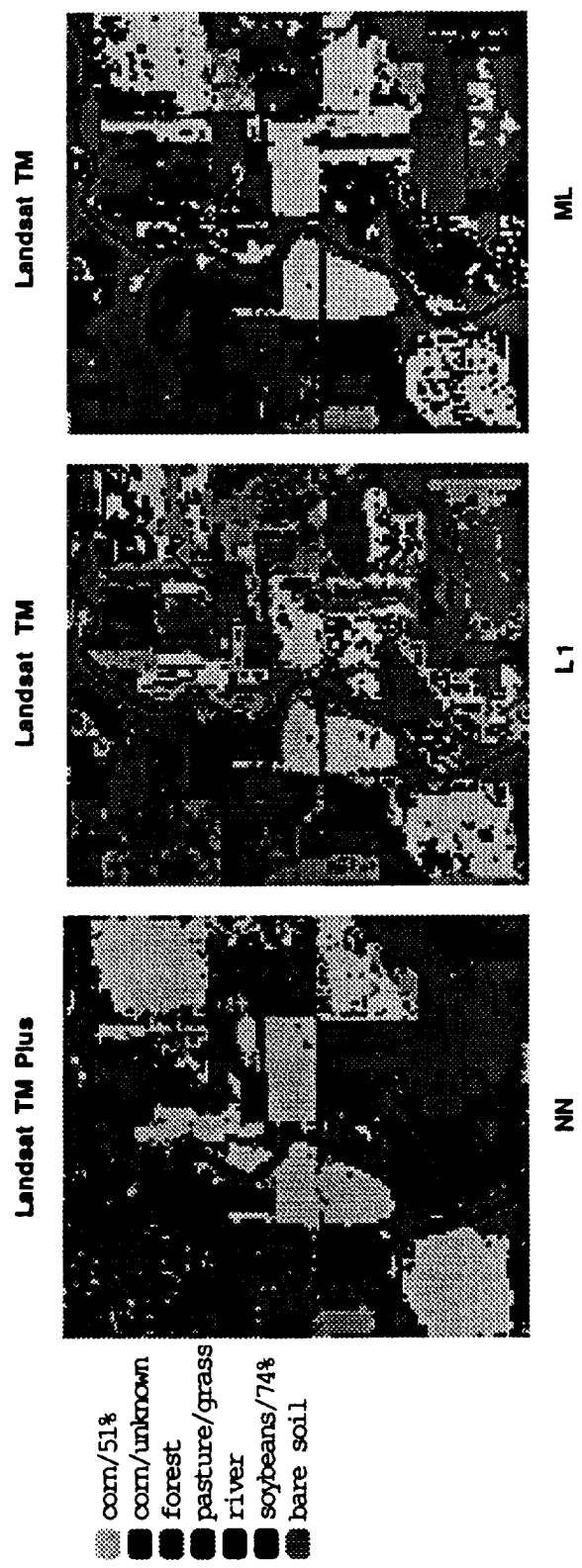


Figure 39. Classification results for the Landsat TM data of April 26, 1988.

4.6 Evaluation of Neural Network Training

Figures 40 and 41 show the neural network training processes and results for all seven images used. Table 28 lists the time spent for each neural network training. The corresponding configurations of the seven neural classifiers were previously listed in Table 7. Although three out of the seven images were produced by applying principal components and spectral ratioing transformations to the original Landsat TM images, the neural classifiers recognized them as new images as mentioned earlier. Therefore, there were a total of seven independent neuro-classifications corresponding to the images used. As seen in Figures 40 and 41, and Table 28, their training characteristics are different from one another, especially the maximum (Max) errors shown in Figure 40. First, the convergence for each eight-band image (March Plus and April Plus) starts at the very beginning of training whereas there is at least a thirty-cycle (half hour or so) plateau period of training for each seven-band image (March, April, PC March, PC April and SR March), and the trainings for both eight-band images arrive at the stable 10% error in less than one hundred cycles as shown in Table 28. Incorporating a GIS-layer made the neural training markedly faster compared to the trainings for all seven-band images except the original March, 1987 data, and made the neural training more predictable because it had no plateau period. Secondly, each seven-band April, 1988 data set took much longer to converge than its corresponding March, 1987 data set most likely because of the closer spectral characteristics for the crop residue classes and the bare soil class as described earlier. This shows again that the seven-band April images, either original or transformed, were more difficult to classify than the corresponding March images in this study. Thirdly, the PC data took a much longer time to converge than the corresponding original data. In addition to the accuracy consideration discussed earlier, it is shown again that the original images cost much less in terms of training time

than the PC images. Fourthly, all transformed data had a longer plateau training period, and the PC April, 1988 data had about twice as long or more of a plateau period as the PC and SR March, 1987 data. This indicates that the training for the transformed data, either principal components or spectral ratioing, was more unpredictable than that for the original data. Finally, the training time for the SR March, 1987 data was longer than that for the original March, 1987 data but shorter than that for the PC March, 1987 data.

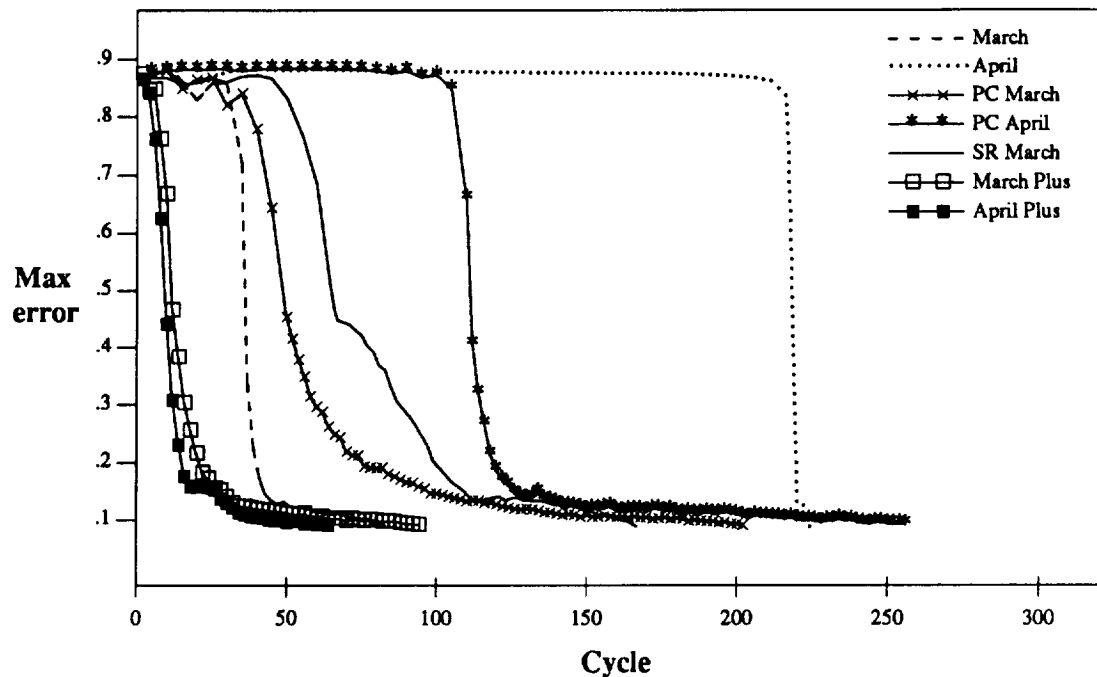


Figure 40. Max errors for all neural trainings.

For the *Root Mean Squared* (RMS) errors shown in Figure 41, the sharp drops start at the very beginning of training the classifiers for the Landsat TM Plus data. All RMS errors decreased relatively smoothly and there was no plateau period although there were a couple of peak points for the PC April, 1988 training data.

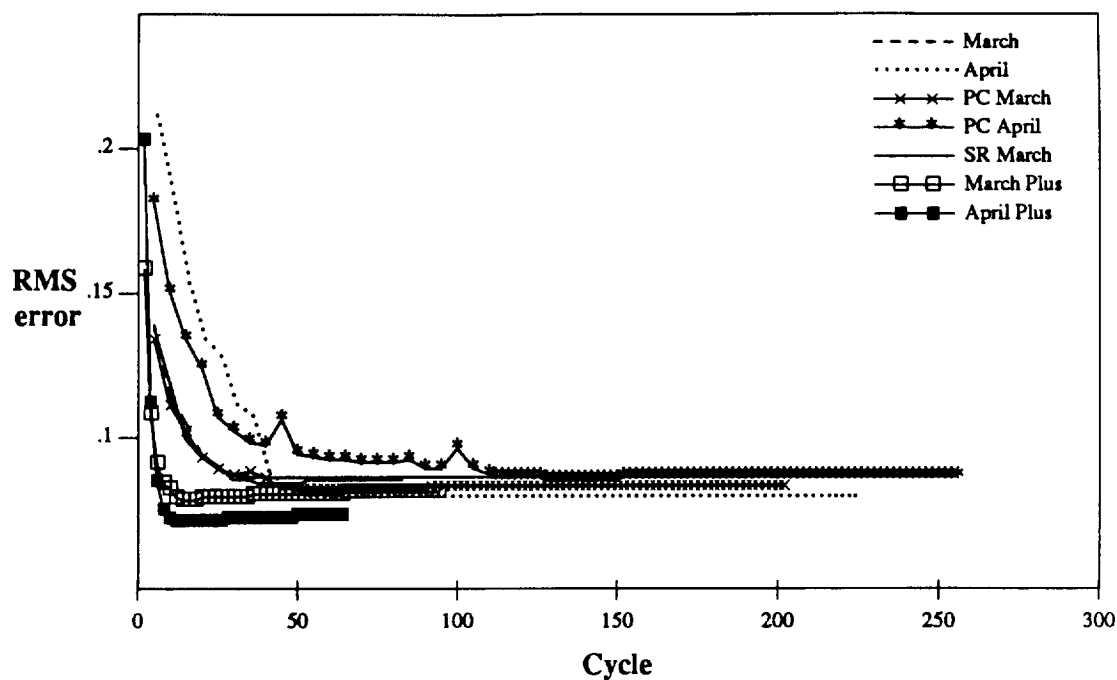


Figure 41. RMS errors for all neural trainings.

Table 28. Training behavior for the neural classifiers.

Data	Training cycles (cycle \approx 65sec)	Max error	RMS error
March	83	0.104	0.088
April	223	0.100	0.082
PC March	202	0.104	0.086
PC April	256	0.105	0.089
SR March	167	0.101	0.090
March Plus	94	0.104	0.084
April Plus	64	0.104	0.076

Maximum and RMS errors are two parameters to monitor and improve the training for neural networks. The RMS errors always decreased if there were adequate hidden layer units. In other words, if RMS errors did not decrease in the way shown in Figure 41, it would be

necessary to increase units for the corresponding hidden layer. However, too many units in a hidden layer would cause training to fall into a local minimum and become static at an undesired error. As seen in Figure 41, all RMS error curves dropped to less than 10% in about fifty cycles. If the error was greater than this percentage, for example 15%, it indicated that the learning rate factor, η , was too large and needed to be reduced. For the maximum errors, if they were unchanged within one hundred cycles, for example they were more than 89% at that time, the momentum, α , needed to be decreased because it was too big to reach the minimum. In summary, the adjustments for the learning rate factor, the momentum, and the number of units in the hidden layer were tradeoffs.

5. SUMMARY AND CONCLUSIONS

Landsat TM data for March 23, 1987 and April 26, 1988 with accompanying ground truth data for the study area in Miami County, Indiana were used to determine crop residue type and class. Three methods for image classification including Maximum Likelihood, L1 Minimum Distance, and neural networks, which are an emerging artificial intelligence technique, were utilized to investigate the best classifier for the estimation of crop residues.

Landsat TM data were able to determine crop residue type and class in a large area. This remote sensing approach overcomes the problems of range and topography that traditional methods of estimating crop residues have, and is suitable for ensuring USDA program compliance.

The spectral characteristics among the crop residue classes and between the crop residue classes and the bare soil class and other biomass classes were investigated using the Landsat TM scenes for the study area. Crop residue classes in the study area were separated from one another and from the bare soil class and other biomass classes, and two types of crop residue with four classes identified from each Landsat TM image. The lower the crop residue cover percentage, the less the moisture content and the higher the reflectance. The reflectance for crop residue classes was higher, and the differences among the crop residue classes and between the crop residue classes and the bare soil class were lower in April, 1988 than in March, 1987 because of the lower moisture content. Therefore, the crop residue classes were less separable in April, 1988 than in March, 1987.

The neural network classifier obtained better accuracies for the GIS-enhanced Landsat TM (Landsat TM Plus) data than the L1 Minimum Distance classifier, whereas the Maximum Likelihood classifier was not able to classify them because of its consideration of inverting the covariance matrix. However, the Maximum Likelihood classifier performed better classifications for the original Landsat TM data than the L1 Minimum Distance classifier and the neural network classifier. The L1 Minimum Distance classifier obtained worse accuracies for the original Landsat TM data and the Landsat TM Plus data.

A GIS layer, *ownership*, was added to each original Landsat TM image as the eighth band of data in an attempt to improve the classification results using the neural network back-propagation classifier. The classification results obtained by using the neural classifier showed clearer fields for crop residues and clear boundaries for these fields, less confusion among the crop residue classes, and no confusion between the crop residue classes and the bare soil class, compared to the results obtained by applying the Maximum Likelihood classifier to the original seven-band Landsat TM image data. Moreover, Maximum Likelihood could not be used for the generated eight-band data because the covariance matrices corresponding to each eight-band image had zero value determinants, and thus, the covariance matrices could not be inverted and thereby Maximum Likelihood could not be utilized. The minimum distance classifier did not obtain satisfactory classification accuracies because it does not consider the second order statistics, the covariances between image bands.

Principal components and spectral ratioing transformations were performed for the two original Landsat TM data sets to investigate the performances of the neural network classifiers. The neural network trainings for the transformed data sets took much longer than those for the original data sets, and the testing accuracies obtained by applying the maximum likelihood classifier and the neural classifier to the spectral ratioing transformed data were less than those

for other types of data. Therefore, using the original data would be less costly because it does not require a transformation. However, the principal components and spectral ratioing transformed images were visually more interpretable than the original ones when displayed on screen, and the neural classifier treated them as new data sets. In addition, the testing accuracies obtained by applying the neural classifier to these transformed images were less than those for the Maximum Likelihood classifier, but the corresponding training took longer times. Therefore, it can be concluded that transformation was not needed for the two original data sets.

The neural training times for the GIS-enhanced Landsat TM data sets were less than the times for other types of data including the original, and principal components and spectral ratioing transformed data, except for the original March data. The training for each GIS-enhanced eight-band data set converged at the very beginning of neural training whereas there was at least a thirty-cycle (half hour or so) plateau period of maximum errors for each seven-band image. The training for the seven-band April, 1988 data took much longer, and had a greater plateau period of maximum errors than that for the seven-band March, 1987 data. Moreover, the training for the transformed seven-band data sets took a longer time, and had a greater plateau period of maximum errors than that for the original seven-band data sets. Therefore, the neural classifier applied to the eight-band data sets, which were generated by incorporating a GIS layer, took the least time to converge to the desired error. However, neural training still required 50 cycles (more than 54 minutes) on SUN SPARC workstations. This was the major disadvantage for the neural networks used for image classification. As new generations of computers (faster and parallel processing computers) evolve, this problem will be overcome.

In the case of the neural classifiers, coding, including *encoding* and *decoding*, was important for the neural networks' convergence and the classification accuracies since neural networks know about nothing except numbers. Although decimal coding did not work for the

neuro-classifications, binary coding always performed well. Thermometer coding was appropriate for an output layer since it increased the accuracy of classification.

A fully interconnected three-layer neural network, which contained input, hidden and output layers, worked well for the neuro-classifications. However, it was necessary to scramble input/output pairs in order to present inputs to it in a random fashion before starting to train the neural network. This is required for back-propagation network theory to behave properly. Otherwise, the neural network training converged very slowly, or did not converge at all.

In the neuro-classification of all types of data, including both seven-band and eight-band, the initial learning rate, η , was 0.30 or 0.35. When the maximum error decreased to 0.1, it was changed to 0.7. Generally speaking, the higher the learning rate factor, the faster the neural network will learn, but the more reckless the learning and the greater the chances of the neural network being unable to accomplish the overall desired result. The final momentum value, α , was 0.9 while its initial value was 0.6 or 0.65 depending on the oscillation of neural network training.

6. RECOMMENDATIONS FOR FURTHER RESEARCH

Results in this study suggest that Landsat TM data can be used to estimate crop residue coverage in a large area for which traditional methods of determining residues would not be economical. Further research, including classifications of a series of images from late October to late May of the next year, and exact date-matching and sound ground truth is essential to investigate how crop residues change along with changing seasons in Indiana and most of the Midwest. The influence of soils beneath crop residues would be considered in the case of lower percent crop residue coverage. An atlas for crop residue spectral characteristics is needed for the future real time monitoring and classification of crop residues. In addition, an interactive satellite image processing linkage with GIS tools is needed in order to really integrate remote sensing with GIS. This would make a spatial database easy to enrich and update, and the classification of multitemporal data would be a daily routine.

In consideration of ground truth, acreage, yields, tillage and planting practices could be input into a spatial database of the study area in forms of GIS layers, and then the residue coverage corresponding to the ground truth could be spatially calculated based on these layers of information using Equation 3.1 listed in Chapter 3. A new layer for the initial residue coverage in the spatial database could be created as a result of the calculation. The new layer could be used for selection of training fields for image classification, or may be added to original satellite images as a new band of data to assist with the classification of multitemporal data.

Since the key point of successful neuro-classification is the representativeness and agreement of its training data, it is necessary to develop an effective selection procedure appropriate to it. Just as described above, map-based ground truth can be very helpful for selection of training data, and probably can make automatic selection of training data possible.

Incorporating other GIS layers of information, such as soil moisture, soil type, elevation, slope and drainage, may improve classification of remotely sensed data to estimate crop residue coverage and should be investigated. Also, neural network techniques should be added to the integrated GIS system.

Reducing training time for neuro-classification could be another area of further research, including unsupervised neuro-classification and neuro-classification with other neural network learning algorithms.

BIBLIOGRAPHY

BIBLIOGRAPHY

1. Anderson, J.A., 1989. Introduction to neural networks. *Proceedings of the 1989 IEEE Videoconferences Seminars Via Satellite*, Vol. 2.
2. Arnold, J.G., X. Zhuang, B.A. Engel, R. Srinivason, R. Muttiah, and C. Rewerts, 1990. Intelligent GIS for natural resource modeling and site selection. *Proceedings of the 1990 EPA Nonpoint Natural Resources and Remote Sensing*, Chicago, IL, Oct. 1-3, 1990.
3. Baffes, P.T., 1989. *Nets User's Manual. Version 2.0*. AIS at NASA/JSC, Athens, GA.
4. Baumgardner, M.F., L.F. Silva, L.L. Biehl, and E.R. Stoner, 1985. Reflectance properties of soils. *Advances in Agronomy*, Vol. 38, pp. 1-44.
5. Beasley, D.B., L.F. Hugins, and E.J. Monke, 1980. ANSWERS: a model for watershed planning. *Transactions of the ASAE*. 23(4), pp. 938-944.
6. Benediktsson J.A., P.H. Swain, and O.K. Ersoy, 1990. Neural network approaches versus statistical methods in classification of multisource remote sensing data. *IEEE Trans. Geoscience Remote Sensing*, GE-28(4), pp. 540-552.
7. Benediktsson J.A., P.H. Swain, and O.K. Ersoy, 1990. Classification of very high dimensional data using neural networks. *IGARSS' 90*, Vol. 2, pp. 1269-1272.
8. Caudill, M., 1987-1989. Neural networks primer. *AI Expert*.
9. Colwell, R.N., 1983. *Manual of Remote Sensing*, 2nd Edition, Vol. 2, pp. 2190-2228.
10. Decatur, S.E., 1989. Application of neural networks to terrain classification. *Proceedings of the 1989 International Joint Conference on Neural Networks*, Washington, D.C., Vol. 1, pp. 283-288.
11. DeGloria, S.D., S.L. Wall, A.S. Benson, and M.L. Whiting, 1986. Monitoring conservation tillage practices using Landsat multispectral data. *Journal of Soil Water Conservation*, May-June, pp. 187-190.
12. Ekmiller, R., and von der C. Malsbury, 1988. *Neural Computers*. Springer-Verlag, New York.
13. ERDAS, Inc., 1988. *ERDAS User's Guide. Version 7.3*.
14. Foster, G.R., L.J. Lane, D.L. Shertz, J.O. Nordin, and G.D. Wingate, 1987. User requirements: USDA-water erosion prediction project(WEPP), *ASAE Technical Paper 87-2539*, ASAE, St. Joseph, MI.
15. Hancock, P.J.B., 1988. Data representation in neural nets: an empirical study. *Proceedings of the 1987 IEEE International Conference on Neural Networks*, San Diego, CA, pp.

11-20.

16. Harwig, R.O., and J.M. Laflen. 1978. A meterstick method for measuring crop residue cover. *Journal of Soil and Water Conservation*, 33(2), pp. 90-91.
17. Heermann, P.D., N. Khazence, 1990. Analysis of large multi-dimensional data with back-propagation neural networks. *Proceedings of IJCNN 90, International Joint Conference on Neural Networks*, San Diego, CA, Vol. 1, pp. 525-530.
18. Hepner, G.F., T. Logan, N. Ritter, and N. Bryant, 1990. Artificial neural network classification using a minimal training set: comparison to conventional supervised classification. *Photogrammetric Engineering and Remote Sensing*, 56(4), pp. 496-473.
19. Hill, P.R., J.V. Mannering, and J.R. Wilcox, 1989. Estimating corn and soybeans residue cover, *Agronomy Guide*, Soils AY-269, Cooperative Extension Service, Purdue University.
20. Key, J., J.A. Maslanik, and A.J. Schweiger, 1989. Classification of merged AVHRR and SMMR Arctic data with neural networks. *Photogrammetric Engineering and Remote Sensing*, 55(9), pp. 1331-1338.
21. Knisel, W.G. (ed.), 1980. CREAMS: a field scale model for chemicals, runoff, and erosion from agricultural management systems. *USDA Conservation Research Report*, No. 26, 643p.
22. Kolm, K.E., and H.L. Case, 1984. The identification of irrigated crop types and estimation of acreages from Landsat imagery. *Photogrammetric Engineering and Remote Sensing*, 50(10), pp. 1479-1490.
23. Kuczewski, R.M., M.H. Myers, and W.J. Crawford, 1987. Neurocomputers workstations and processors: approaches and applications. *Proceedings of the 1987 IEEE International Conference on Neural Networks*, San Diego, CA. pp. 487-500
24. Laflen, J.M., M. Amemiya, and E.A. Hintz, 1981. Measuring crop residue cover. *Journal of Soil Water Conservation*, November-December, pp. 341-343.
25. Landgrebe, D.A., and L.L. Biehl, 1990. *An introduction to MacLARSYS. Version 1.25*. Laboratory of Applications for Remote Sensing, Purdue University, West Lafayette, IN.
26. Lillesand, T.M., and R.W. Kiefer, 1987. *Remote Sensing and Image Interpretation*, John Wiley and Sons, New York, N.Y., pp. 531-699.
27. Lowery, B., T.M. Lillesand, D.H. Mueller, P. Weiler, F.L. Scarpace, and T.C. Danial, 1984. Determination of crop residue cover using scanning microdensitometry. *Journal of Soil and Water Conservation*, November-December, pp. 402-403.
28. Maas, S.J., 1988. Using satellite data to improve model estimates of crop yield. *Agronomy Journal*, Vol. 80, July-August, pp. 655-662.
29. Mannering, J.V., 1989. Conservation tillage to maintain soil productivity and improve water quality. *Agronomy Guide*, Tillage AY-222, Cooperative Extension Service, Purdue University.
30. Mather, P.M., 1987. *Computer Processing of Remotely-Sensed Images : An Introduction*, John Wiley & Sons, Inc., pp. 179-241.

31. NeuralWare, Inc. 1989. *NeuralWorks User's Manual, reversion 2.00*, NeuralWare, Inc., Sewickly, PA. pp. 1-45.
32. Nguyen, D.D., and J.S. Lee, 1989. A new LMS-based algorithm for rapid adaptive classification in dynamic environments. *Neural Networks, Vol. 2*, pp. 15-228
33. Olsen, M.V., and T.L. Fisher, 1986. Land cover classification of agricultural lands utilizing Landsat TM Data. *Report No. TS-AMD-84141*, Lockheed Engineering Management Services Corp., USEPA-EMSL, Las Vegas, Nevada 89114.
34. Oschwald, W.R., M. Stelly, D.M. Kral, and J.H. Nauseef, 1978. *Crop Residue Management Systems*. ASA Special, Vol. 31, pp. 1-48.
35. Richards, J.A., 1986. *Remote Sensing Digital Image Analysis : An Introduction*. Springer-Verlag, Berlin, West Germany, 281p.
36. Rumelhart, D.E., G.E. Hinton, and R.J. Williams, 1986. *Parallel Distributed Processing*. MIT Press, Cambridge, Mass. chapter 9, 10 and 11.
37. Ryerson, R.A., R.N. Dobbins, and C. Thibault, 1985. Timely crop area estimates from Landsat. *Photogrammetric Engineering and Remote Sensing*, 51(11), pp. 1735-1743.
38. Schaal, G.M., 1986. Analysis of thematic mapper classification of tillage practices in Seneca county, Ohio: including a discussion on the selection of ground truth sites. *Grant No. R-005845-01*, Great Lakes National Program Office, USEPA Region 5, Chicago, IL 60605.
39. Schowengerdt, R.A., and H. Wang, 1990. A general purpose expert system for image processing. *Photogrammetric Engineering and Remote Sensing*, 55(9), pp. 1277-1284.
40. Sloneker, L.L., and W.C. Moldenhauer, 1977. Measuring the amounts of crop residue remaining after tillage. *Journal of Soil and Water Conservation*, September-October, pp. 231-236.
41. Srinivasan A., and J.A. Richards, 1990. Knowledge-based techniques for multi-source classification. *International Journal Remote Sensing*, 11(3), pp. 505-525.
42. Stephens, P.R., J.K. Macmillan, J.L. Daigle, and J. Cihlar, 1985. Estimating universal soil loss equation factor values with aerial photography. *Journal of Soil and Water Conservation*, May-June, pp. 293-296.
43. Swain, P.H., and S.M. Davis, 1978. *Remote Sensing : The Quantitative Approach*. McGraw-Hill International Book Co.
44. Tank, D.W., and J.J. Hopfield, 1987. Collective computation in neuronlike circuits. *Scientific American*, Dec., pp. 104-114.
45. Touretzky D.S., 1989. What's hidden in the hidden layer?. *Byte*, Aug., pp. 227-233.
46. Wasserman, P.D., 1989. *Neural Computing, Theory and Practice*. Van Nostrand Reinhold Press, New York, 230p.
47. Widrow, B., and M.E. Hoff, 1960. Adaptive switching circuits. *IRE WESCON, Conv. record*, New York, pp. 96-104

48. Widrow, B. and R. Winter, 1988. Neural nets for adaptive filtering and adaptive pattern recognition. *IEEE Computer*, 21, pp. 25-39.
49. Wischemier, W.M., and D.D. Smith, 1978. *Predicting runoff erosion losses-A guide to conservation planning*. Agr. Handbook. No. 537. U.S. Dept. Agr., Washington, D.C., 58p.
50. Wu, Y., 1988. *Quantitative Assessment of Landsat TM Data for Detailed Soil Mapping*, M.S. thesis, the Department of Agronomy, Purdue University.
51. Zhuang, X., and B.A. Engel, 1990. Neural networks for applications in agriculture. *ASAE Technical Paper 90-7024*, ASAE, St. Joseph, MI.
52. Zhuang, X., and B.A. Engel, 1990. Classification of multispectral remote sensing data using neural networks vs statistical methods. *ASAE Technical Paper 90-7552*, ASAE, St. Joseph, MI. *to be presented at the ASAE Winter Meeting in Chicago, IL, December 18-21.*

APPENDICES

Appendix A. Ground Truth Data Survey Form

Table 1. Ground truth survey form A, 1986.

CROPPING HISTORY FOR FARMS IN SECTIONS SELECTED
FOR NASA SATELLITE RESEARCH PROJECT
SOIL MANAGEMENT PHASE

Farmer's (or operator's) name: RALPH GRANDSTAFF
Farm location: SECTION 9/28N/5E SOUTHEAST CORNER
RD 900N AND 500E

Cropping year (1986 - 1987 - 1988) Circle one
-- Fill out one sheet for each year --

Field Number:	<u>1</u>				
No. of Acres:	<u>21.5</u>				
Crop:	<u>Fallow</u>				
Primary Tillage System Used: (check)					
No-Till		<u>Working on field to control</u>			
Ridge Till		<u>CANADA THISTLE</u>			
Chisel Straight or Twisted Pts					
MB Plow					
Disk 3 or 6 inches					
Planter has: Smooth or no coulters:					
Narrow Ripple Coulter (<1.5"):					
Date of Fall or Spring tillage:					
Date of Planting:					
Date of Harvest:					
Soil Mgt. Practices: (Answer yes No)					
Terraces:	<u>NO</u>				
Contours:	<u>NO</u>				
Strip Crop:	<u>NO</u>				
Tile Drained:	<u>YES</u>				
Irrigation:	<u>NO</u>				
If Crop was CRP or Set-a-side What was Seeded?					

Table 2. Ground truth survey form A, 1987.

CROPPING HISTORY FOR FARMS IN SECTIONS SELECTED
FOR NASA SATELLITE RESEARCH PROJECT
SOIL MANAGEMENT PHASE

Farmer's (or operator's) name: RALPH GRANDSTAFF
Farm location: SECTION 9/28N/5E SOUTHEAST CORNER
RD 900N AND 500E

Cropping year (1986 - (1987) - 1988) Circle one
-- Fill out one sheet for each year --

Field Number:	<u>1</u>				
No. of Acres:	<u>21.5</u>				
Crop:	<u>Fallow</u>				
Primary Tillage System Used: (check)					
No-Till		<u>working on field to control CANADA THISTLE</u>			
Ridge Till					
Chisel Straight or Twisted Pts					
MB Plow					
Disk 3 or 6 inches					
Planter has: Smooth or no coulters:					
Narrow Ripple Coulters (<1.5"):					
Date of Fall or Spring tillage:					
Date of Planting:					
Date of Harvest:					
Soil Mgt. Practices: (Answer yes No)					
Terraces:	<u>NO</u>				
Contours:	<u>NO</u>				
Strip Crop:	<u>NO</u>				
Tile Drained:	<u>YES</u>				
Irrigation:	<u>NO</u>				
If Crop was CRP or Set-a-side What was Seeded?					

ORIGINAL PAGE IS OF POOR QUALITY

Table 3. Ground truth survey form A, 1988.

CROPPING HISTORY FOR FARMS IN SECTIONS SELECTED
FOR NASA SATELLITE RESEARCH PROJECT
SOIL MANAGEMENT PHASE

Farmer's (or operator's) name: Ralph GRANDSTAFF

Farm location: SECTION 9/2EN/SE SOUTHEAST CORNER
Rd 900N AND 502E

Cropping year (1986 - 1987 - 1988) Circle one
-- Fill out one sheet for each year --

Field Number:	<u>1</u>				
No. of Acres:	<u>21.5</u>				
Crop:	<u>OTS</u>				
Primary Tillage System Used: (check)					
No-Till					
Ridge Till					
Chisel Straight or Twisted Pts					
HB Plow					
Disk 3 or 6 inches	<input checked="" type="checkbox"/>				
<u>3"</u>					
Planter has: Smooth or no couller:					
Narrow Ripple Couller (<1.6"):					
Date of Fall or Spring tillage:	<u>APR</u>				
Date of Planting:	<u>APR</u>				
Date of Harvest:	<u>July</u>				
Soil Mgt. Practices: (Answer yes No)					
Terraces:	<u>NO</u>				
Contours:	<u>NO</u>				
Strip Crop:	<u>NO</u>				
Tile Drained:	<u>YES</u>				
Irrigation:	<u>NO</u>				
If Crop was CRP or Set-a-side What was Seeded?					

ORIGINAL PAGE IS
OF POOR QUALITY

Table 4. Ground truth survey form B.

CROPPING HISTORY FOR FARMS IN SECTIONS SELECTED
FOR NASA SATELLITE RESEARCH PROJECT
SOIL MANAGEMENT PHASE

Farmer's (or operator's) name: Johil Livingood
 Farm location: SECTION 9/28N/5E SOUTHSIDE OF
Rd 900N 1/4-1/2 MILE EAST OF 500 EAST

Cropping year (1986 - 1987 - 1988) Circle one
 -- Fill out one sheet for each year --

Field Number:	<u>1</u>				
No. of Acres:	<u>60</u>				
Crop:	<u>PERM PASTURE</u>				
Primary Tillage System Used: (check)					
No-Till					
Ridge Till					
Chisel					
Straight or Twisted Pts					
MB Plow					
Disk					
3 or 6 inches					
Planter has:					
Smooth or no coulters:					
Narrow Ripple Coulters (<1.5"):					
Date of Fall or Spring tillage:					
Date of Planting:					
Date of Harvest:					
Soil Mgt. Practices: (Answer yes No)					
Terraces:	<u>NO</u>				
Contours:	<u>NO</u>				
Strip Crop:	<u>NO</u>				
Tile Drained:	<u>NO</u>				
Irrigation:	<u>NO</u>				
If Crop was CRP or Set-a-side What was Seeded?					

Table 5. Ground truth survey form C, 1986.

CROPPING HISTORY FOR FARMS IN SECTIONS SELECTED
FOR NASA SATELLITE RESEARCH PROJECT
SOIL MANAGEMENT PHASE

Farmer's (or operator's) name: DEARBORFF FARMS INC

Farm location: SECTION 9/28N/5E SOUTH SIDE OF
Rd 900N 1/2 MILE EAST OF 500E

Cropping year (1986 - 1987 - 1988) Circle one
-- Fill out one sheet for each year --

Field Number:	<u>7</u>				
No. of Acres:	<u>57.0</u>				
Crop:	<u>CORN</u>				
Primary Tillage System Used: (check)					
No-Till					
Ridge Till					
Chisel Straight or Twisted Pts					
MB Plow	<input checked="" type="checkbox"/>				
Disk 3 or 6 inches					
Planter has: Smooth or no coulter:	<input checked="" type="checkbox"/>				
Narrow Ripple Coulter (<1.5"):					
Date of Fall or Spring tillage:	<u>MAY 5</u>				
Date of Planting:	<u>MAY 7</u>				
Date of Harvest:	<u>OCT 7</u>				
Soil Mgt. Practices: (Answer yes No)					
Terraces:	<u>NO</u>				
Contours:	<u>NO</u>				
Strip Crop:	<u>NO</u>				
Tile Drained:	<u>NO</u>				
Irrigation:	<u>YES</u>				
If Crop was CRP or Set-a-side What was Seeded?					

ORIGINAL PAGE IS
OF POOR QUALITY

Table 6. Ground truth survey form C, 1987.

CROPPING HISTORY FOR FARMS IN SECTIONS SELECTED
FOR NASA SATELLITE RESEARCH PROJECT
SOIL MANAGEMENT PHASE

Farmer's (or operator's) name: DEARDORFF FARMS INC

Farm location: SECTION 10 1/2 28N/5E SOUTH SIDE OF
Rd 900N 1/2 MILE EAST OF Rd 500E

Cropping year (1986 - (1987) - 1988) Circle one
-- Fill out one sheet for each year --

Field Number:	<u>7</u>				
No. of Acres:	<u>57</u>				
Crop:	<u>CORN</u>				
Primary Tillage System Used: (check)					
No-Till					
Ridge Till					
Chisel	<input checked="" type="checkbox"/>				
Straight or Twisted Pts:	<u>TWISTED</u>				
MB Plow					
Disk 3 or 6 inches					
Planter has: Smooth or no coulters:	<input checked="" type="checkbox"/>				
Narrow Ripple Coulters (<1.5"):					
Date of Fall or Spring tillage:	<u>FALL 86</u> <u>OCT 22</u>				
Date of Planting:	<u>APR 25</u>				
Date of Harvest:	<u>SEP 19</u>				
Soil Mgt. Practices: (Answer yes No)					
Terraces:	<u>NO</u>				
Contours:	<u>NO</u>				
Strip Crop:	<u>NO</u>				
Tile Drained:	<u>NO</u>				
Irrigation:	<u>YES</u>				
If Crop was CRP or Set-a-side What was Seeded?					

ORIGINAL PAGE IS
OF POOR QUALITY

Table 7. Ground truth survey form C, 1988.

CROPPING HISTORY FOR FARMS IN SECTIONS SELECTED
FOR NASA SATELLITE RESEARCH PROJECT
SOIL MANAGEMENT PHASE

Farmer's (or operator's) name: DEARDORFF FARMS INC
 Farm location: SECTION 9/28N/5E SOUTH SIDE OF
RD 900N 1/2 MILE EAST OF 500E

Cropping year (1986 - 1987 - (1988)) Circle one
 -- Fill out one sheet for each year --

Field Number:	<u>7</u>				
No. of Acres:	<u>59</u>				
Crop:	<u>CORN</u>				
Primary Tillage System Used: (check)					
No-Till					
Ridge Till					
Chisel	<input checked="" type="checkbox"/>				
Straight or Twisted Pts:	<u>TWISTED</u>				
MB Plow					
Disk 3 or 6 inches					
Planter has: Smooth or no coulters:	<input checked="" type="checkbox"/>				
Narrow Ripple Coulters (<1.5"):					
Date of Fall or Spring tillage:	<u>Nov 9</u>				
Date of Planting:	<u>APR 30</u>				
Date of Harvest:	<u>SEP 27</u>				
Soil Mgt. Practices: (Answer yes No)					
Terraces:	<u>NO</u>				
Contours:	<u>NO</u>				
Strip Crop:	<u>NO</u>				
Tile Drained:	<u>NO</u>				
Irrigation:	<u>YES</u>				
If Crop was CRP or Set-a-side What was Seeded?					

ORIGINAL PAGE IS
OF POOR QUALITY

Table 8. Ground truth survey form D, 1986.

CROPPING HISTORY FOR FARMS IN SECTIONS SELECTED
FOR NASA SATELLITE RESEARCH PROJECT
SOIL MANAGEMENT PHASE

Farmer's (or operator's) name: GENE GRISMORE

Farm location: SECTION 9/28N/5E WESTSIDE OF
Rd 600E PART OF NORTHEAST 1/4 SECTION

Cropping year (1986 - 1987 - 1988) Circle one
-- Fill out one sheet for each year --

	1986	1987	1988			
Field Number:	12	11	7			
No. of Acres:	27	32 1/2	13			
Crop:	ALFALFA	BEANS	CORN			
Primary Tillage System Used: (check)						
No-Till						
Ridge Till						
Chisel						
Straight or Twisted Pts						
MB Plow	✓		✓			
Disk		✓				
3 or 6 inches		3				
Planter has: Smooth or no coulters:		✓	✓			
Narrow Ripple Coulters (< 1.5"):						
Date of Fall or Spring tillage:	AUG 85	MAY 17	APR 10-15			
Date of Planting:	AUG 85	MAY 18	APR 28			
Date of Harvest:	JUNE July Aug	Late Sep	Early Oct			
Soil Mgt. Practices: (Answer yes No)						
Terraces:	NO	NO	NO			
Contours:	NO	NO	NO			
Strip Crop:	NO	NO	NO			
Tile Drained:	NO	NO	NO			
Irrigation:	NO	NO	NO			
If Crop was CRP or Set-aside What was Seeded?						

ORIGINAL PAGE IS
OF POOR QUALITY

Table 9. Ground truth survey form D, 1987.

CROPPING HISTORY FOR FARMS IN SECTIONS SELECTED
FOR NASA SATELLITE RESEARCH PROJECT
SOIL MANAGEMENT PHASE

Farmer's (or operator's) name: GENE CRISMORE

Farm location: SECTION 9/28N/5E WESTSIDE OF
RD 600E PART OF NORTHEAST 14 SECTION

Cropping year (1986 - (1987) - 1988) Circle one
-- Fill out one sheet for each year --

Field Number:	7	11	11A & 11B	12		
No. of Acres:	13.0	6.4	26	27		
Crop:	SOY BEANS	PCR	Soybeans	WRY		
Primary Tillage System Used: (check):						
No-Till						
Ridge Till						
Chisel Straight or Twisted Pts						
MB Plow	✓			✓		
Disk 3 or 6 inches		✓	✓			
		3"	3"			
Planter has: Smooth or no coulters:	✓		✓			
Narrow Ripple Coulters (<1.5"):						
Date of Fall or Spring tillage:	NPR	APR	MAY 10	Aug 85		
Date of Planting:	MAY	APR	MAY 20	Aug 85		
Date of Harvest:	LATE SEP		SEP	JUNE JULY AUG		
Soil Mgt. Practices: (Answer yes No)						
Terraces:	NO	NO	NO	NO		
Contours:	NO	NO	NO	NO		
Strip Crop:	NO	NO	NO	NO		
Tile Drained:	NO	NO	NO	NO		
Irrigation:	NO	NO	NO	NO		
If Crop was CRP or Set-a-side What was Seeded?		LEGUME MIX				

ORIGINAL PAGE IS
OF POOR QUALITY

Table 10. Ground truth survey form D, 1988.

CROPPING HISTORY FOR FARMS IN SECTIONS SELECTED
FOR NASA SATELLITE RESEARCH PROJECT
SOIL MANAGEMENT PHASE

Farmer's (or operator's) name: GENE GRISMORE

Farm location: SECTION 9/28N/5E WEST SIDE OF
RD 600 E PART OF NORTHEAST 1/4 SECTION

Cropping year (1986 - 1987 - 1988) Circle one
-- Fill out one sheet for each year --

Field Number:	11	7	12			
No. of Acres:	32.5	13	27			
Crop:	Soybeans	Soybeans	Alf. Hay			
Primary Tillage System Used: (check)						
No-Till						
Ridge Till						
Chisel Straight or Twisted Pts						
HB Plow			✓			
Disk 3 or 6 inches	✓ 3"	✓ 3"				
Planter has: Smooth or no coulters:	✓	✓				
Narrow Ripple Coulters (<1.5"):						
Date of Fall or Spring tillage:	MAY 10	MAY 10	AUG 85			
Date of Planting:	MAY 10	MAY 10	AUG 85			
Date of Harvest:	LATE SEP	SEP	MAY JUNE JULY			
Soil Mgt. Practices: (Answer yes No)						
Terraces:	NO					
Contours:	NO					
Strip Crop:	NO					
Tile Drained:	NO					
Irrigation:	NO					
If Crop was CRP or Set-a-side What was Seeded?						

ORIGINAL PAGE IS
OF POOR QUALITY

Table 11. Ground truth survey form E, 1986.

CROPPING HISTORY FOR FARMS IN SECTIONS SELECTED
FOR NASA SATELLITE RESEARCH PROJECT
SOIL MANAGEMENT PHASE

Farmer's (or operator's) name: JOHN W. WILSON

Farm location: SECTION 9/28N/5E EAST SIDE OF
Rd 500E SOUTHWEST 1/4 SECTION

Cropping year (1986) - 1987 - 1988) Circle one
-- Fill out one sheet for each year --

Field Number:	1A	1B	2A	2B		
No. of Acres:	10	131.8	6.9	26.6		
Crop:	ACR	CORN	CORN	ACR		
Primary Tillage System Used: (check)						
No-Till						
Ridge Till						
Chisel Straight or Twisted Pts		✓	✓			
MB Plow		Twisted	Twisted			
Disk 3 or 6 inches						
Planter has: Smooth or no coulters:						
Narrow Ripple Coulters (<1.5"):		✓	✓			
Date of Fall or Spring tillage:		Nov 15	Oct 15			
Date of Planting:		APR 25	APR 25			
Date of Harvest:		SEP 28	SEP 28			
Soil Mgt. Practices: (Answer yes No)						
Terraces:	NO	NO	NO	NO		
Contours:	NO	NO	NO	NO		
Strip Crop:	NO	NO	NO	NO		
Tile Drained:	NO	NO	NO	NO		
Irrigation:	NO	NO	YES	NO		
If Crop was CRP or Set-a-side What was Seeded?	GRASS MIXTURE			GRASS MIXTURE		

ORIGINAL PAGE IS
OF POOR QUALITY

Table 12. Ground truth survey form E, 1987.

CROPPING HISTORY FOR FARMS IN SECTIONS SELECTED
FOR NASA SATELLITE RESEARCH PROJECT
SOIL MANAGEMENT PHASE

Farmer's (or operator's) name: JOHN W. WILSON

Farm location: SECTION 9/28N/5E EAST SIDE
OF ROAD 300 E SOUTHWEST 1/4 SECTION

Cropping year (1986 - 1987 - 1988) Circle one
-- Fill out one sheet for each year --

Field Number:	1A	1B	2A	2B		
No. of Acres:	10	131.8	6.9	26.6		
Crop:	ACR	CORN	CORN	ACR		
Primary Tillage System Used: (check)						
No-Till						
Ridge Till						
Chisel Straight or Twisted Pts:		✓ Twisted	✓ Twisted			
HB Plow						
Disk 3 or 6 inches						
Planter has: Smooth or no coulters:						
Narrow Ripple Coulters (<1.5"):		✓	✓			
Date of Fall or Spring tillage:		OCT 28	OCT 28			
Date of Planting:		APR 25	APR 25			
Date of Harvest:		OCT 1	OCT 1			
Soil Mgt. Practices: (Answer yes No)						
Terraces:	NO	NO	NO	NO		
Contours:	NO	NO	NO	NO		
Strip Crop:	NO	NO	NO	NO		
Tile Drained:	NO	NO	NO	NO		
Irrigation:	NO	YES	YES	NO		
If Crop was CRP or Set-aside What was Seeded?	GRASS MIXTURE			GRASS MIXTURE		

Table 13. Ground truth survey form E, 1988.

CROPPING HISTORY FOR FARMS IN SECTIONS SELECTED
FOR NASA SATELLITE RESEARCH PROJECT
SOIL MANAGEMENT PHASE

Farmer's (or operator's) name: JOHN W. WILSON

Farm location: SECTION 9/28N/5E EASTSIDE OF
Rd 500E Southwest 1/4 SECTION

Cropping year (1986 - 1987 - (1988)): Circle one
-- Fill out one sheet for each year --

Field Number:	1A	1B	2A	2B		
No. of Acres:	10	131.8	6.9	26.6		
Crop:	ACP	CORN	CORN	ACP		
Primary Tillage System Used: (check)						
No-Till						
Ridge Till						
Chisel Straight or Twisted Pts		✓ Twisted	✓ Twisted			
MB Plow						
Disk 3 or 6 inches						
Planter has: Smooth or no coulters:						
Narrow Ripple Coulters (<1.5"):						
Date of Fall or Spring tillage:		NOV 1 APR 15	NOV 1			
Date of Planting:		APR 20	APR 20			
Date of Harvest:		SEP 25	SEP 25			
Soil Mgt. Practices: (Answer yes No)						
Terraces:	NO	NO	NO	NO		
Contours:	NO	NO	NO	NO		
Strip Crop:	NO	NO	NO	NO		
Tile Drained:	NO	NO	NO	NO		
Irrigation:	NO	YES	YES	NO		
If Crop was CRP or Set-a-side What was Seeded?	GRASS MIXTURE			GRASS MIXTURE		

ORIGINAL PAGE IS
OF POOR QUALITY

Table 14. Ground truth survey form F, 1986.

CROPPING HISTORY FOR FARMS IN SECTIONS SELECTED
FOR NASA SATELLITE RESEARCH PROJECT
SOIL MANAGEMENT PHASE

Farmer's (or operator's) name: LESTER & DORIS RAY
Farm location: SECTION 9/28N/5E SOUTHEAST 1/4
Rd 800 N WEST OF GODE

Cropping year (1986 - 1987 - 1988) Circle one
-- Fill out one sheet for each year --

Field Number:	1	2	3	4
No. of Acres:	44	22.2	12.5	8.2
Crop:	Soybeans	Soybeans	Soybeans	Soybeans
Primary Tillage System Used: (check)				
No-Till				
Ridge Till				
Chisel Straight or Twisted Pts:	✓	✓	✓	✓
MB Plow				
Disk 3 or 6 inches				
Planter has: Smooth or no couler:	✓	✓	✓	✓
Narrow Ripple Couler (<1.5"):				
Date of Fall or Spring tillage:	APR 86	APR 86	APR 86	APR 86
Date of Planting:	MAY 15	MAY 15	MAY 15	MAY 15
Date of Harvest:	OCT	OCT	OCT	OCT
Soil Mgt. Practices: (Answer yes No)				
Terraces:	NO	NO	NO	NO
Contours:	NO	NO	NO	NO
Strip Crop:	NO	NO	NO	NO
Tile Drained:	NO	NO	NO	NO
Irrigation:	NO	NO	NO	NO
If Crop was CRP or Set-a-side What was Seeded?				

ORIGINAL PAGE IS
OF POOR QUALITY

Table 15. Ground truth survey form F, 1987.

CROPPING HISTORY FOR FARMS IN SECTIONS SELECTED
FOR NASA SATELLITE RESEARCH PROJECT
SOIL MANAGEMENT PHASE

Farmer's (or operator's) name: LESTER & DORIS RAY
Farm location: SECTION 9/28N/5E SOUTHEAST 1/4
RD 800N WEST OF 600E

Cropping year (1986 - 1987 - 1988) Circle one
-- Fill out one sheet for each year --

Field Number:	1	2	3	4		
No. of Acres:	44	22.2	12.5	8.2		
Crop:	Soybeans	Soybeans	Soybeans	Soybeans		
Primary Tillage System Used:(check)						
No-Till						
Ridge Till						
Chisel	✓	✓	✓	✓		
Straight or Twisted Pts:	TWISTED	TWISTED	TWISTED	TWISTED		
MB Plow						
Disk 3 or 6 inches						
Planter has: Smooth or no coulter:	✓	✓	✓	✓		
Narrow Ripple Coulter (<1.5"):						
Date of Fall or Spring tillage:	APR 87	APR 87	APR 87	APR 87		
Date of Planting:	MAY 20	MAY 20	MAY 20	MAY 20		
Date of Harvest:	OCT	OCT	OCT	OCT		
Soil Mgt. Practices: (Answer yes No)						
Terraces:	NO	NO	NO	NO		
Contours:	NO	NO	NO	NO		
Strip Crop:	NO	NO	NO	NO		
Tile Drained:	NO	NO	NO	NO		
Irrigation:	NO	NO	NO	NO		
If Crop was CRP or Set-a-side What was Seeded?						

ORIGINAL PAGE IS OF POOR QUALITY

Table 16. Ground truth survey form F, 1988.

CROPPING HISTORY FOR FARMS IN SECTIONS SELECTED
FOR NASA SATELLITE RESEARCH PROJECT
SOIL MANAGEMENT PHASE

Farmer's (or operator's) name: LESTER & DORIS RAY

Farm location: SECTION 9/28N/5E SOUTHEAST 1/4
Rd 800N WEST OF 600E

Cropping year (1986 - 1987 - (1988)) Circle one
-- Fill out one sheet for each year --

Field Number:	1	2	3	4		
No. of Acres:	44	22.2	12.5	8.2		
Crop:	CRP	CRP	CRP	CRP		
Primary Tillage System Used: (check)						
No-Till						
Ridge Till						
Chisel Straight or Twisted Pts						
MB Plow						
Disk 3 or 6 inches	✓ 3"	✓ 3"	✓ 3"	✓ 3"		
Planter has: Smooth or no coulters:						
Narrow Ripple Coulters (<1.5"):						
Date of Fall or Spring tillage:	APR 88	APR 88	APR 88	APR 88		
Date of Planting:	APR	APR	APR	APR		
Date of Harvest:						
Soil Mgt. Practices: (Answer yes No)						
Terraces:	NO	NO	NO	NO		
Contours:	NO	NO	NO	NO		
Strip Crop:	NO	NO	NO	NO		
Tile Drained:	NO	NO	NO	NO		
Irrigation:	NO	NO	NO	NO		
If Crop was CRP or Set-a-side What was Seeded?	CRP & Clover	CRP & Clover	CRP & Clover	CRP & Clover		

Appendix B. Flown Aerial Photographs

Section 3:

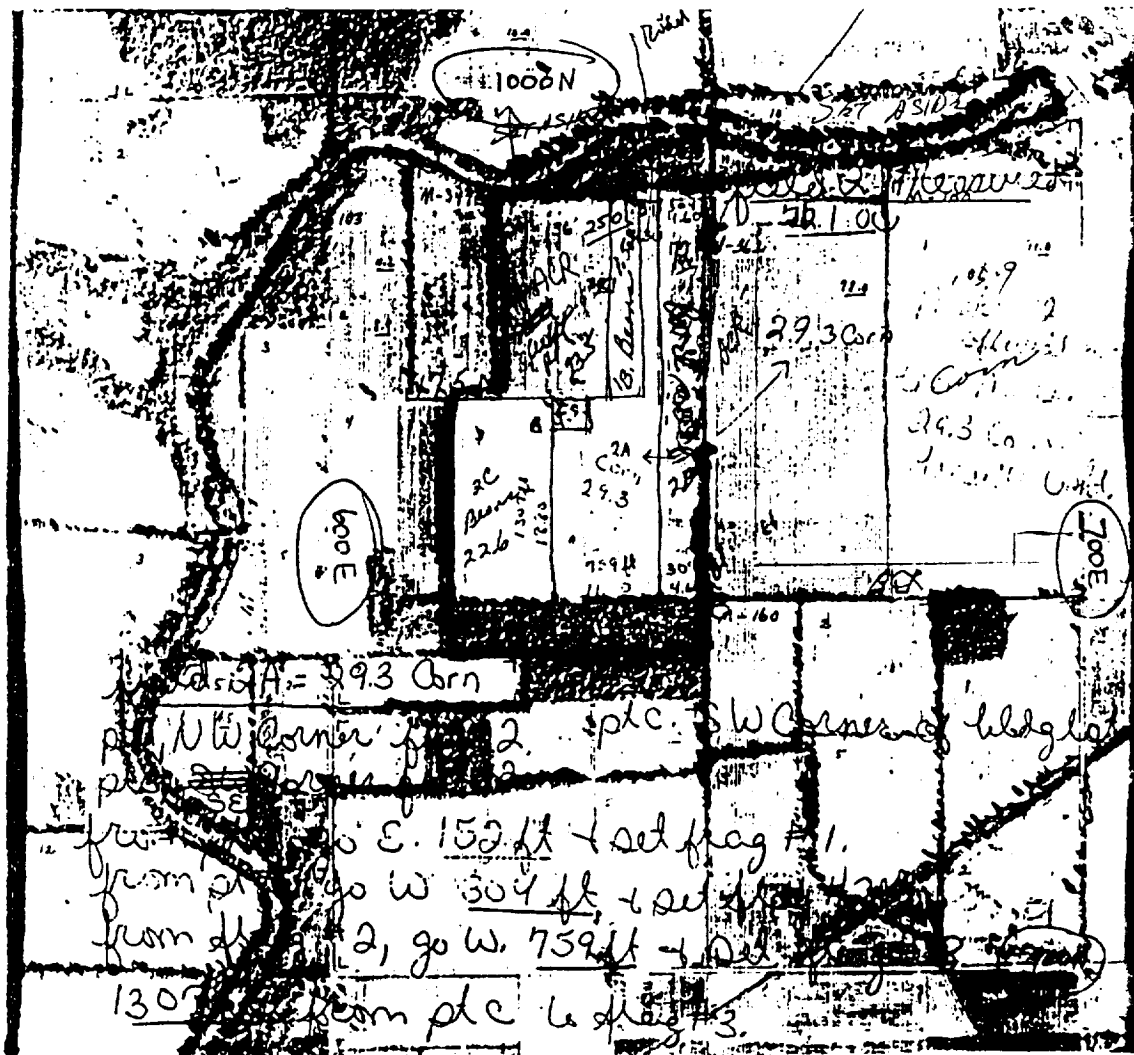


Figure 1. Photocopy A of flown aerial photograph for section 3.

ORIGINAL PAGE IS
OF POOR QUALITY

Section 4:

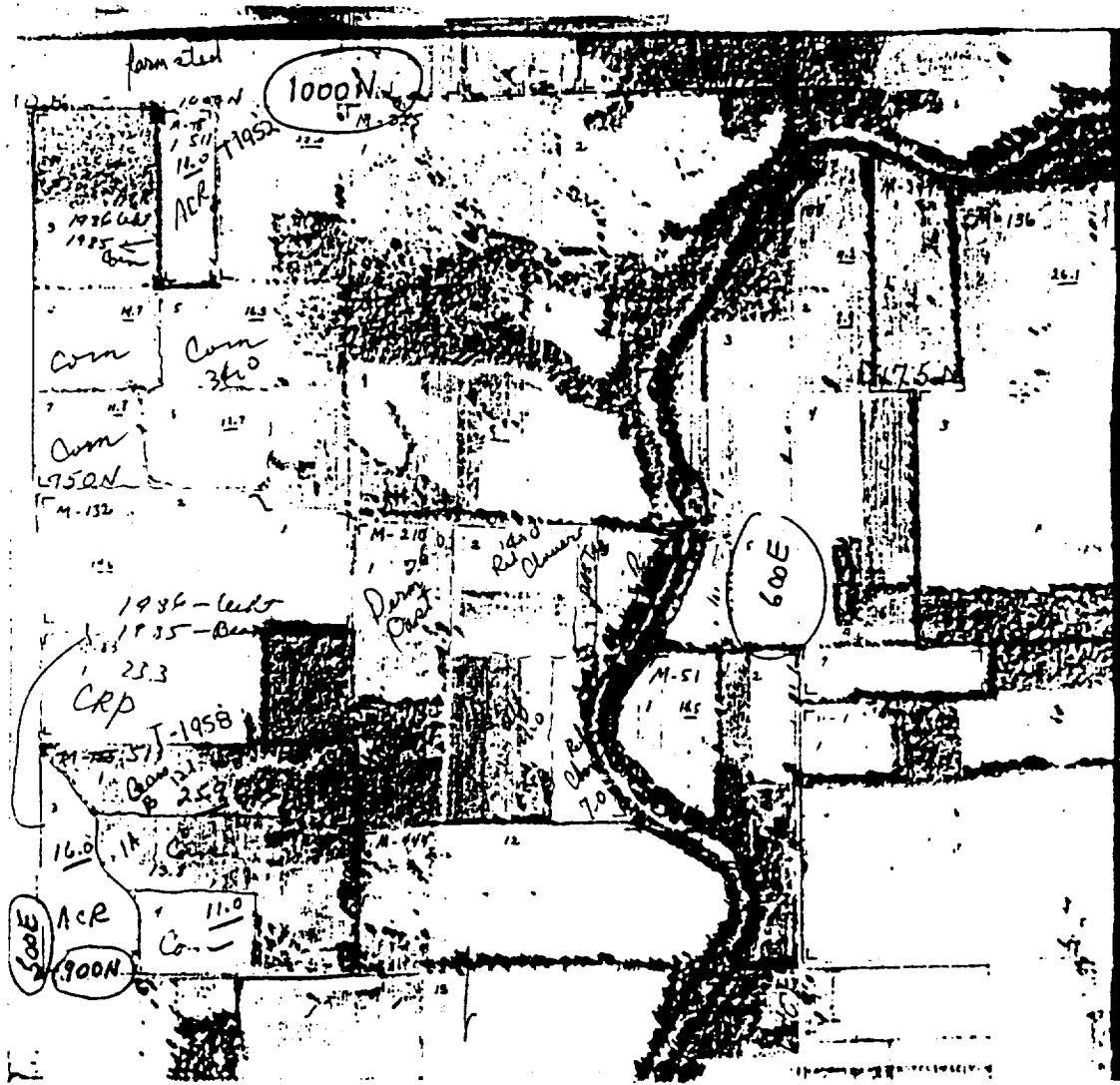


Figure 2. Photocopy A of flown aerial photograph for section 4.

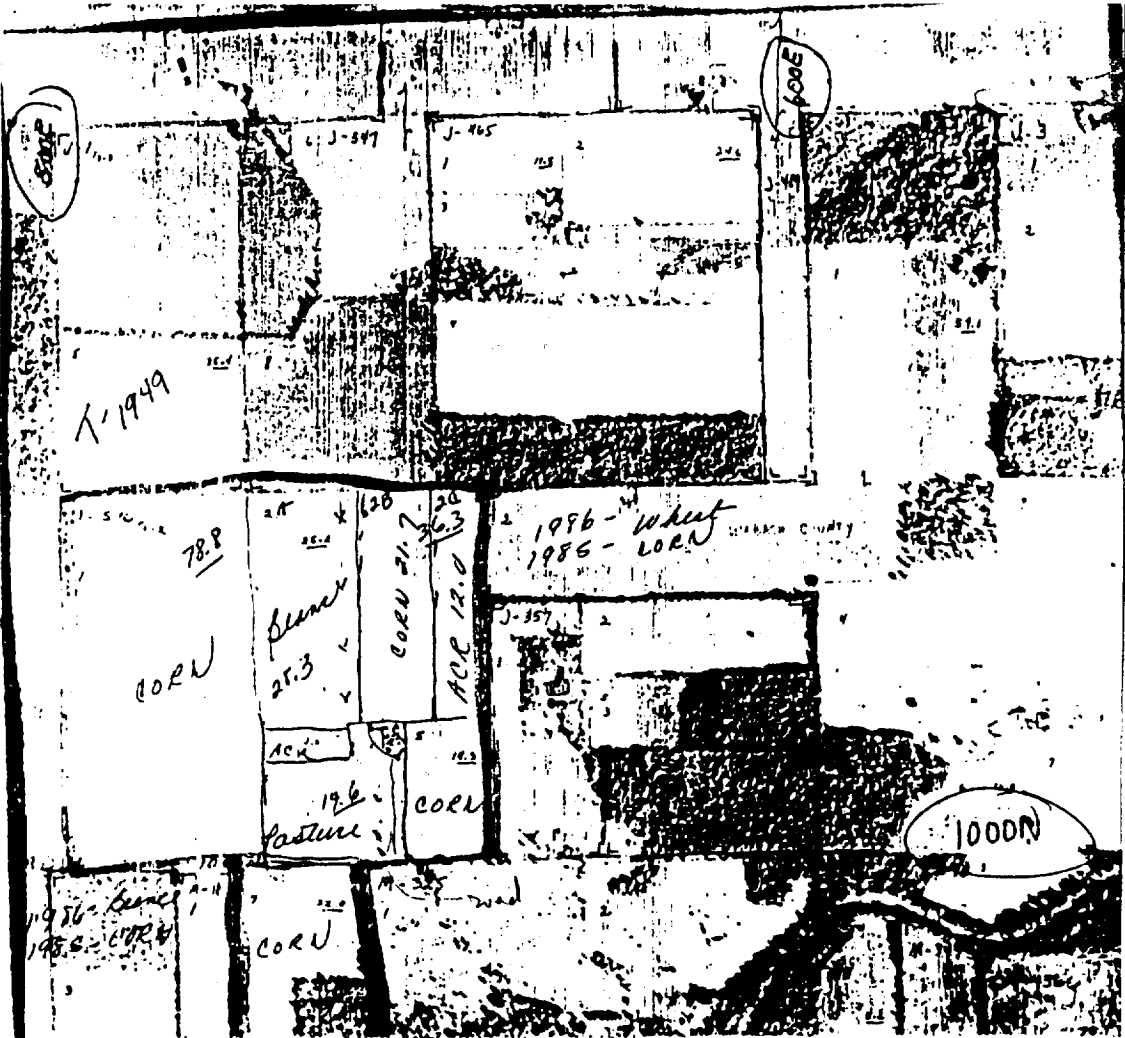


Figure 3. Photocopy B of flown aerial photograph for section 4.

ORIGINAL PAGE IS
OF POOR QUALITY

Section 10:

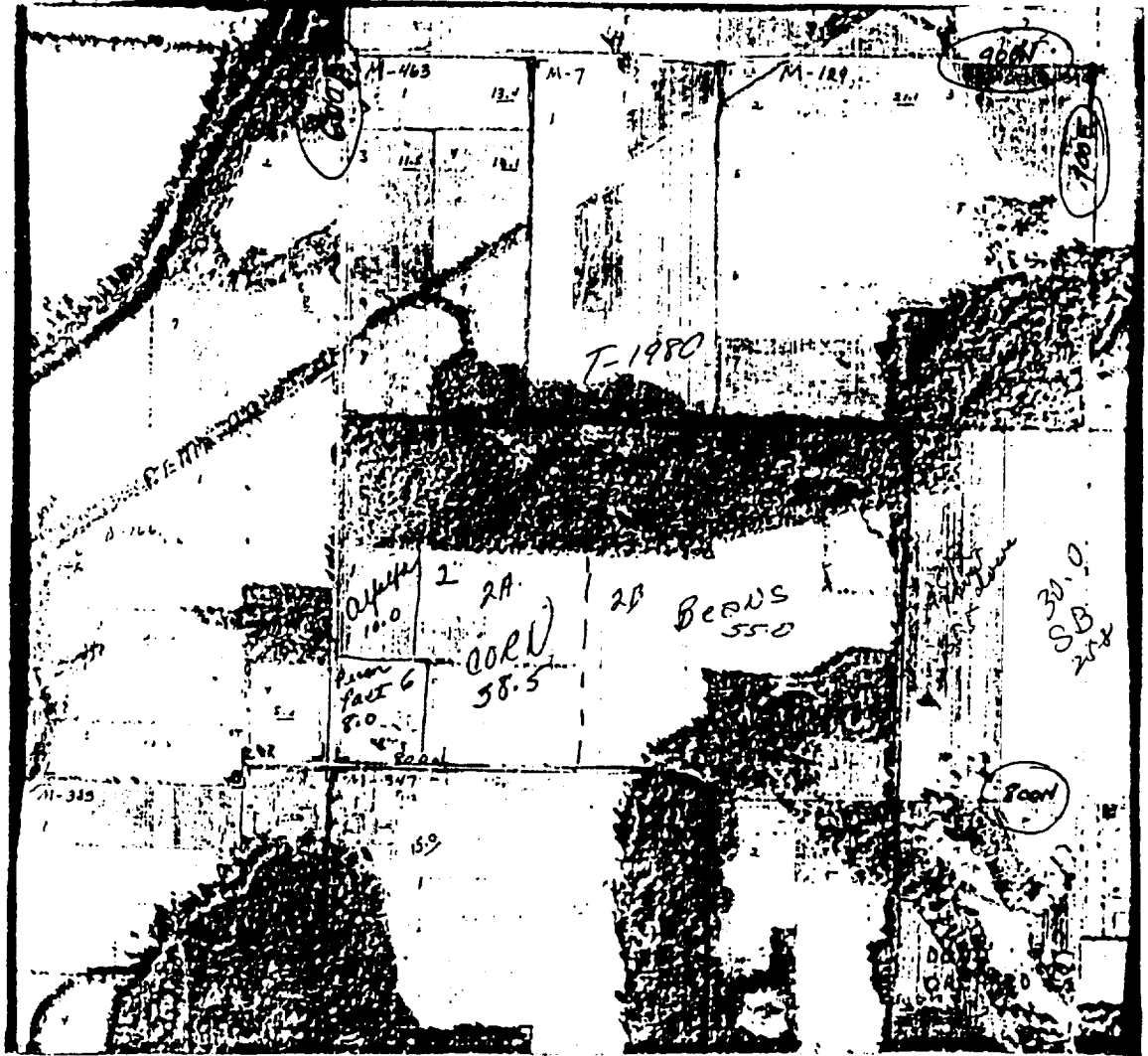


Figure 5. Photocopy A of flown aerial photograph for section 10, 1987.

ORIGINAL PAGE IS
OF POOR QUALITY

Appendix C. NETS Interface Routine Code

Mac_to_NETS.c

```

/*****
Date:          6/17/90
Programmer:    Xin Zhuang, AGEN, Purdue Univ.,
               W. Lafayette, IN 47906
Routine name:  Mac_to_NETS.c
Description:   Converting an ASCII data file listed on
               MacLARSYS to NASA NETS format
               which is binary-coded.
*****/

```

```
#include <stdio.h>
```

```
#define YES 1
#define NO 0
```

```
#define minus(y,x) (y-x)
```

```
FILE *fopen();
FILE *infile;
FILE *infile_image;
FILE *infile_class;
FILE *outfile_image; /* a file for a multi-band image */
FILE *outfile_class; /* a file for classes */
FILE *outfile_jop; /* a NETS training file */
```

```
int MaxClass = 7;
```

```
char MacFile[10];
char Image[10];
char Class[10];
char NetsFile[10];
```

```
main()
{
```

```
    Get_MacFile_Name();
```

```
    Get_ImageFile_and_ClassFile_Names();
```

```
    MacFile_to_Image_and_Class();
```

```
    /*****
Degroup a MacFile to a image file and a class file
getting rid of the row & colum # and Field #.
*****/
```

```
    Create_NetsFile();
```

```
    /*****
Generate the ASCII-type binary codes for NETS.
*****/
```

```
}
```

```
Get_MacFile_Name()
```

```
{
    printf("Enter MacFile Name==> ");
    scanf("%s", MacFile);
}
```

```
Get_ImageFile_and_ClassFile_Names()
```

```
{
    int ij;

    i = j = 0;

    while ((Image[i++] = MacFile[j++]) != ' ')
        ;
    --i;

    Image[i++] = '.';
    Image[i] = 'I';
    /****
The corresponding image file name is with extension "I".
*****/
```

```
    i = j = 0;
```

```
    while ((Class[i++] = MacFile[j++]) != ' ')
        ;
    --i;
```

```
    Class[i++] = '.';
    Class[i] = 'C';
```

```
    /****
The corresponding class file name is with extension "I".
*****/
```

```
}
```

```
MacFile_to_Image_and_Class()
```

```
{
    int Row, Col, class, field;

    int band1, band2, band3, band4, band5, band6, band7, band8;

    infile = fopen(MacFile, "r");

    outfile_image = fopen(Image, "w");
    outfile_class = fopen(Class, "w");

    while( fscanf(infile, "%d%d%d%d%d%d%d%d%d%d",
```

```

                                &Row, &Col, &class, &field,
                                &band1, &band2, &band3, &band4, &band5,
                                &band6, &band7, &band8) != EOF)
{
    fprintf(outfile_image, "(");
    fprintf(outfile_image, "%d %d %d %d %d %d %d %d",
            band1, band2, band3, band4, band5, band6, band7, band8);
    fprintf(outfile_image, ")");
}
/*****
The parentheses are for the Make_Bin routine.
*****/

    fprintf(outfile_class, "%d0, class);

}

    fprintf(outfile_class, " ");

fclose(infile);

fclose(outfile_image);
fclose(outfile_class);
}

Create_NetsFile()
{
    int c;

    infile_image = fopen(Image, "r");
    infile_class = fopen(Class, "r");

    Get_NETS_iopFile_Name();

    printf("%s0, NetsFile);
    outfile_iop = fopen(NetsFile, "w");

    printf("%s0, NetsFile);

    Write_ASCII_Bin_Image();

    fclose(infile_image);
    fclose(infile_class);
    fclose(outfile_iop);
}

Get_NETS_iopFile_Name()
{
    int i, j;

    i = j = 0;

    while ((NetsFile[i++] = MacFile[j++]) != ' ')
        ;
    --i;

```

```

    NetsFile[i++] = '.';
    NetsFile[i++] = 'i';
    NetsFile[i++] = 'o';
    NetsFile[i] = 'p';
}
/*****
The corresponding class file name is with extension "iop".
*****/
}

```

Write_ASCII_Bin_Image()

```

/*****
This function was written by Ranjan Mutiah for
converting a ASCII file to a ASCII-binay file.
It was modified to be suitable for converting
an image fiel.
*****/
{

```

```

    int c, k, i, ok, l, junk, temp=0;
    char ch[5];
    unsigned number;

```

```

    putc('(', outfile_iop);

```

```

    while ((c = getc(infile_image)) != EOF) {

```

```

        ungetc(c, infile_image);
        ok = YES;
        junk = NO;

```

```

        for (i=0; i<=5; i++) ch[i] = 0;

```

```

        i = 0;
        while((ok == YES) && ((c = getc(infile_image)) != ' ')) {
            if(((c == EOF)|(c == '0')|(c == '-')|(c == ')')|(c == '(')))
                ok = NO;
            else { ch[i++] = c; temp++; }
        }

```

```

        if (c == '-') { while ((c = getc(infile_image)) != '0'); if (temp == 0)junk = YES; }

```

```

        if (i != 0) number = atoi(ch); /* First element is '(' */

```

```

        l = 0; k = 0;

```

```

        while ((l++ < 8) && (i != 0))

```

```

        {
            if ((number & 1) == 1)

```

```

                {
                    putc('0', outfile_iop);
                    putc('.', outfile_iop);
                    putc('9', outfile_iop);
                    if (ch[i] != '0')

```

```

                        putc(' ', outfile_iop);

```

```

                    if ((ch[i] == '0') && (k++ < 7))

```

```

                        putc(' ', outfile_iop);

```

```

                }
            else

```

```

                {

```

```

        putchar('0', outfile_iop);
        putchar('.', outfile_iop);
        putchar('1', outfile_iop);
        if (ch[i] != '0')
            putchar(' ', outfile_iop);
        if ((ch[i] == '0') && (k++ < 7))
            putchar(' ', outfile_iop);
    }
    number = number >> 1;
}

if (c == '0' && junk == NO && (c = getc(infile_image)) != EOF)
{
    Write_ASCII_Bin_Class();
    putchar(')', outfile_iop);
    putchar('0', outfile_iop);
    putchar('(', outfile_iop);

    ungetc(c, infile_image);
    temp = 0;
}
}
Write_ASCII_Bin_Class();
putchar(')', outfile_iop);
}

```

```

atoi(s)
char s[];
{
    int i, n;
    n = 0;
    for (i=0; s[i] >= '0' && s[i] <= '9'; ++i)
        n = 10 * n + s[i] - '0';
    return(n);
}

```

```

Write_ASCII_Bin_Class()
{
    int class; /* variable for the class number */
    int zero; /* # of zero in class thermometer coding */

    fscanf(infile_class, "%d", &class);

    zero = minus(MaxClass, class);
    Print_out_Class_Code(zero, class);
}

```

```

Print_out_Class_Code(num_null, num_one)
int num_null, num_one;
{
    int i;

```

```

        for (i=1; i<=num_one; i++)
        {
            fprintf(outfile_iop, ".9");
        }

        for (i=1; i<=num_null; i++)
        {
            fprintf(outfile_iop, ".1");
        }
}

```

decode.c

```

/*****
Date:          6/17/90
Programmer:    Xin Zhuang, AGEN, Purdue Univ.,
               W. Lafayette, IN 47906
Routine name:  decode.c
Description:    Decoding a NASA NETS result to a
               ASCII-binary file.
*****/

#include <stdio.h>

#define minus(y,x) (y-x)

#define MXPXL  940*220 /* maximum # of pixels */
#define MXGRY_LEVEL 16 /* maximum # of pixels */
#define THRSHLD 0.70 /* decoding threshold
                    (if THRSHLD>0.51, then the code value is 1) */
#define MXCLSS 13 /* maximum # of classes */

#define NAMELEN 32 /* maximum length of output filename */

FILE *fopen();
FILE *infile;
FILE *outfile;
FILE *logfile;

int row_num, /* # of lines of the source file */
    col_num, /* # of pixels of the source file */
    total_num_pixel;

char file_out[NAMELEN]; /* name of the output file */
char file_in[NAMELEN]; /* name of the output file */

float image_gis[MXCLSS];
int class[MXCLSS];

```

```

main(argc,argv)
int argc;
char *argv[];
{
    int i_pixel, j;

    char indication[4][10], bracket_left, bracket_right;

    input_para();

    infile = fopen(file_in, "r");
    outfile = fopen(file_out, "w");

    get_total_num_pixel();

    for (i_pixel=0; i_pixel<total_num_pixel; i_pixel++)
    {
        for (j=0; j<4; j++)
        {
            fscanf(infile, "%s", indication[j]);
            /* printf("%s0, indication[j]);*/
        }
        fscanf(infile, "0");

        fscanf(infile, "%c", &bracket_left);
        /* printf("%c", bracket_left);*/

        input_image_gis_data();
        output_gis_gray_code();

        fscanf(infile, "%c0, &bracket_right);

    }

    fclose(infile);
    fclose(outfile);
}

input_para()
{
    printf("Enter image_gis data file ==> ");
    scanf("%s", file_in);

    printf(" >> Enter # of lines of each input file : ");
    scanf("%d", &row_num);

    printf(" >> Enter # of pixels in a line : ");
    scanf("%d", &col_num);

    printf("Each source file is [%d x %d].0, row_num, col_num);

    printf(" >> Enter the name of the output file : ");
    scanf("%s", file_out);
}

get_total_num_pixel()
{
    total_num_pixel = row_num * col_num;
}

input_image_gis_data()
{
    int i_class;

    for (i_class=0; i_class<MXCLSS; i_class++)
    {
        fscanf(infile, "%f", &image_gis[i_class]);
        /* printf(" %f ", image_gis[i_class]);*/
        /* printf("0");*/
    }

    fscanf(infile, "0");
}

output_gis_gray_code()
{
    int i_class;

    for (i_class=0; i_class<MXCLSS; i_class++)
    {
        if ( image_gis[i_class] < THRSILD )
            fprintf(outfile, "0.1 ");
        else
            fprintf(outfile, "0.9 ");
    }

    fprintf(outfile, "0");
}

```

makegis.c

```

/******
Date:          6/17/90
Programmer:    Xin Zhuang, AGEN, Purdue Univ.,
               W. Lafayette, IN 47906
Routine name:  makegis.c
Description:    Making a GIS file which both MacLARSYS
               and ERDAS can read based on the result
               decoded using "decode.c".
*****/

#include <stdio.h>

#define THRSHL  0.7 /* decoding threshold
                   (if THRSHL>0.7, then the code value is 1) */

#define nil_or_one(x) (x > THRSHL ? 1 : 0)

#define MXPXL   940*220 /* maximum # of pixels */
#define MXGRY_LEVEL 16 /* maximum # of pixels */
#define MXCLSS  13 /* maximum # of classes */

#define NAMELEN 32 /* maximum length of output filename */

FILE *fopen();
FILE *infile;
FILE *outfile;
FILE *logfile;

int row_num, /* # of lines of the source file */
    col_num, /* # of pixels of the source file */
    total_num_pixel,
    class_gray_level;

char file_out[NAMELEN]; /* name of the output file */
char file_in[NAMELEN]; /* name of the input file */

float image_gis[MXCLSS];
int class[MXCLSS];

main(argc,argv)
int argc;
char *argv[];
{
    int i_row, i_col, j;

    input_para();

    infile = fopen(file_in, "r");
    outfile = fopen(file_out, "w");

    get_total_num_pixel();

    for (i_row=0; i_row<row_num; i_row++)
    {
        for (i_col=0; i_col<col_num; i_col++)
            {
                input_image_gis_data();
                output_gis_gray_code();
            }

        fprintf(outfile,"0");
    }

    fclose(infile);
    fclose(outfile);
}

input_para()
{
    printf("Enter image_gis data file ==> ");
    scanf("%s", file_in);

    printf(" >> Enter # of lines of each input file : ");
    scanf("%d", &row_num);

    printf(" >> Enter # of pixels in a line : ");
    scanf("%d", &col_num);

    printf("Each source file is [%d x %d].0, row_num, col_num);

    printf(" >> Enter the name of the output file : ");
    scanf("%s", file_out);
}

get_total_num_pixel()
{
    total_num_pixel = row_num * col_num;
}

input_image_gis_data()
{
    int i_class;

    /* # of NTES output equals # of classes, */
    /* so each output has MXCLSS digits. */

    for (i_class=0; i_class<MXCLSS; i_class++)
    {

```

```

        fscanf(infile, "%f", &image_gis[i_class]);
/*   printf(" %f ", image_gis[i_class]);*/
/*   printf("\n");*/
    }

    fscanf(infile, "\n");
}

output_gis_gray_code()
{
    int i_class;
    char gray_level;

    class_gray_level = 0;

    for (i_class=0; i_class<MXCLSS; i_class++)
    {
        if (mil_or_one(image_gis[i_class]) > 0.1)
            class_gray_level++;
        else
            i_class = MXCLSS;
    }

    switch (class_gray_level) {
    case 0:
        gray_level = '0';
        break;
    case 1:
        gray_level = '1';
        break;
    case 2:
        gray_level = '2';
        break;
    case 3:
        gray_level = '3';
        break;
    case 4:
        gray_level = '4';
        break;
    case 5:
        gray_level = '5';
        break;
    case 6:
        gray_level = '6';
        break;
    case 7:
        gray_level = '7';
        break;
    case 8:
        gray_level = '8';
        break;
    case 9:
        gray_level = '9';
        break;
}

```

```

    case 10:
        gray_level = 'A';
        break;
    case 11:
        gray_level = 'B';
        break;
    case 12:
        gray_level = 'C';
        break;
    case 13:
        gray_level = 'D';
        break;
}

fprintf(outfile, "%c", gray_level);
}

```

percent.c

```

/*****
Date:      6/17/90
Programmer:  Xin Zhuang, AGEN, Purdue Univ.,
            W. Lafayette, IN 47906
Routine name: percent.c
Description:  This routine is for calculating
            correct percentage of classification.
*****/

#include <stdio.h>

#define NAMELEN 32
/* maximum length of output filename */

#define Get_Correct_Percent(x, y) 100*x/(x + y)

FILE *fopen();
FILE *infile;
FILE *outfile;
FILE *logfile;

char file_out[NAMELEN]; /* name of the output file */
char file_in[NAMELEN]; /* name of the output file */

int class_num;
float true = 0;
float false = 0;

float Percent;

main(argc, argv)
int argc;
char *argv[];
{
    char c;

```



```

int one_or_zero;
float true_plus_false;

input_para();
/* Get_OutputFile_Name();*/

infile = fopen(file_in, "r");

while( (c =getc(infile)) != EOF )
{
    if ( c != '0' )
    {
        one_or_zero = atoi(c);

        if ( one_or_zero == class_num )
            true = true + 1;
        else
            false = false + 1;
    }
}

Percent = Get_Correct_Percent(true, false);

fclose(infile);

true_plus_false = true + false;

printf("%4.2f0, Percent);
outfile = fopen(file_in, "a");

fprintf(outfile, " %7.2f / %7.2f ) = %4.2f0, true, true_plus_false, Percent);
fclose(outfile);
}

input_para()
{
    printf("Enter file ==> ");
    scanf("%s", file_in);

    printf("class num");
    scanf("%d", &class_num);
}

Get_OutputFile_Name()
{
    int i,j;

    i = j = 0;
    while ((file_out[i++] = file_in[j++]) != ' ')
        ;
    --i;

    file_out[i++] = '.';
    file_out[i] = 'P';
}

atoi(c)
char c;
{
    int image_gis;

    switch (c) {
        case '0':
            image_gis = 0;
            break;
        case '1':
            image_gis = 1;
            break;
        case '2':
            image_gis = 2;
            break;
        case '3':
            image_gis = 3;
            break;
        case '4':
            image_gis = 4;
            break;
        case '5':
            image_gis = 5;
            break;
        case '6':
            image_gis = 6;
            break;
        case '7':
            image_gis = 7;
            break;
        case '8':
            image_gis = 8;
            break;
        case '9':
            image_gis = 9;
            break;
        case 'A':
            image_gis = 10;
            break;
        case 'B':
            image_gis = 11;
            break;
        case 'C':
            image_gis = 12;
            break;
        case 'D':
            image_gis = 13;
            break;
    }
}

```

```

    return(image_gis);
}

```

subset.c

```

/*****
Date:      6/17/90
Programmer:  Xin Zhuang, AGEN, Purdue Univ.,
            W. Lafayette, IN 47906
Routine name: subset.c
Description:  This routine is for subsetting and
            converting a binary ERDAS file, which
            has been removed its header, to an
            ASCII one.
*****/

#include <stdio.h>
#include <math.h>

#define MXBUF 256 /* maximum size of buffer */
#define MXBND 12 /* maximum number of data channels */
#define NAMELEN 32 /* maximum length of output filename */

FILE *fopen();
FILE *outfile;

main(argc,argv)
int argc;
char *argv[];
{
    int fd[MXBND+1], /* file descriptor of files */
        nl, /* # of lines of the source file */
        np, /* # of pixels of the source file */
        cl,
        max,
        maxcl,
        ndum,
        nval[MXBND][MXBUF][MXBUF],
        cc,i,j,ii,jj,kk,
        UL_X, UL_Y,
        BR_X, BR_Y,
        UL_BR_X, UL_BR_Y;

    unsigned char img[MXBND][MXBUF],
        output[MXBUF]; /* buffer */
    char outf[NAMELEN]; /* name of the output file */

    printf(" >> Enter # of lines of each input file : ");
    scanf("%d", &nl);
    printf(" >> Enter # of pixels in a line : ");
    scanf("%d", &np);
    printf("Each source file is [%d x %d].0, nl,np);
    printf(" >> Enter the name of the output file : ");

```

```

        scanf("%s", outf);
    printf(" >> Enter (row,col) of the upper-left: ");
    scanf("%d%d", &UL_Y, &UL_X);
    printf(" >> Enter (row,col) of the bottom-right: ");
    scanf("%d%d", &BR_Y, &BR_X);

    UL_BR_Y = BR_Y - UL_Y + 1;
    UL_BR_X = BR_X - UL_X + 1;

    printf(" >> The subset is [%d x %d].0, UL_BR_Y, UL_BR_X);

    outfile = fopen(outf, "w");

    for(jj=1;jj<argc;++jj)
    {
        fd[jj]=open(argv[jj],0);
    }

    /* read image data */

    for(ii=1;ii<=nl;++ii)
    {
        for(jj=1;jj<argc;++jj)
        {
            cc=read(fd[jj],img[jj],np);
        }
        for(kk=0;kk<np;++kk)
        {
            for (jj=1; jj<argc;++jj)
            {
                nval[jj][kk][ii] = img[jj][kk];

                if (ii >= UL_Y && ii <= BR_Y)
                    if (kk >= UL_X - 1 && kk <= BR_X - 1)
                    {
                        fprintf(outfile,"%d ",nval[jj][kk][ii]);
                    }
            }
        }
    }
    if (ii >= UL_Y && ii <= BR_Y)
        fprintf(outfile,"0");
    }
    fclose(outfile);
}

```